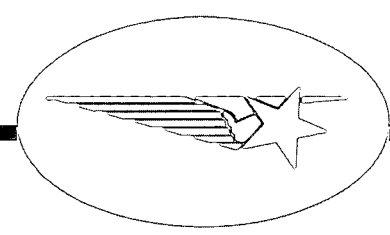


CR 114523

AVAILABLE TO THE PUBLIC

X
M/1X



(NASA-CR-114516) STAR FIELD ATTITUDE
SENSOR STUDY FOR THE PIONEER VENUS
SPACECRAFT M.P. Rudolf, et al (Lockheed
Missiles and Space Co.) NOV. 1972 154 p
CSCL 22B G3/31

N73-12924

Unclass
49082

Lockheed

MISSILES & SPACE COMPANY

A GROUP DIVISION OF LOCKHEED AIRCRAFT CORPORATION

SUNNYVALE, CALIFORNIA

Reproduced by
**NATIONAL TECHNICAL
INFORMATION SERVICE**
U S Department of Commerce
Springfield VA 22151

147

NASA CR 114516

Available to the Public

STAR FIELD ATTITUDE SENSOR STUDY

FOR THE PIONEER VENUS SPACECRAFT

By W. P. Rudolf and D. R. Reed

November 1972

Distribution of this report is provided in the
interest of information exchange. Responsibility
for the contents resides in the author or
organization that prepared it.

Prepared under contract NAS2-7171 by

LOCKHEED MISSILES AND SPACE CO.

Sunnyvale, California

for

AMES RESEARCH CENTER

NATIONAL AERONAUTICS AND SPACE ADMINISTRATION

LOCKHEED MISSILES & SPACE COMPANY

FOREWORD

This report was prepared by Lockheed Missiles and Space Company for the National Aeronautics and Space Administration, Ames Research Center under Contract NAS2-7171.

The Lockheed Project Engineer was W. P. Rudolf. Other contributing authors of this report were D. R. Reed, T. T. Tarshis, R. T. Garcia, W. E. Uplinger, and C. P. Eggen.

Lockheed would like to acknowledge the technical guidance provided by the Program Technical Monitor D. Chisel.

TABLE OF CONTENTS

Title Page	i
Foreword	iii
Table of Contents	v
Section (1) Summary	1
Section (2) Introduction	5
Section (3) Symbols	9
Section (4) Pioneer Venus Attitude Determination Requirements	11
Section (5) Star Scanners - Techniques and Classifications	15
Section (6) Stellar Targets and Backgrounds	21
Section (7) Conversion of Star Light into Electrical Signals	31
Section (8) Signal to Noise Requirements	55
Section (9) Stray Light - Sources, Symptoms, and Cures	73
Section (10) Preliminary Sensor System Design	105
Section (11) Options to Simplify Attitude Determination System	125
Section (12) Survey of Applicable Star Scanner Technology	129
Section (13) Conclusions	143
Section (14) References	145

111

Section 1

SUMMARY

Lockheed Missiles and Space Company has conducted a study for the National Aeronautics and Space Administration, Ames Research Center, to assess the applicability of using a star field scanner to determine the spin axis orientation of the spinning Pioneer Venus Spacecraft. A survey was conducted to determine the methods and techniques currently employed in star scanner systems, including various slit configurations and detector types. Star scanners have been classified into several categories depending on the number of detectors, the slit or detector configuration, and the characteristics of the detectors employed.

Star scanners determine attitude by identifying and measuring the positions of stars as they cross the detector field of view due to vehicle rotation. The spectra, intensity, and distributions of stars are important considerations in the design. Silicon detectors which respond to longer wavelength light have an advantage over visual light detectors such as most photomultiplier tubes, because there are more cooler stars in the sky which have the peak of their radiance distributions at longer wavelengths.

The various possible detectors are examined in detail, and compared under operating conditions found in star scanner applications. Photomultiplier detectors are generally limited by background noise from the general sky background, while silicon detectors are limited by dark current noise. Developmental low leakage silicon diode detectors can outperform the photomultiplier detector in this star scanner application when they are used as an array of a number of detectors.

The signal to noise required for proper sensor operation is determined not by the accuracy requirements, but rather by the necessity of minimizing "false alarms", mostly due to dimmer stars crossing the detector which will have a low but still significant detection probability. Using a 50% margin of safety, this leads to a requirement that at normal cruise spin speed, the minimum intensity star that must be detected under the worst case

orientation conditions must produce a signal to noise ratio of 20.

Stray light, that is light reaching the detector from light sources outside the field of view, is a major problem in the design of star scanners. Stray light can come from the sun directly or from planetary albedo. Stray light can cause an increase in noise level, or can appear as an interfering signal. The stray light rejection required depends on the details of sensor design and the definition of rejection, but can be as high as 10^{12} for a typical sensor using a photomultiplier tube detector. Sensors using silicon detectors are generally less sensitive to stray light; depending on design details, they require stray light rejection ratios one or two (or even more) orders of magnitude smaller than required by a photomultiplier detector sensor.

Rejection of stray light is accomplished primarily by a sunshield or baffle which prevents most out-of-field light from reaching the optical system. The design of the optical system, the optical cavity, the detector geometry, and the information processing techniques are important also. A two stage cone baffle is recommended for this application, and a set of parametric curves for this design is presented.

Baffle rejection must be measured in order to have confidence in the design, but conventional measurement techniques are limited in their capabilities and are not adequate to measure the high rejection ratios required. Two techniques are recommended which could potentially be developed into suitable measurement systems for this application.

Based on the attitude determination requirements, and the parameter relationships developed in the study, preliminary design specifications have been developed for two sensor systems which will meet all requirements. One sensor design is a photomultiplier "V-slit" reticle type. It features a 5 centimeter diameter aperture and a 45 centimeter long baffle. Two separate mechanisms are included to protect the photomultiplier tube from damage due to high light levels.

The second sensor uses an array of eight silicon photodiode detectors which make the sensor more sensitive than the first sensor, so that an

aperture diameter of only 3.2 centimeters and a baffle length of only 28 centimeters can be employed. No protection mechanisms are required. This sensor design is considered more developmental than the photomultiplier tube sensor.

Both sensor designs can meet all attitude determination requirements, and allow complete freedom to modify the mission profile without constraint due to attitude determination ability. Several ways have been investigated, however, in which the requirements could be relaxed to simplify the sensor system; or to reduce its size, weight, power, or cost. These include reducing redundancy requirements, the spin speed or speed range requirements, or the ability to operate in worst case orientations. Reducing the accuracy does not produce significant benefits.

Fifteen organizations which have been associated with star sensor design, development, or operation were contacted to determine if they had any applicable hardware or technology. Several operational sensor systems have been identified which have capabilities somewhat similar to those required for this mission. All are sufficiently different, however, that they would require extensive modification to be suitable, and it is felt that a new design employing proven concepts or components from some of these present systems, is the most cost effective approach.

SECTION 2

INTRODUCTION

The Pioneer Venus program will conduct scientific exploration of the planet Venus and its environment. The spacecraft will consist of a basic bus, which will carry additional systems to carry out either entry probe missions or Venus orbiter missions.

The Pioneer Venus spacecraft will be a spin stabilized system, capable of propulsive maneuvers to perform mid-course trajectory corrections during the inter-planetary flight from Earth to Venus, and capable of attitude maneuvers for probe deployment, orbit injection, and orbit correction at Venus. The performance of these maneuvers requires that the orientation of the spacecraft spin axis be determined and controlled with respect to an inertial reference. A previous study (Reference R 7) for the Pioneer Venus missions showed selection of a Star Field Scanner concept together with a solar aspect sensor for spacecraft attitude measurement. A system of this type has been previously flown in Earth orbit, but due to lack of interplanetary flight experience, further study is necessary to properly assess technical feasibility, system interface considerations, and cost of flight hardware development.

The objectives of this study, as listed in the statement of work, are:

- (1) To identify and clearly understand the critical factors which determine design and performance of Star Sensor/Scanner systems in configurations as they would apply to the Pioneer Venus missions.
- (2) To identify and analyze the important tradeoffs which relate performance to design, and design to cost, reliability, spacecraft interface, and operational flexibility.
- (3) To provide preliminary design definition for the concept or concepts which show greatest potential for the Pioneer Venus application.

4,

- (4) To determine and assess the feasibility of implementing the candidate design or designs.
- (5) To identify any critical problem or development areas associated with the selected designs.

An additional objective was to determine if there are any existing star scanner systems which could be applicable to this mission, perhaps with modification.

To meet the objectives, the work was organized into five tasks. They are:

- (1) Survey current aerospace program hardware and technology and identify any candidate hardware, systems, and/or system concepts applicable to the Pioneer Venus missions. Considerations should include PM tube as well as solid state sensor devices. Describe the systems identified in terms of basic design, approach and development status.
- (2) Define the critical design and integration parameters for the star sensor/scanner systems and determine the sensitivity of these parameters to system performance characteristics.
- (3) Evaluate, by tradeoff and analysis, the effectiveness of the identified systems and system concepts in terms of:
 - (a) Attitude determination performance
 - (b) Spacecraft integration requirements
 - (c) Operational Constraints
 - (d) Design Feasibility, Complexity and Cost
 - (e) System Reliability
- (4) Select a preferred system and promising alternates. Provide preliminary design specifications for these systems.
- (5) Identify potential or known problem areas associated with the designs considered, and describe alternative solutions. Describe the critical failure modes and their effects as related to performance of the system.

Preceding page blank

The work performed under these tasks has been reorganized for this report. The work of tasks (2) and (3) are primarily found in Sections 5 through 9, the preliminary design is in Section 10, and task (1), the survey, is covered in Section 12.

The major problem area identified is the rejection of stray light, which is covered in Section 9. Other potential problems are the susceptibility of photomultipliers to damage from high light levels and the developmental status of the very low leakage silicon diode detectors. Both topics are discussed in Section 7.

SECTION 3

SYMBOLS

A	pulse amplitude
A_D	area of detector, cm^2
A_O	area of optical aperture, cm^2
a	resolution element size, degrees
D, D_O	diameter of optical aperture, cm
e	electronic charge, 1.6×10^{-19} coulombs/electron
$\overline{\text{FAR}}$	average false alarm rate, per second
FOV	field of view, degrees
f_l	focal length, centimeters
Δf	bandwidth, Hertz
I	intensity, watts/cm^2
I_B	background generated current, amperes
I_D	dark current, amperes
I_{NB}	background generated noise current, amperes
I_{ND}	dark noise current, amperes
I_{NJ}	Johnson noise current, amperes
I_{NS}	signal generated noise current, amperes
I_O	incident intensity, watts/cm^2
I_s	signal generated current, amperes
i_T	total detector current, amperes
i_s	detector signal current per square centimeter of optical aperture
K	Boltzmann's constant, 1.38×10^{-73} watt-sec/ $^{\circ}\text{K}$
L	length of inner baffle, cm.
L'	length of total baffle, cm.
L_D	length of detector, cm.
M,m	magnitude of star
M_v	visual magnitude
$M_{(Si)}$	Silicon (detector) magnitude
N	number of surfaces
n	number of detectors

6/

NEP	noise equivalent power, watts/ $\sqrt{\text{Hz}}$
P_d	probability of detection
R	resistance, ohms
R_A, R_B	stray light rejection, definitions (A) and (B)
r	response factor of filter
T	temperature, degrees Kelvin
t	time, seconds
W	width of inner baffle
W'	width of total baffle
W_D	width of detector, cm.
α	slit or detector width, degrees
λ	wavelength, micrometers
η_T	optical transmission
θ_r	inner baffle rejection angle, degrees
θ'_r	outer baffle rejection angle, degrees
τ_d	dwelt time of light signal, seconds
τ_r	rise time of pulse, seconds
σ	standard deviation of distribution
Ω	solid angle field of view, steradians
Ω_w	angular width of detector, radians
ω, ω_s	vehicle spin speed, radians/second

SECTION 4

PIONEER VENUS ATTITUDE DETERMINATION REQUIREMENTS

The requirements for the attitude determination system for the Pioneer Venus mission are based on the earlier Planetary Explorer Studies by the AVCO Corporation and the Goddard Space Flight Center. These requirements are described in the statement of work for this study, and have been considered as the maximum requirements of the mission. The study team also addressed the question of how these requirements could be relaxed to simplify the sensor system or reduce its costs, size, weight, power or other parameters, yet retain sufficient capability to perform the missions as they are currently conceived. The requirements as listed in the Star Field Attitude Sensor Study Statement of Work are reproduced below.

(1) General.

The Pioneer Venus spacecraft will be spin stabilized for attitude control. The primary spin axis orientation (cruise mode) will be either perpendicular to the ecliptic plane or parallel to the ecliptic plane; the choice to be made based on the results of system design studies currently being initiated. For the case where the spin axis is oriented perpendicular to the ecliptic plane, attitude reference accuracies require Sun sensors and star sensors/scanners. In general, maneuvers, involving precession of the spacecraft spin axis would be performed by first ascertaining or confirming the cruise or premaneuver attitude, commanding a series of reaction jet pulses aboard the spacecraft to effect the required precession, and then determining the new spacecraft attitude with respect to inertial reference. The attitude orientations conceivably required include the full 4π steradian angle.

After performance of a function at the new attitude, (i.e., velocity correction, probe release, etc.), the spacecraft would then be precessed back to its cruise orientation. Attitude measurement would confirm that the cruise orientation was properly restored.

(2) Attitude Determination

The system must be capable of determining the spacecraft spin axis orientation with respect to inertial reference throughout the Earth-Venus interplanetary trajectory, the probe mission terminal trajectory, or the orbit injection and the Venus orbital trajectory (excluding eclipse periods).

(3) Accuracy

The orientation of the spacecraft spin axis is to be determinable to within $\pm 0.1^\circ$, as the maximum accuracy requirement; up to $\pm 1.0^\circ$ as the minimum accuracy requirement. This range of accuracy is given to provide latitude in the analysis of design considerations, so that tradeoffs for this key performance parameter can be developed.

(4) Spacecraft Spin Rate

The system must be capable of functioning with its required accuracy for spin rates of 5 rpm or greater.

(5) Spacecraft Nutation

The system must be capable of proper function with a spacecraft nutation of 2° at wobble frequencies of up to 3 rad/sec.

(6) Stray Light

The system must be capable of proper function with the spacecraft in full sunlight, maximum Earth albedo and Venus albedo as are anticipated for the interplanetary and near planetary trajectory conditions.

(7) Response Period for Attitude Measurement

The time required between initiation of the attitude measurement function, and receipt on the ground of the actual orientation data should be minimized. A near-real-time (excluding light time considerations) availability of attitude measurement is highly desirable.

(8) Spacecraft Integration Requirements

The system must be integratable with a spin stabilized spacecraft with minimum impact. Weight and power requirements are to be minimized. Considerations should be given to magnetic cleanliness, number of discrete commands required, unusual power conditioning requirements, etc.

(9) Operational Constraints

The system should be designed to avoid conditions which would prohibit or limit the function of other elements of the spacecraft system or reduce maneuver flexibility during the re-orientation and attitude measurement sequence. All commandable functions should effectively be reversible.

(10) Redundancy.

The system must include provisions for redundancy and backup which strictly remove the mission critical functions from the vulnerability of single point failures.

(11) Assumptions for Initial Conditions

It may be assumed that a priori knowledge of approximate orientation is available for all attitude determination requirements, however, this dependence should be minimized and considerations given to strategies and designs which would permit independent function for recovery from an initially random orientation.

SECTION 5

STAR SCANNERS - TECHNIQUES AND CLASSIFICATIONS

Star field scanners, or simply star scanners, have a number of basic similarities, and are all basically designed to perform the same function, that of determining attitude. The technology survey (Section 12) reveals that a number of star scanners have been built, designed, or proposed for a variety of applications, and have many widely differing parameters such as various slit configurations, fields-of-view, and such. A number of studies have examined star field scanners for various applications, and have made a variety of recommendations. Reports describing the results of many of these studies are listed among the references (Section 14). This section attempts to isolate the essential features of all star scanners, and to classify the various types into meaningful categories.

WHAT IS A STAR SCANNER?

A star scanner is an instrument which scans the sky and responds to light from stars it views in this process. These "star crossings" permit determination of the spin axis orientation once the stars have been identified. All star scanners have the same basic components, namely an optical system, a means of scanning the optical line of sight through a search field (for spinning vehicles, the use of the vehicle rotation is most practical), a reticle at the focal plane defining one or more instantaneous fields of view, and one or more detectors which respond when a star is in the field-of-view, and appropriate processing electronics.

Determination of the vehicle attitude requires four basic steps:

- (1) Measurement of the location of the stars in the search field (vehicle coordinate system)
- (2) Identification of the measured stars.
- (3) Knowledge of the star positions in celestial coordinates.
- (4) Transformation between the vehicle coordinates and the celestial coordinates.

At least three independent measurements must be made in order to perform the transformation which determines the vehicle attitude. These can involve two separate measurements on the same star, such as measuring both elevation and azimuth. If one has other knowledge, the required number of measurements may be reduced. For example, if the position of the sun is known in both elevation and azimuth, only one further measurement is required. For this reason, it is highly desirable to include a sun aspect angle sensor on the spacecraft to provide redundancy and simplify the requirements on the star scanner.

CLASSIFICATIONS OF STAR SCANNERS

Star scanners may be classified in three major ways.

- (1) They employ a single detector, or more than one detector.
- (2) They use a single slit (to make measurements in one axis only) or they use multiple slits or an array of detectors (to measure star position in both azimuth and elevation).
- (3) They employ a photomultiplier detector or a solid state detector or array.

There are many other ways in which star scanners may be classified, but these appear to be the most fundamental and meaningful for this spinning vehicle application.

Classification (1) - Single or Multiple Detectors

This classification is important for two reasons. First, multiple detector sensors generate more information per star crossing, and thus require somewhat different signal processing methods. Second, for a given total sensor field-of-view, and slit or detector configuration, the sensitive area of each detector will be smaller when more than one detector is employed. Since most noise sources such as background noise and dark current noise are directly dependent on the sensitive area of the detector, the noise is smaller in a multiple detector sensor and thus its sensitivity is higher. All else being equal, the sensitivity will increase as $(n)^{1/2}$ where n is the number of detectors.

Preceding page blank

Classification (2) - Single Slit or Multiple Slit

A single slit sensor can perform only one measurement on a star that it views, that of measuring the azimuth position. The elevation of the star can be anywhere within the elevation field-of-view. Multiple slit detectors generally measure a star position in both azimuth and elevation, thus obtaining two of the three measurements required for attitude determination on a single star. Essentially all multiple detector sensors are also multiple slit sensors as well, but single detector sensors can fall in either category.

The single slit approach has one major advantage, that of minimizing background noise for a given field scanned. The scheme does require more stars to be observed, however, a minimum of three stars when the sun position is not known. Maximum accuracy is achieved when the sensor is oriented near the spin axis, but this reduces the solid angle of sky scanned. Because more stars are required for attitude determination, the field of view must be larger than the multiple slit approach and/or the sensor must be more sensitive so that dimmer stars may be detected. These features place a more severe requirement on baffling and make baffling more difficult. Because a star crosses the detector only once per scan, false alarms can be distinguished only by observing repeated scans, which means that, all else being equal, the single slit sensor requires a larger signal to noise ratio than a multiple slit sensor where false alarms can be rejected if they do not fall into an acceptable pattern. Star identification is a major problem with a single slit, and a priori attitude information is nearly essential. This is because star identification is based primarily on measuring angular distances between the various stars observed. The single slit sensor provides only very crude information on these angular separations because it only measures the azimuth position of each star. The multiple slit sensor, on the other hand, measures both azimuth and elevation of each star and the angular separation of all stars observed can be easily calculated.

The multiple slit approach does present a larger sensitive area and consequently has a larger background noise for a given elevation f.o.v. when only one detector is employed. However, the f.o.v. can be much smaller with this scheme due to the fact that only two stars are required for attitude determination. In the case where sun aspect angle is known, only one star

need be observed. The smaller field of view is also very desirable from a stray light rejection view point. Because only one star need be observed when the sun position is known, because stray light rejection is improved, and because star identification is much easier, the multiple slit method is recommended over the single slit approach for the Pioneer Venus application.

A wide variety of multiple slit designs have been built and proposed. The simplest is the "V-slit" which consists of two separate linear sensitive areas placed at an angle to each other. Most of the more elaborate multiple slit arrays such as the "N-slit" or the "W-slit" configurations are merely somewhat fancier versions of the simple "V-slit." The basic purpose in adding extra elements to the basic configuration is to resolve some of the ambiguities which can arise when stars are more closely spaced than the maximum-spacing between slits so the series of pulses from each star overlap. Although this does serve to reduce the ambiguity, when a single detector is employed, the noise also increases. Ambiguities can be removed in most cases, by encoding the amplitude of the star crossing signal, and this is the recommended approach rather than adding additional slits to the basic V-slit design.

A second way in which multiple slits can be employed, is by "coding" the slit pattern by using parallel slits which will then produce a coded signal when a star crosses. This was used on the Project Scanner sensor. It has been shown (Reference R 3) that this is generally an undesirable scheme since as more slits are added to generate or increase the code length, the noise increases also such that the sensor becomes less sensitive.

Classification(3)- Photomultiplier Tube or Solid State Detector

The operating characteristics of these two types of detectors are radically different and thus sensors employing them have different characteristics. The photomultiplier tube is a high vacuum electron tube requiring high voltages and is sufficiently bulky so that it is practical to employ only one tube per sensor. Such devices then obviously also fall in the single detector classification. Solid state detectors, on the other hand, are small and require only low voltages for operation, and can be easily fabricated into arrays. The two detector types differ in their

limiting noise mechanisms and their sensitivity under various operating conditions, their susceptibility to damage, and in many other ways. Detectors are discussed in detail in Section 8.

Classification of Existing Star Scanners

All the sensors covered in the technology survey can be classified in each of these three ways. Although these sensors are discussed in more detail in Section 12, it is informative to examine them in light of these classification schemes. Table 5-1 shows these classifications. It is not clear from the information available whether either of the Pioneer Venus proposals use a single detector or multiple detectors.

Most operational systems use a single P.M. tube detector and employ a multiple slit reticle which measures star positions in two axes. The solid state sensors also use the multiple slit reticle except for the Pioneer Jupiter sensor which is designed as only a roll position indicator. The SCADS system is the only operational single slit sensor of the general type required for Pioneer Venus. It uses a 25 degree long slit which does not compromise stray light rejection because it is mounted on the spacecraft so that it always points more than 90 degrees from the sun. Unfortunately, the Pioneer Venus sensor can't use such a simple solution.

SENSOR CLASSIFICATIONS

Sensor	CLASSIFICATION 1		CLASSIFICATION 2		CLASSIFICATION 3	
	Single Detector	Multiple Detector	Single Slit	Multiple Slit	P.M. Tube	Solid State
SCADS (GSFC)	*		*		*	
QAO-7 (Ball Bros.)	*			*	*	
SAS-A,B (AS&E, APL)	*			*	*	
ATS-3 (CDC)	*			*	*	
SCANNER (Honeywell)	*			*	*	
Pioneer Jupiter (TRW)	*		*			*
Pioneer Venus (Kollsman)	?	?		*		*
Pioneer Venus (CDC)	?	?		*		*
SPARS (CDC)		*		*		*

SECTION 6

STELLAR TARGETS AND BACKGROUND

A star scanner provides information for attitude determination whenever a sufficient number of stars (at appropriate angular separations) are detected and identified. The number of stars detected depends upon sensor parameters which can be varied by the sensor designer, such as field of view, sensor angle to the spin axis, and upon sensor sensitivity. The number and identity of the stars detected will depend on the attitude of the spacecraft.

Given knowledge of the field of view, aspect angle, and sensitivity of the sensor, the number of stars which would be detected can be determined for any attitude of the spacecraft. In some instances, sensor aspect angle can be preadjusted for detection of an optimum number of stars when the spacecraft is at its nominal cruise mode, or for particularly important maneuvers or operations.

To meet the Pioneer Venus attitude determination requirements, the sensor system must be able to determine attitude at all orientations. Since it is impractical to simulate all possible vehicle attitudes, fields-of-view, sensitivities, and aspect angles, we must make use of general analytic methods.

Stellar Irradiance

The apparent brightness of stars (irradiance received at the earth at a given wavelength) is measured in modern astronomy on a logarithmic scale derived from the visual magnitude scale of ancient Greek astronomers. The "apparent magnitude" of a star refers to its observed brightness, which depends on its actual brightness, its size, and its distance from us. In the modern system irradiance is defined for a fictional star which is "zero magnitude" at all wavelengths (and, therefore, in each selected spectral band). The magnitude of a particular star (at wavelength λ or bandwidth λ_1 to λ_2) is then determined by the relationship, $\log (I_n/I_m) = 0.4 (m-n)$. If n refers to one "zero magnitude" star, the magnitude of the star is

given by $m = 2.5 \log (I_n/I_m)$. If the star irradiance, I_m , is 100 times that of our reference star, $\log (I_n/I_m) = \log 1/100 = -2$, so the star has a magnitude $m = -5$. If the reference star is 100 times as bright as the star, then $m = +5$. Thus, our magnitude scale for describing stellar irradiance has the property that bright stars have small or negative magnitudes, and dim stars have large positive magnitudes. Excepting the sun ($m_v = -26.8$), the visual magnitude of observed stars range from $-1.4 m_v$ for the brightest star, (Sirius) to about $+24$ for the faintest star recorded with the 200 inch telescope. The irradiance received from the moon and planets is also frequently expressed in equivalent magnitude, but varies with viewing geometry and distance.

Figure 6-1 from reference P1 indicates the relationship between viewed magnitude of the planets and brighter stars, their intensities, and the number of stars brighter than a given magnitude. The observed intensities at visual and photographic wavelengths are well documented for all of the brighter stars. Forbes and Mitchell (Reference P2) using narrow band spectral measurements on 964 bright stars, have calculated the response of six different photocathode materials and the silicon detector to light from these stars. Although none of these stars are south of declination - 20 degrees, the response of such stars can be readily determined from a knowledge of star operational characteristics and viewed magnitude relative to a similar observed star in the northern hemisphere.

Star Distribution and Required Sensor Scan Field

The angular distribution of the stars observed from the earth is determined to a large extent by the location of the sun near the edge of our galactic system. Figure 6-2 (Ref. R 1) illustrates the general distribution of integrated starlight seen from the earth in a spherical coordinate system with its poles parallel to the poles of our galaxy. It can be seen that most of the star energy observed is concentrated in the plane of the galaxy (commonly known as the Milky Way). It can be seen from the figure that the total light varies over a wide range, from well below the average level of 100 tenth magnitude stars per square degree to over 700 tenth magnitude stars per square degree. This star background is the limiting noise source for sensors using

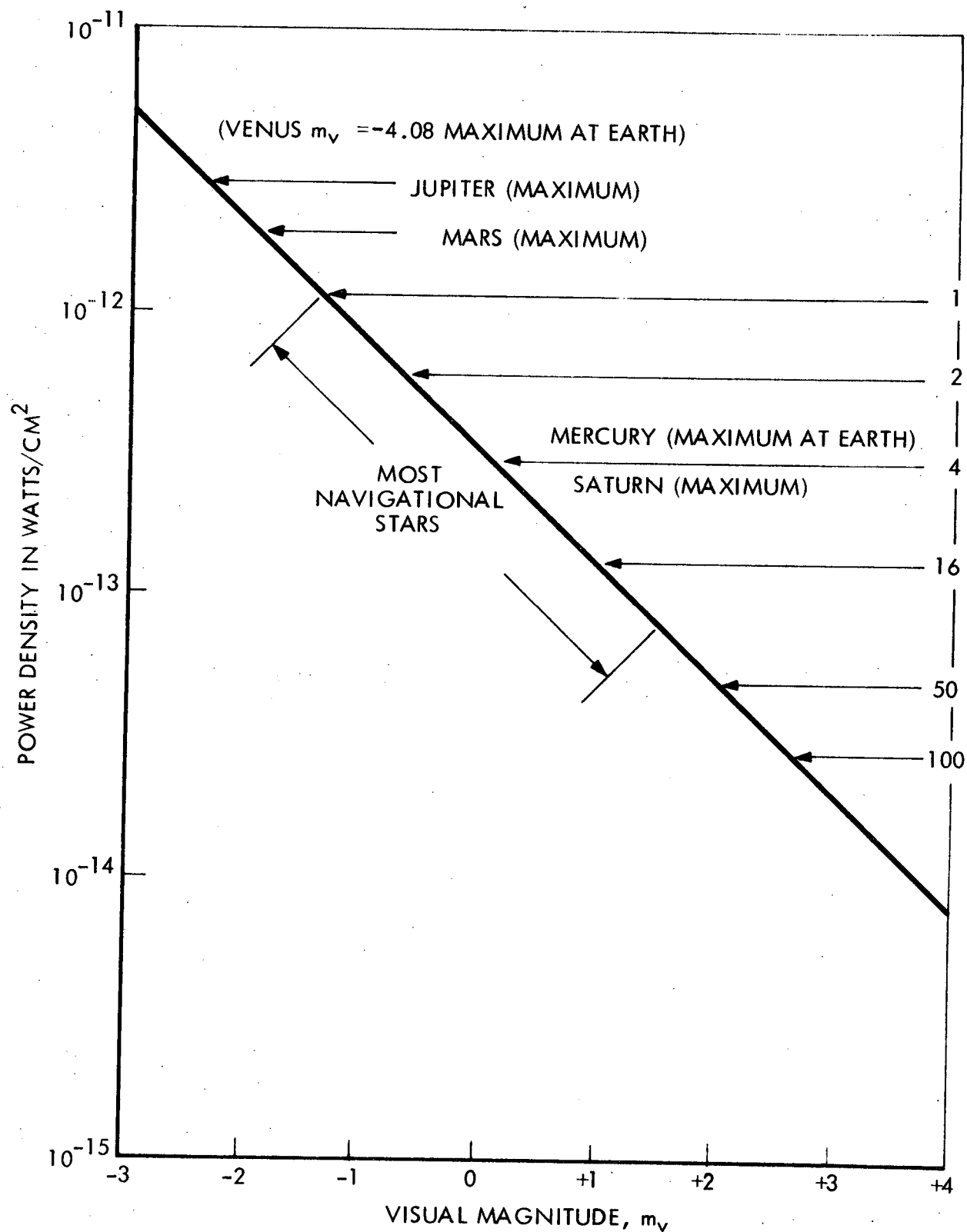


FIGURE 6-1
INTENSITY OF PLANETS AND STARS

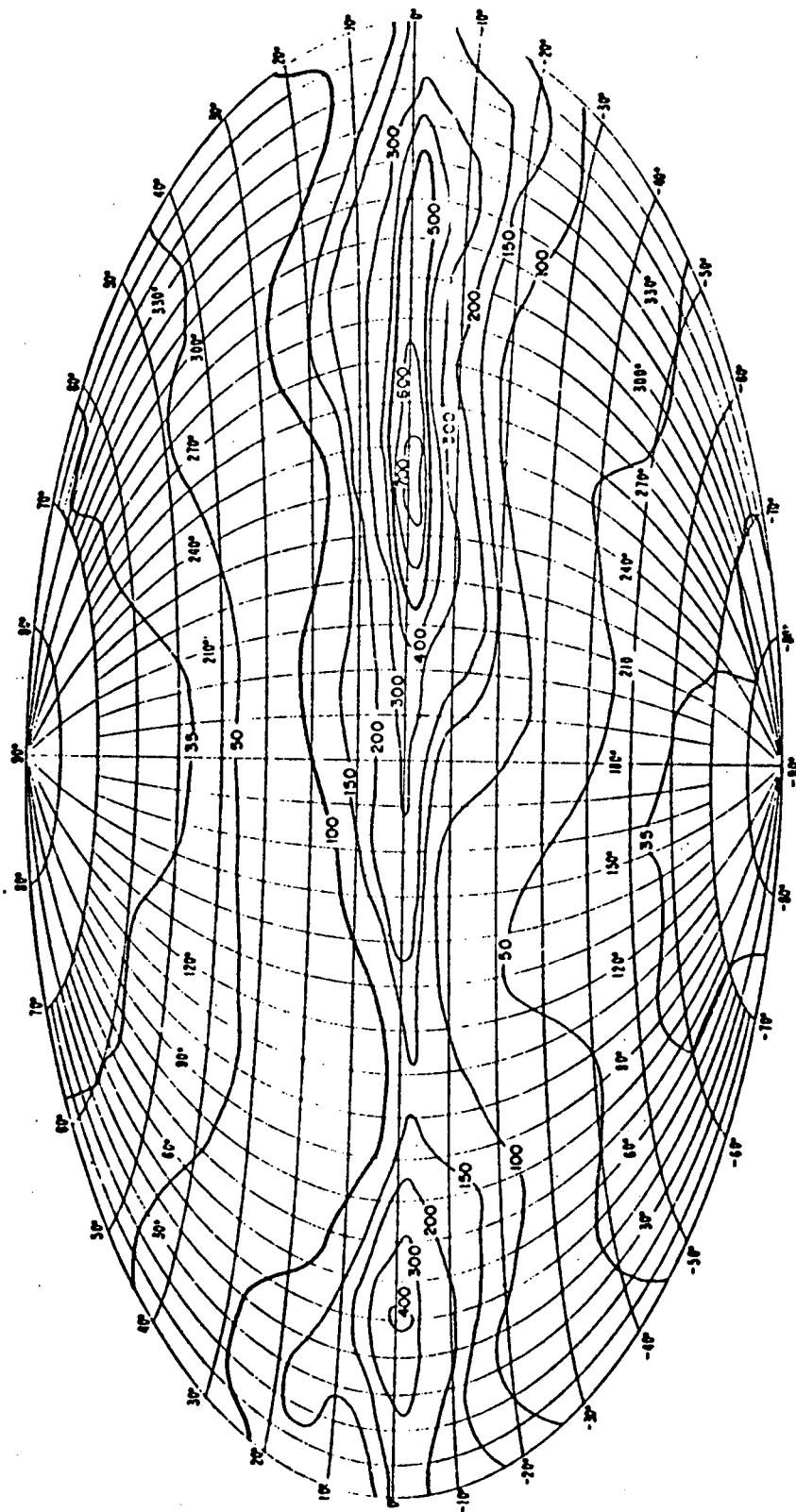


FIGURE 6-2
TOTAL INTEGRATED STARLIGHT IN NUMBER OF TENTH-MAGNITUDE (VISUAL)
STARS PER SQUARE DEGREE IN GALACTIC CO-ORDINATES

(From Reference R1)

photomultiplier detectors. Many of the bright stars we see appear bright primarily because they are near to us, and, therefore, are distributed in more nearly random directions than the majority of stars.

For any given sensor field of view, aspect angle on the vehicle, and limiting magnitude sensitivity, one can determine which stars will be seen by the sensor at any given orientation. This procedure can be used to insure adequate star scanner performance for critical attitudes of the spacecraft. It is also possible to compare results from attitudes spaced around the celestial sphere and thus, estimate the probability of detecting a given number of stars at random attitudes.

Simulations for statistical analysis have been made for a number of types of star sensors, most considering stars in or near the visual spectrum. Studies have been performed for both circular fields of view and annular fields of view typical of star sensors on spinning vehicles. Such simulations are valid for specific cases of size and shape of field of view, and for the investigated sensitivity. It is desirable, however, to have a means of predicting the probability of detecting the required number of stars for the general case.

In Figure 6-3 the lower curves show (as a function of limiting visual magnitude) the area of the sky which would have to be viewed (in either a circular or annular field of view) to detect one or two stars, if stars were uniformly distributed on the celestial sphere. The curves at the upper right show, for spinning vehicles, an empirical boundary for the requirement of one star 99-100 percent of the time. This curve is based on a number of specific studies. It has also been found that studies considering circular fields of view result in approximately the same curve for the worst case orientations and visual stars.

In order to extrapolate the coverage requirement for visual star magnitude to other spectral regions it is necessary to consider the relative number of stars in the selected spectrum and the visual spectrum at various magnitudes. In addition, since the individual stars which will be brightest vary with sensor spectral response, the spatial distribution of the

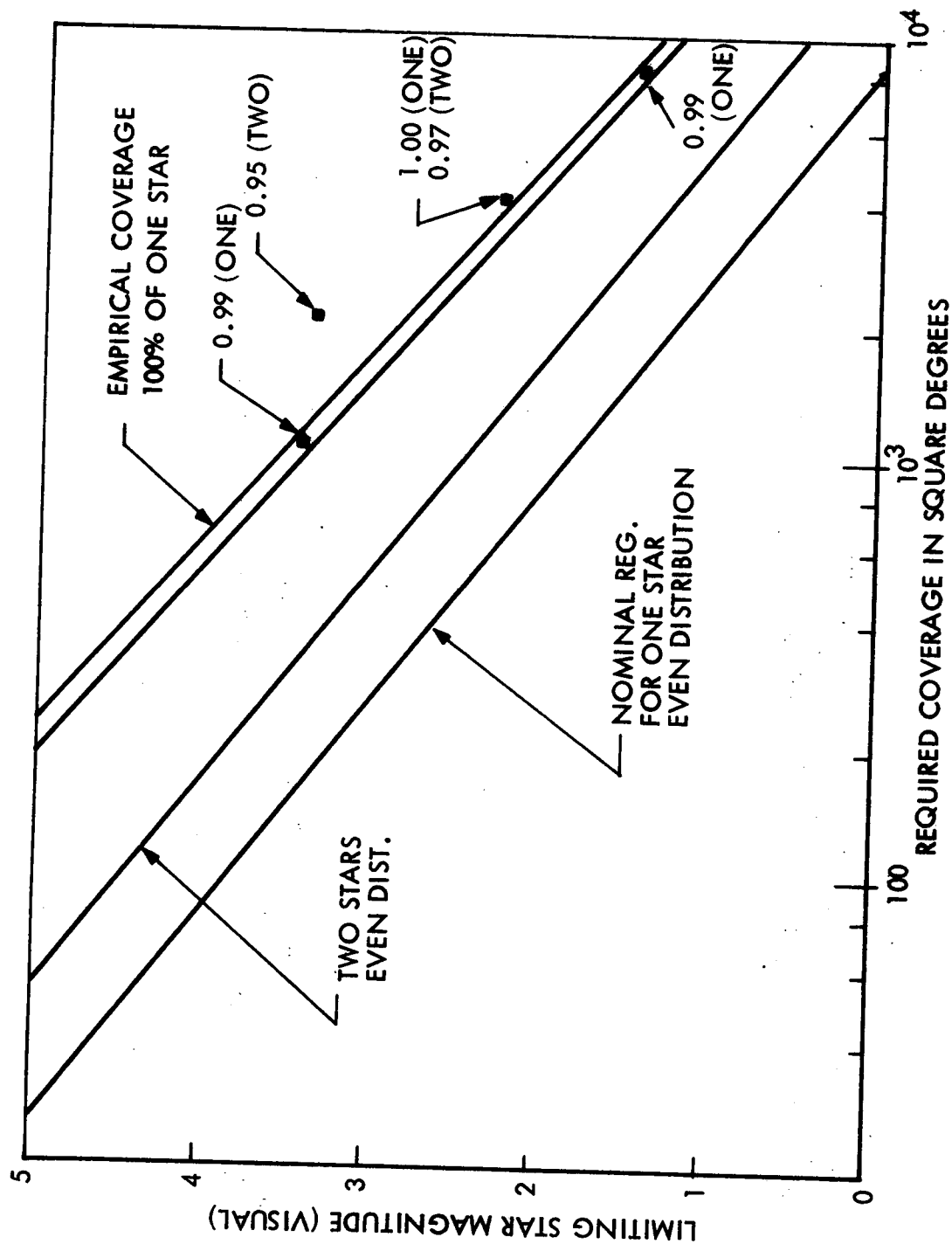


FIGURE 6-3
SKY COVERAGE REQUIRED TO SEE STARS

stars will vary. The distribution generally becomes somewhat more uniform for bright stars at longer (redder) wavelengths but is probably not significantly improved for silicon over visual sensors.

Figure 6-4 shows the number of stars brighter than a given magnitude for visual and silicon detector. The silicon curve is derived from an analysis of the data of Forbes and Mitchell for the 964 bright stars mentioned above. This shows that for any given magnitude, the silicon detector "sees" significantly more stars than a detector which responds to visual light such as many photomultipliers. This constitutes a significant advantage for the silicon detector.

Figure 6-5 shows the area of sky which must be scanned to see a certain number of stars brighter than a given magnitude. If the sensor scans 6 percent of the sky, for example, a silicon detector must be sensitive to stars as dim as 2.5 magnitude, and a visual detector must be sensitive to stars as dim as 3 magnitude to be assured of seeing at least one star in the scanned field. It may be noted that the average number of stars seen is much greater than the worst case. The percentage of sky scanned by a sensor with a given elevation field of view and mounted at a given aspect angle is shown in Figure 6-6.

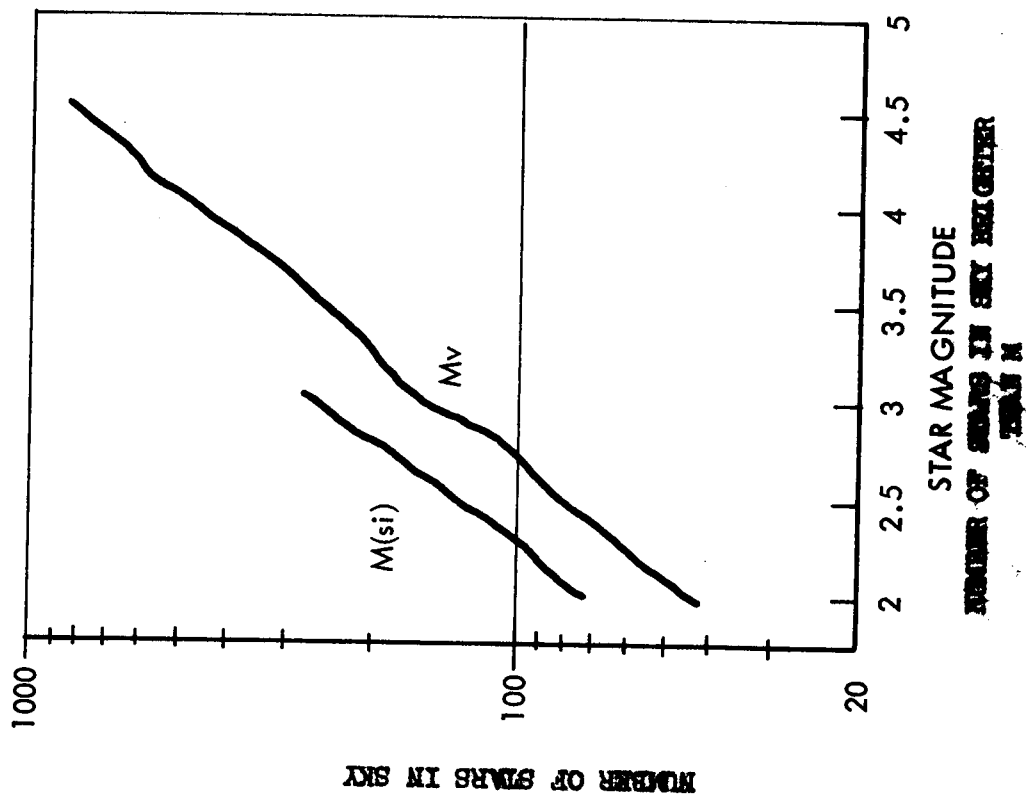


FIGURE 6-4

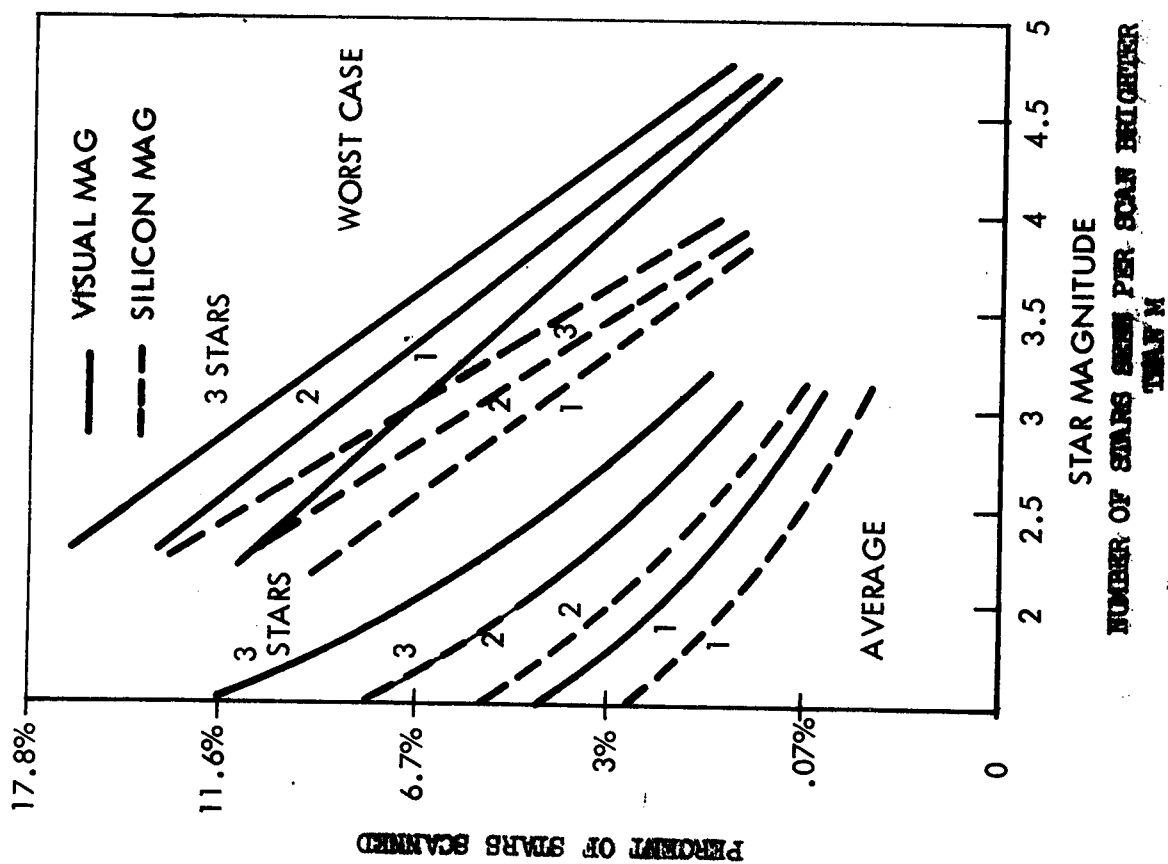


FIGURE 6-5

FRACTION OF SKY VIEWED BY SPINNING SENSOR

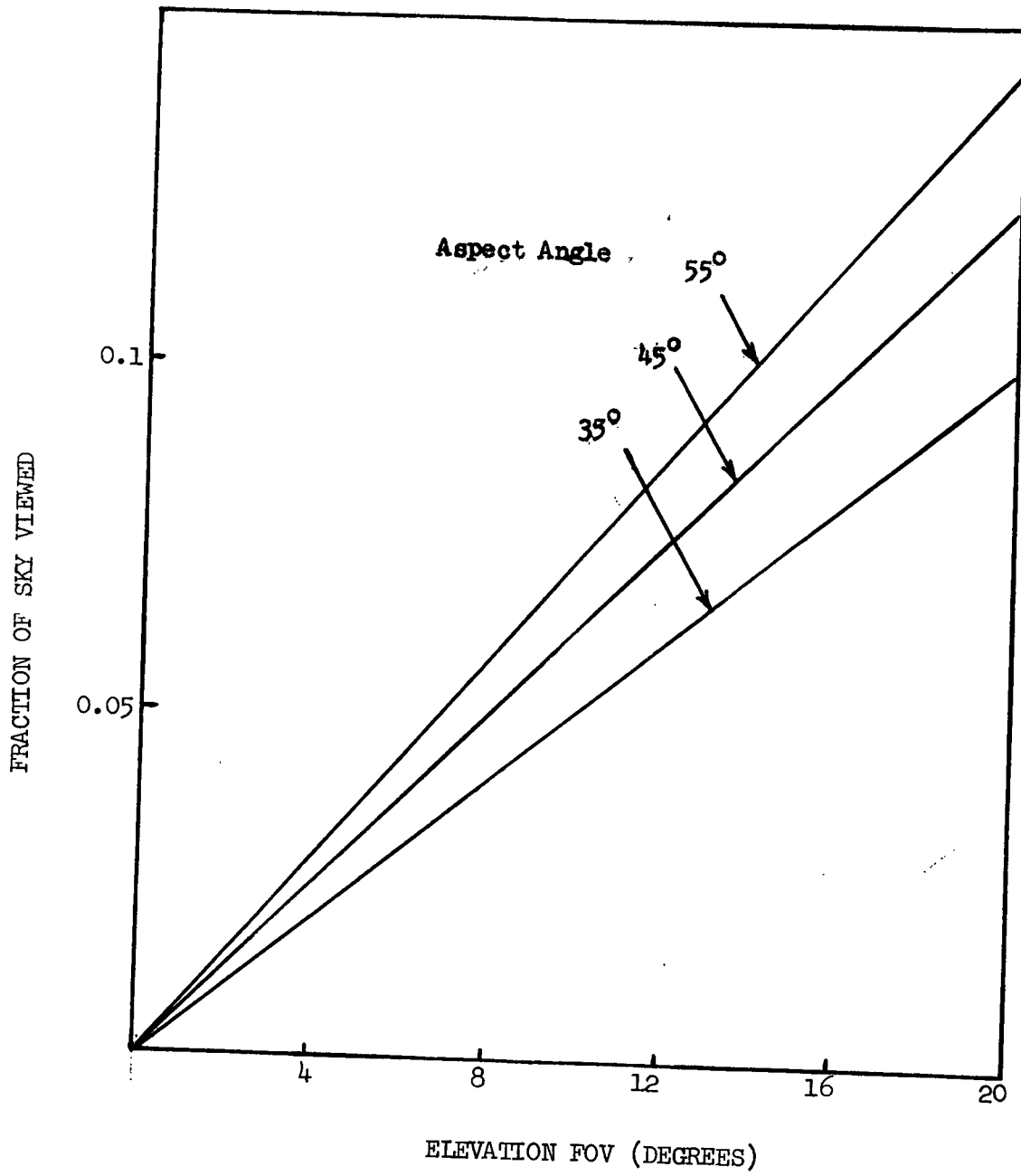


FIGURE 6-6

SECTION 7

CONVERSION OF STAR LIGHT INTO ELECTRICAL SIGNALS

One of the fundamental elements of all star scanner systems is a device which converts the light radiation from stars into electrical signals. These devices are known as detectors, and there are several types of detectors that could potentially be used in star scanners.

Detectors which have greatest sensitivity in the general region where many stars have their radiance peak are of most interest. This region is the visible spectrum plus narrow regions of the ultraviolet and infrared spectrums to either side of the visible. Star energy falls off rapidly in the ultraviolet as one passes to the short wavelength side of the star radiance peak, and detectors for the infrared region require cooling for maximum sensitivity if their cutoffs approach two microns or so. The search for suitable detectors then centers on a comparative few in and near the visible region. These are photoemissive devices, particularly photomultipliers, silicon or germanium photodiode detectors, and photoconductors such as cadmium sulfide and cadmium selenide.

These detectors fall into two basic categories, the photomultiplier detectors and the solid state detectors. All the solid state detectors are similar in that they can be fabricated in arrays, are small in size, and require low voltages and consume little power. Because they are similar in these fundamental characteristics, these detectors may be compared fairly directly. The silicon and germanium diodes are particularly similar, both being diamond lattice structure intrinsic semiconductors and forming diodes with impurity doping. The germanium diodes are sensitive to slightly longer wavelengths, (i.e. a cutoff wavelength of about 1.8 μm vs. about 1.1 μm for silicon.) The technology of silicon diodes is much better developed for detector purposes, with much better dark current characteristics, and as a consequence the germanium devices are little used compared to silicon detectors. Silicon

photodiodes are clearly the choice over germanium photodiodes for star sensor applications.

Cadmium sulfide and cadmium selenide are photoconductors rather than photovoltaic devices. They change in resistance when illuminated rather than generating a current as do the photodiodes. These devices are produced by depositing thin films of these materials on suitable substrate, and the active areas are defined by depositing masks and electrodes. The production of these devices is somewhat an art, and the characteristics of the materials can be modified by impurities and heat treatments. They have two characteristics which make them unsuitable for this star sensor application. First, they exhibit "hysteresis" or "light history" effects which means that their response depends to a great extent on their exposure to light levels previously. This effect is significant enough to cause major calibration and threshold errors. A second related effect which is even more important is that these detectors exhibit very long time constants at the low light levels of interest, and the time constants change with light intensity. This, too, makes calibration difficult. The only star scanner system to use cadmium sulfide or selenide detectors was the earlier SPARS system under development by CDC.* To control the time constant, the detectors were illuminated by a constant light source which stabilizes the time constant but also reduces the detector sensitivity significantly. Later SPARS designs did not use cadmium detectors. Because of these characteristics of the cadmium sulfide and selenide detectors which make them unsuited for use in the star scanner systems, and the superiority of the silicon photodiode over the germanium photodiode, the only type of solid state detector which will be considered further for this application is the silicon photodiode.

The detectors of interest for this star scanner application are thus the photomultiplier tube with various possible types of photocathode materials, and silicon photodiode detectors. Most of the operational star scanner systems which were covered in the technology survey employ photomultipliers, all of them manufactured by EMR Photoelectric Division of Weston Instruments, and they use photocathode materials with the highest quantum efficiency and which have the largest response for most stars which are the bi-alkali and the S-20 types.

* Control Data Corporation

The Pioneer Jupiter star sensor is the only item of flight hardware covered in the survey to use a photodiode detector. A number of manufacturers have proposed and/or are developing other silicon detector star sensors, but they have not been demonstrated in flight hardware. The following sections will examine these two types of detectors in more detail.

PHOTOMULTIPLIER DETECTORS

The photomultiplier tube is a form of high vacuum electron tube where light falling on the photocathode surface liberates electrons. This electron current is amplified in a series of dynodes by the process of secondary emission, so that the output current at the anode is larger than the cathode current by a factor of typically a million or so. For many applications, including the star sensor application, this amplification process introduces only negligible noise, so that the signal to noise ratio at the output is essentially the same as that at the cathode. This "noiseless gain" of the photomultiplier is the essence of its advantage over solid state detectors, because the noise (usually background noise in this sensor application) is amplified in the tube to a level such that it dominates noise introduced in the following electronics.

It is not the purpose of this section to describe in detail the construction and operating characteristics of the various forms of photomultiplier tubes. Many volumes have been written on this subject and a few are listed in the reference section of this report. Rather the characteristics of the tubes suitable for star sensor applications will be reviewed, and sensor design criteria will be developed based on these characteristics.

Being an electron tube, the photomultiplier has a significant physical size, typically about 1 3/8 inches in diameter and 4 1/4 to 5 inches long for the tubes used in operational star scanner systems. High voltages are required for their operation since a minimum potential is required between successive dynode stages to accelerate the electrons sufficiently to produce secondary electrons upon impact. The total tube potentials must be a minimum of about 1000 volts and generally run in the range of 2000 to 3000 volts. Thus a high voltage power supply is required in the instrument and the high

voltage areas must be carefully potted to eliminate corona discharge problems in the low pressure environment of the space vehicle. Because of the size of the photomultiplier tube and its power supplies, it is impractical to include more than one tube in a Pioneer Venus star scanner, and thus such an instrument is limited to a single detector channel which imposes restrictions on the sensitivity of the system and provides a critical failure path.

There are many different photocathode materials in use in photomultiplier tubes, with many different spectral characteristics. The S-20 and bi-alkali cathodes are of most interest in this application because their spectral range matches most stars well and they have comparatively high quantum efficiency. Both materials have their spectral peak at about 0.4 microns and cutoff at about 0.3 microns on the short wavelength side. The S-20 response extends to nearly 0.8 microns while the bi-alkali cuts off at less than 0.7 microns. Quantum efficiency is the probability that a photon striking the photocathode will release an electron, and both these materials have a quantum efficiency of about 20% at the spectral peak.

The response time of photomultiplier tubes is much faster than is required for this star scanner application. The limiting factor is the time spread of an electrical pulse as it is amplified in the dynode chain due to the variation in possible path length the various electrons travel. Photomultiplier tubes of the "venetian blind" structure, which is the structure typically used in star scanners, have a rise time of 12 to 15 nanoseconds and focused dynode configurations are much faster. Since this star scanner application only requires frequency response to a few kilocycles at most, depending on spin speed and slit width, all photomultiplier tubes have more than sufficient speed.

The photomultiplier tubes that have been flown in space have been of a rugged construction in which Kovar rings supporting the elements are sealed between glass rings to form a very strong one piece structure. Such tubes are rated to withstand 100g's shock and 30g's vibration and have been tested to much higher levels. Because of the rugged structure, the microphonic

response of these tubes is very low. The presence of the magnetic alloy Kovar in the tube structure provides some magnetic shielding for the "electron optics" in the tube, and make these structures less susceptible to degradation by magnetic fields. Conventional tubes can be severely degraded by fields as low as two gauss, while the venetian blind tube with Kovar rings can operate with only a few percent degradation up to 10 gauss or so. The Kovar in the tube can be a problem, however, if other instruments in the spacecraft are sensitive to weak magnetic fields. A similar venetian blind tube structure using a ceramic rather than a glass uses much less Kovar and can reduce such a potential problem.

Photomultiplier Noise Sources

The limiting noise of a photomultiplier tube under very low light level conditions is shot noise due to dark current in the tube. Dark current is random emission of electrons from the photocathode, and it is generally due to a thermal mechanism so the current can be reduced by cooling the tube. The sensitivity of such detectors can be measured in terms of a figure of merit known as noise equivalent power or NEP. This is simply the light signal level which results in a unity signal to noise ratio when measured in a one hertz bandwidth. Typical photomultiplier tubes have NEP of the order of 10^{-16} watts/ $\sqrt{\text{Hz}}$.

In the star sensor application, the photomultiplier is not completely in the dark but receives radiation from the sky. This background radiation generates a current which is generally larger than the dark current and thus the shot noise from this current is the limiting noise mechanism for practical cases. At high signal levels, shot noise due to the signal current may also be significant. These noise mechanisms are discussed in greater detail later in this section.

Damage Mechanisms

Although photomultiplier tubes can be made very rugged to withstand the expected mechanical environment, there are other mechanisms by which they can be temporarily degraded or permanently damaged. These mechanisms include damage to the cathode, dynodes, and anode by large currents, and direct cathode damage due to high light levels. The currents can be controlled by

electrical means so that damage does not occur. High value biasing resistors can limit current in the dynode chain, and the power supply may be controlled so that the voltage is reduced, or even turned off when the input light signal gets too high. Such circuits, of course, add to the complexity and affect the reliability of the instrument, but are capable of preventing any significant damage to the dynodes which are most susceptible to current damage. The cathode, however, can not be completely protected in this way.

Two effects occur in the photocathode at high light levels, the first being a large increase in dark current due to excitation of metastable states in the cathode material which decay with a spectrum of time constants. The recovery time required after exposure to high light levels is dependent on the product of the duration of the exposure and its intensity. In an application such as the star scanner where at certain orientations the photomultiplier would see a pulse of light once a revolution (from the sun or planetary albedo for example), the dark current would build up to an equilibrium value over many revolutions.

The second effect is permanent damage at yet higher light levels due to "burning" the photocathode. This would almost certainly occur in a star sensor if the unit were oriented such that the sun is imaged directly on the reticle slit, although if an extremely narrow slit were employed and the vehicle spin speed was fast enough so that the dwell time was very short, complete damage might not occur in a single exposure. Such narrow slits, however, require a very high resolution optical system which is a disadvantage for stray light rejection as is shown in Section 9.

These damage mechanisms mean that if a photomultiplier tube is used as the detector in the Pioneer Venus star scanner, protection devices must be included to prevent degradation and damage. Certainly, the currents must be limited by the biasing resistors and provision must be made to reduce the power supply voltages. If the sun will ever strike the reticle slit directly, or if it is required that the unit recover quickly after being exposed to Venus albedo, or other high light levels, a shutter must be employed to shield the

photocathode from light which will increase dark current significantly or cause permanent damage.

SILICON DIODE DETECTORS

The second type of detector which may be considered for this star scanner application is the silicon diode detector. This detector has significant advantages over other solid state detectors as mentioned earlier and is the only type to be examined in detail here. The principles of operation are much different than those of the photomultiplier tube, and thus it has different physical and operational characteristics which give it a number of advantages and some disadvantages as compared to the photomultiplier.

The silicon diode is a photovoltaic device which generates a current when illuminated. The silicon solar cell is identical to the photodiode detector in principle of operation although the processing details are somewhat different. A junction is formed near the surface of a silicon wafer, usually by diffusion of an impurity at high temperature. Using photo-resist, etching, diffusion, and passivation techniques common in transistor and integrated circuit processing, many separate diode detectors may be formed at one time on a single silicon wafer, and complex configurations can be easily produced.

The silicon diode detector has a wider spectral band than the photocathode materials of interest, and extends farther into the infrared region where there are more bright stars as shown in Section 6. Also, the quantum efficiency is much higher than the photocathode materials, being typically about 70%. Here quantum efficiency is defined as the probability that a light photon will separate an electron hole pair across the diode junction, thus generating current.

One major advantage of the silicon diode detector is that it only requires low voltages. Where the photomultiplier tube requires thousands of volts bias for proper operation, and thus a high voltage power supply, the silicon detector requires only a few volts reverse bias at almost zero power. Another attractive feature is that no magnetic materials are necessary for its construction as compared to the ruggedized photomultiplier which uses a large

amount of Kovar. This could be a significant difference if magnetic cleanliness is important.

Silicon Detector Noise Sources

The sensitivity of silicon diode detectors at low light levels is determined by the dark current which has two components. When a reverse bias is applied (which is desirable to reduce the junction capacitance), leakage across the diode can occur. This is often a function of the surface passivation and defects in the junction. This can be kept small by keeping the bias low. The second component of the dark noise is due to thermal generation of carriers which is thought to be primarily due to deep level impurities in the junction region. This current will flow at zero bias, and is a strong function of temperature, falling off rapidly at lower temperatures. Recent developments have made significant improvement in the dark currents due to both these mechanisms. Significantly greater sensitivity is now possible than was obtainable a few years ago, although the best detectors must be considered as still developmental. As an example of current technology, United Detector Technology, Inc. claims, in their form 1000 data sheet, a dark current of 50 picoamps at a five volt reverse bias for their PIN-020A detector which has an area of 2×10^{-3} square centimeters. Fairchild Camera and Instrument Corporation (Reference 02) has been developing much lower dark current diode detectors for a different application, and have measured leakage currents of about 10 picoamps or less in a 10^{-2} square centimeter detector, which is an improvement in dark current per unit area of a factor of 25. The Microelectronics department of Lockheed Missiles and Space Company has been producing low dark current phototransistors using processing methods similar to those employed by Fairchild, and sample detectors have been produced which have similarly low leakage currents.

Even with the low dark currents demonstrated in this developmental technology, the silicon diode detectors are somewhat less sensitive than the photomultiplier detectors when directly compared on an equal area basis. A typical silicon diode NEP would be about 2×10^{-15} watts/ $\sqrt{H_z}$ as compared to 10^{-16} watts/ $\sqrt{H_z}$ for the photomultiplier. The silicon diode, however, because

of its compact size and low voltage requirements, can be incorporated in a star scanner in the form of an array of electrically separate detectors, each of which is of much smaller area than the photomultiplier detector, and the net effect is that the silicon diode sensor can be more sensitive. A more detailed and quantitative comparison is included later in this section.

To take full advantage of the low dark currents of the silicon diode detectors, large value load resistors must be employed so that the Johnson noise from the load resistor will not be greater than the noise due to the dark current itself. Both these noise sources are discussed later in this section. The load resistor and diode capacitance combine to limit the frequency response of the silicon diode detector. The signal and noise will both roll off at 6 db per octave from the frequency determined by the RC product, and the sensitivity will be unchanged up to the point where these noise sources become less than the amplifier noise. Thus the frequency response of the silicon detector does not compare with that of the photomultiplier, but fortunately the frequency response requirements of this application are sufficiently low so that available amplifier technology will not degrade the performance of the system.

This discussion is based on a simple "voltage mode" amplifier, while actually it may be advantageous to use a "current mode" feedback amplifier to reduce crosstalk and facilitate further signal processing, but the basic sensitivity limits are the same for either configuration.

Silicon Detectors Not Susceptible to Light Damage

One of the most important features of silicon photodiodes for this star scanner application is that they are not susceptible to damage from high light levels. They can, in fact, survive when the sun is focused directly on them in a star sensor application, and can tolerate being heated by such means to several hundred degrees centigrade without permanent damage. The dark current will increase drastically at such elevated temperatures, so that the detector will be inoperable, but then will cool quickly if properly mounted to a heat sink. This means that no protective devices need be included in a star scanner using such detectors.

When illuminated with high light levels, the current generated will cause the potential across the diode to rise to about one volt where the diode becomes forward biased and the current will flow back across the detector preventing further buildup of voltage. This voltage will saturate the following electronics, and when the light is removed, the recovery time will be determined by the RC time constant of the circuit which, depending on the circuit values, may be fast enough to provide recovery well within a revolution period, especially at the lower spin speeds. If faster recovery is required, it may be possible to sense this situation and provide a means of discharging the diode capacitance with an active device to shunt the load resistor.

NOISE MECHANISMS

In the discussions of the characteristics of the photomultiplier tube and the silicon diode detectors, several noise sources were mentioned including background noise, dark current noise, and Johnson noise. This section examines these and other noise sources which limit the sensitivity of detectors used in star scanner systems.

Shot Noise

There is a noise associated with every current which is due to the quantization of charge and the statistical fluctuations which occur as the charges flow in a circuit. Whenever a current is present, a shot noise is associated with that current no matter whether the current is a dark current, generated by background radiation, or generated by signal radiation.

Shot noise is a "white noise" in that it is uniformly distributed across the frequency spectrum, and thus the RMS noise is proportional to the square root of the electrical bandpass. The shot noise per root Hertz is given by

$$\frac{I_{NS}}{(\Delta f)^{1/2}} = \left[2e (I_D + I_B + I_S) \right]^{1/2} \quad (7-1)$$

where

- e = electronic charge
 $= 1.6 \times 10^{-19}$ coulombs/electron
- I_D = dark current
- I_B = background generated current
- I_S = signal generated current
- $I_T = I_D + I_B + I_S$ = total detector current

As mentioned earlier, the dark current due to spontaneous emission from the photocathode of a photomultiplier is usually smaller than the background radiation from the sky for typical star scanner systems, so background noise is the limiting noise source. When the signal current exceeds the background and dark currents, the total current and thus the noise increases. Since this occurs only when signal is present, it does not affect the false alarm rate, but only the detection probability.

The dark current of a silicon diode detector exceeds the background generated current for the sky background levels seen by a star scanner, so that a silicon photodiode sensor will be limited by the dark current shot noise. Only for very small detectors where the dark current is small, and for very large signals will the signal current exceed this dark current so for most operation with a silicon diode detector the sensitivity of the star scanner will be determined by the dark current noise.

Johnson Noise

Another form of noise which effects silicon diode applications is Johnson noise. This is a fundamental noise associated with resistors, and depends only on the value of the resistor and its temperature.

The Johnson noise current from a resistor is given by

$$\frac{I_{NJ}}{(\Delta f)^{1/2}} = \left[\frac{4KT}{R} \right]^{1/2} \quad (7-2)$$

where K = Boltzmann's Constant
 $= 1.38 \times 10^{-23}$ watt-sec/ $^{\circ}K$
 T = temperature ($^{\circ}K$)
 R = resistance (ohms)

Johnson noise is a white noise as is shot noise so that for a given resistance and dark current the shot noise and Johnson noise will have a constant ratio independent of frequency or electrical bandwidth. Since Johnson noise current varies inversely with resistance, it can always be made smaller than the shot noise by making the resistance large enough. For example, if the dark current is one picoampere the load resistor must be about 5×10^{10} ohms for the Johnson noise to be equal to the dark current shot noise. Because such high value load resistors are required for the highest sensitivity detectors, the frequency response of such units is limited.

"Excess" Noise

Another noise source which can enter is "excess" noise which can have several components such as "1/f" noise and "popcorn" noise. Both these noise sources occur in semiconductors but are not expected to present any practical problem in this type of star scanner application. Both these noise mechanisms are dependent on material processing during device manufacture, but with proper controls and modern techniques they are well controlled. Popcorn noise in particular, occurs infrequently and devices can easily be selected which are free of it. The 1/f noise only occurs, as its name suggests, at lower frequencies and is not expected to be of concern in the detector element itself for the frequencies of interest in this application. The amplifiers will have a 1/f noise component which extends into the operating frequency range but will be well below the other noise sources such as shot or Johnson noise.

Structured Background Noise

Another noise source is due to structured or modulated background. When we discussed background noise earlier, we assumed that the background radiation was uniformly distributed and so the background light intensity did not vary as the instrument scanned the sky. Such is obviously not the case, since as was shown in Section 6, the background is made up primarily of stars which are point sources and they are not uniformly distributed. In other words, as the instrument scans the sky, light at the detector will fluctuate as the various sources come into and out of the instrument field of view, and this fluctuation or modulation will appear as a signal. The major

effect will be caused by the individual brighter stars which may be below detection threshold but which will have the same frequency spectrum as the desired star signals. Other fluctuations due to clusters of dimmer stars will generally generate response at much lower frequencies and will not add significantly to the noise. This structured noise is significantly different in character than the white noise sources of shot noise and Johnson noise, and thus can't simply be added to these other noise sources but must be considered separately. This is discussed in Section 8.

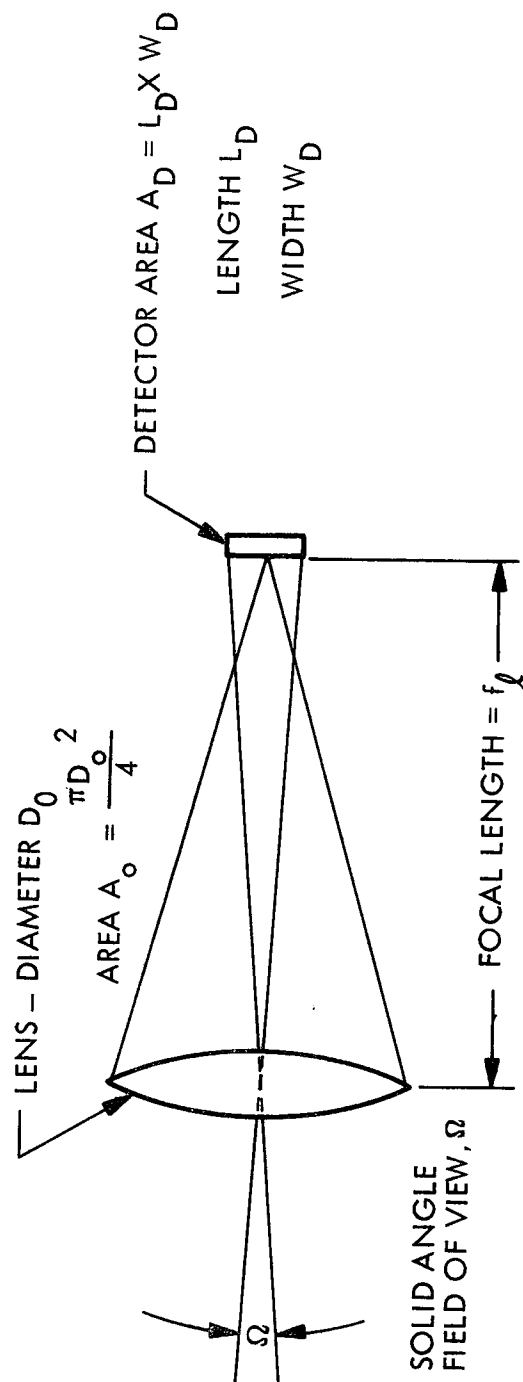
Stray Light Noise

The final noise source is stray light which can come from the sun directly or reflected from planets or spacecraft appendages, and can add to the noise in two ways. Stray light can add to the background, generating a current and thus contributing shot noise, and because the spacecraft is spinning it will be modulated and can have some frequency components in the electronic bandpass. Section 9 discusses this source of interference in more detail.

NOISE DEPENDENCE ON SENSOR PARAMETERS

It has been stated above, that the dominant RMS noise sources occurring in star scanning systems are shot noise due to background light in the case of the photomultiplier detector sensor, and from the dark current when a silicon diode detector is employed. This section will discuss the dependence of these and other noise sources on various sensor parameters such as field of view, aperture area, f/number, spin speed, and the detector dimensions of length and width.

Figure 7-1 schematically illustrates some of the basic parameters of the sensor optical system. All light striking the surface of the lens at angles within the solid angle Ω which is the detector field of view will be imaged onto the detector. The solid angle Ω is determined by the physical area of the detector and the focal length of the optical system. The optical system f/number is simply the ratio of the focal length to the diameter of the aperture, e.g. an f/2 system has a focal length twice the lens aperture diameter.



SOLID ANGLE FIELD OF VIEW

$$\Omega = \frac{A_D}{f_l^2}$$

OPTICAL SYSTEM F/NUMBER

$$F/\text{no.} = \frac{f_l}{D_o}$$

Figure 7-1 Optical System Parameters

The field of view can be thought of as having two dimensions - an angular width in the scan direction which is determined by the detector width and the focal length, and an angular length in the direction normal to the scan direction determined by the detector length and the focal length. The area of sky scanned per revolution will depend on the angular length of the detector, while the detector angular width will determine the dwell time of a signal at a given spin speed.

As shown earlier, background noise is due to the current generated in the detector by the background radiation.

$$\frac{I_{NB}}{(\Delta f)^{1/2}} = [2eI_B]^{1/2} \quad (7-3)$$

The background generated current is proportional to the background radiation collected by the lens in the field of view or

$$I_B \propto A_o \Omega \quad (7-4)$$

So that the noise will increase as $(A_o)^{1/2}$ and as $(\Omega)^{1/2}$ for a fixed background. The system f/number does not enter into this calculation.

Dark current noise, on the other hand, depends on the physical area of the detector, since the dark current is directly proportional to the area (when surface leakage is negligible).

$$\frac{I_{ND}}{(\Delta f)^{1/2}} = [2eI_o]^{1/2} \quad (7-5)$$

$$I_o \propto A_D \quad (7-6)$$

This term is independent of the optical system.

For a given field of view $\Omega = A_0/f_1$, the dark current noise density $I_{N0}/(\Delta f)^{1/2}$ will vary directly as focal length. This means then for a fixed aperture, A_0 , the dark current noise will vary directly as the optical system f/number, i.e. an f/2 system will result in twice the dark current noise as an f/1 system.

Thus background noise and dark current noise have significantly different dependences on the optical system parameters. For a fixed detector field of view Ω , background noise varies directly as the optics diameter (square root of optics area), but is independent of the focal length. In contrast, for the same field of view Ω , dark current noise varies directly as the focal length but is independent of the optics diameter. It is important then for a star scanner using silicon diode detectors to have a "fast" optical system (small f/number), but a photomultiplier system which is limited by background noise does not reduce its noise by reducing the f/number.

Both shot noise and Johnson noise are "white" noise sources, and as such, vary as the square root of the electrical bandwidth. The electrical bandwidth depends on the dwell time of the light signal which in turn depends on the detector width (angular field of view width) and the spin speed. If we assume for simplicity, that the sensor is viewing normal to the vehicle spin axis, and the spin speed is ω radians per second and the detector has a field of view in the scan direction of $\Omega_w = W_0/f_1$ radians, then the dwell time τ_d for a light spot smaller than the detector is

$$\tau_d = \frac{\Omega_w}{\omega} = \frac{W_0}{f_1 \omega} \quad (7-7)$$

The electrical bandwidth required, Δf , is given approximately by

$$\Delta f = 1/2 \tau_d \quad (7-8)$$

So
$$\Delta f = \frac{\omega}{2 \Omega_w} = \frac{f_1 \omega}{2 W_0} \quad (7-9)$$

We have shown earlier that the dark current and background current are both proportional to the total solid angle field of view of the detector, and thus the noise current per root hertz is dependent on the square root of Ω .

$$I_0, I_s \propto \Omega = A_0/(f_1)^2 = \frac{W_0 L_0}{(f_1)^2} \quad (7-10)$$

$$\frac{I_{No,B}}{(\Delta f)^{1/2}} (\Omega)^{1/2} = \frac{1}{f_1} (W_D L_D)^{1/2} \quad (7-11)$$

$$I_N \propto \frac{1}{f_1} (\cancel{W_D} L_D)^{1/2} \left(\frac{f_1 \omega}{2 \cancel{W_D}} \right)^{1/2} = \left(\frac{L_D \omega}{2 f_1} \right)^{1/2} \quad (7-12)$$

which is independent of the detector width.

This is an interesting result because it means that as the detector width is changed the electrical bandwidth changes in such a way to make the noise constant, and thus the signal to noise ratio is independent of the detector width. It is also apparent from Eq. 7-12, that the noise varies as the square root of the spin speed, so the signal to noise ratio will vary inversely as the square root of the spin speed.

If the sensor field of view is not normal to the vehicle spin axis, the situation is somewhat more complicated. The detector width must decrease to keep the dwell time constant, varying as the sine of the aspect angle (the angle between the spin axis and the sensor field of view). At the same time the area of the sky scanned per revolution decreases in the same way, so a longer slit must be used to scan the same percentage of sky. These two effects exactly compensate each other, in that as the aspect angle of the sensor field of view changes the length and width of the slit varies to scan a constant area of the sky and maintain a constant dwell time in such a way as to make the detector area a constant independent of the aspect angle. Constant detector area means a constant total field of view solid angle Ω , which means that the noise and hence the signal to noise ratio is independent of sensor aspect angle for a given scan area coverage and spin speed. This relationship breaks down, however, for small aspect angles where the detector width becomes smaller than the blur spot size.

SIGNAL TO NOISE RATIOS FOR SENSOR CONFIGURATIONS

The various noise sources which limit the sensitivity of star scanners using photomultiplier and silicon diodes have been discussed above. This section will discuss the signal to noise ratios that will result when such detectors are used in a star scanner system. To facilitate direct comparison of the two different types of detectors, a number of parameters will be fixed for the purpose of calculating signal to noise ratios for the two systems.

The dependence of the noise on these system parameters as given above will allow these results to be easily adjusted for other conditions.

The signal current generated in the detector from a given target star can be directly calculated from the current information given in Reference P2 . These currents i_s are per square centimeter of aperture area and assume 100% optical transmission. For a given sensor system with collecting optics area A_o , an optical transmission η_T , the signal current is given by

$$I_s = i_s A_o \eta_T \quad (7-13)$$

The noise is generally shot noise due to the dark current, background generated current, or signal current and for a given electrical bandwidth Δf the noise current I_n is determined from equation 7-1.

$$I_n = [2e(I_o + I_b + I_s)\Delta f]^{1/2} \quad (7-14)$$

The dark current depends on the detector area, and the background current depends on the number of equivalent background stars per steradian, the detector field of view, and the collecting area and optical transmission as in the signal case above. The signal to noise ratio at the sensor output is therefore

$$SNR = \frac{I_s}{I_n} (r) \quad (7-15)$$

where r is the filter response factor, which for this case is approximately 0.67.

Figures 7-2, 7-3, 7-4 show the signal to noise ratios which result from viewing stars with sensors of various types. For purposes of preparing these curves, the following sensor parameters are assumed.

$$A_o = 5 \text{ cm}^2 \text{ (2.54 cm. = 1 inch diameter)}$$

$$\eta_T = 0.8$$

$$\omega_s = 1.26 \text{ rad/sec (12 RPM)}$$

$$f/\text{number} = 1$$

$$r = 0.67 \text{ filter response factor}$$

Figure 7-2 shows signal to noise vs star magnitude for a photomultiplier tube sensor with an S-20 photocathode. At low signal levels, the sensor is limited by the background generated current. Two backgrounds have been assumed: 100 tenth magnitude stars per square degree which is the average background over the entire sky, and 500 tenth magnitude stars per square degree which is a value typical of bright areas of the milky way. As mentioned earlier, when background noise limited, the noise is independent of slit width, and only depends on the length of the slit. The 20 degree long slit would be typical of a two slit (V slit) sensor with an elevation field of view of 10 degrees. For brighter stars, the sensor becomes signal noise limited when the current due to the signal exceeds the background current. In this area, the noise varies inversely as the square root of the detector or slit width, and is independent of length. Several slit widths are shown in the figure.

In this signal noise limited region, the signal continues to vary linearly with light intensity, but now the noise is no longer constant. The noise varies as the square root of the signal intensity, so the signal to noise ratio is no longer linear with signal light intensity as was the case when background limited, but now varies as the square root of the signal level. In the region where the two curves cross, the noise sources will be comparable and the total noise will be the root sum of squares of the two. The net effect is to smoothly round the signal to noise curve in the transition region from the linear behavior in the background limited low signal level region to the square root dependence of the signal noise limited region. This refinement has been omitted from the figures for simplicity.

The SCADS star scanner which is currently in use on the S³* satellite employs a single slit which is 25° long and 0.3° wide. The signal to noise ratios for this slit configuration with the same sensor parameters is also shown in the figure. The actual SCADS sensor uses a slightly larger aperture and spins at a slower speed, so the signal to noise ratios are somewhat larger for the actual system.

A similar set of curves for a silicon diode sensor is presented in Figure 7-3. Dark current noise is the limiting noise source for weak signal levels, with a dark current of one picoampere in a 1° x 1/2° f.o.v. detector typical of

* Small Scientific Satellite

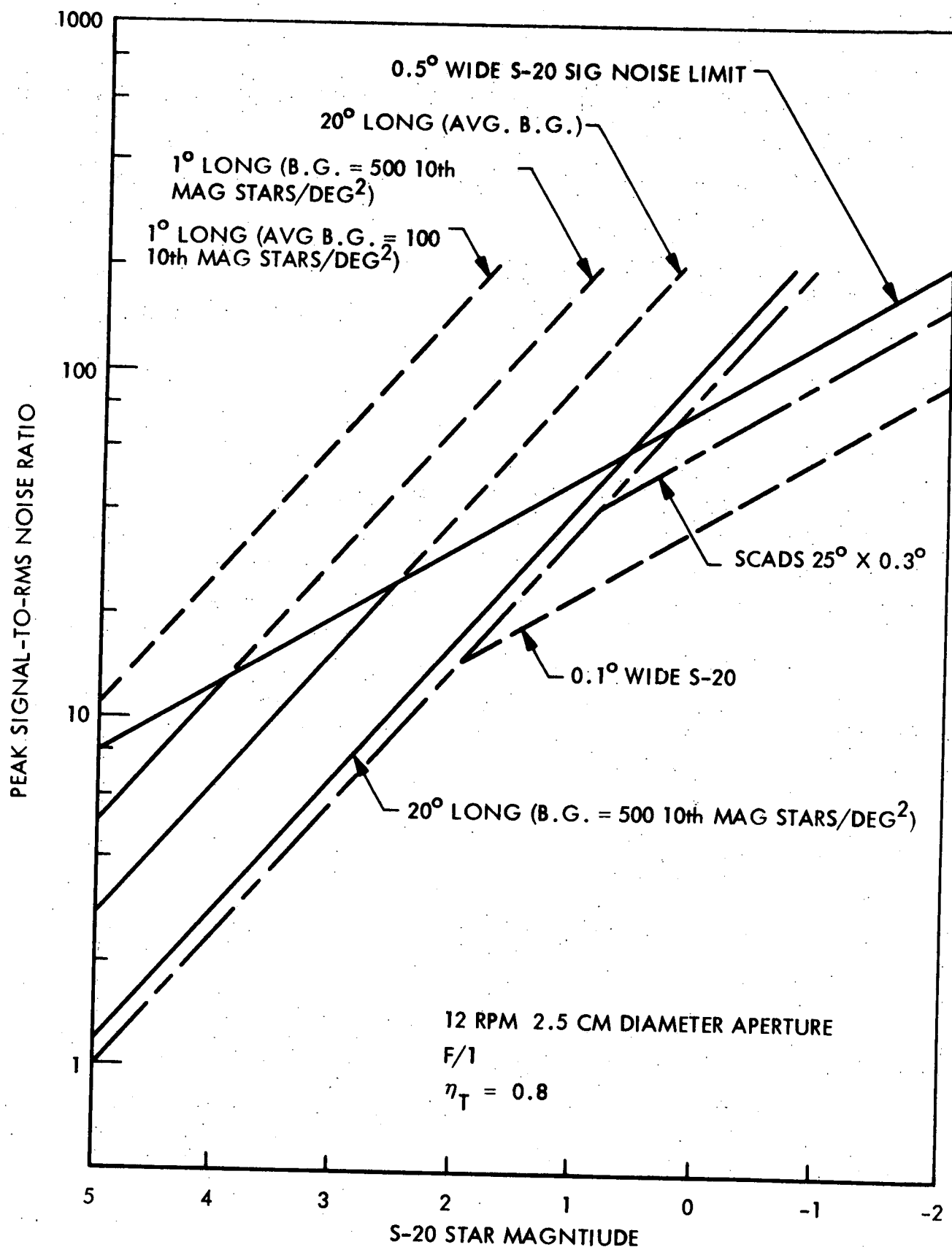


Figure 7-2 Signal-to-Noise Ratios for Star Scanner Employing Photomultiplier With S-20 Photocathode

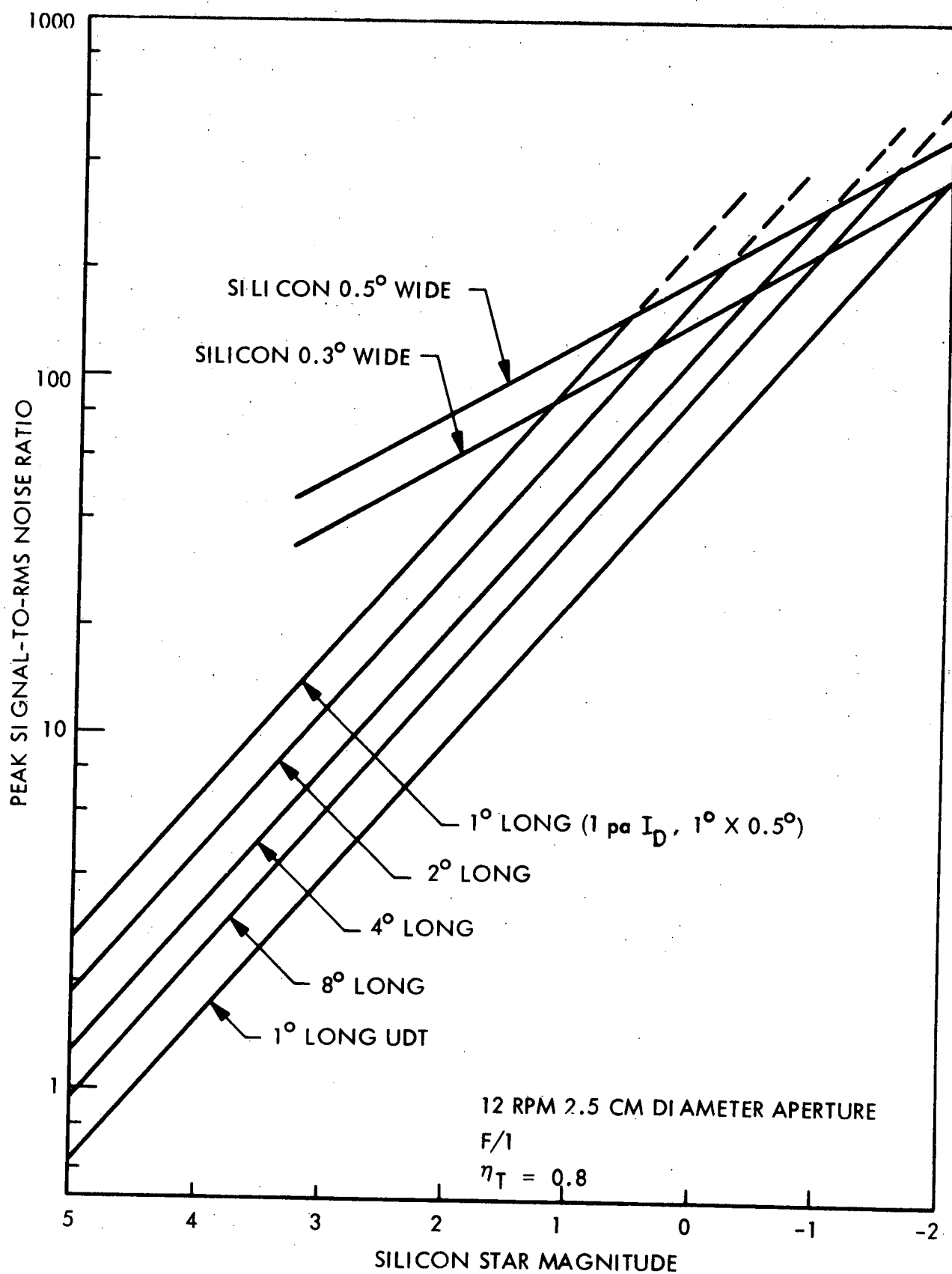


Figure 7-3 Signal-to-Noise Ratio for Star Scanner Employing Silicon Photodiode Detectors

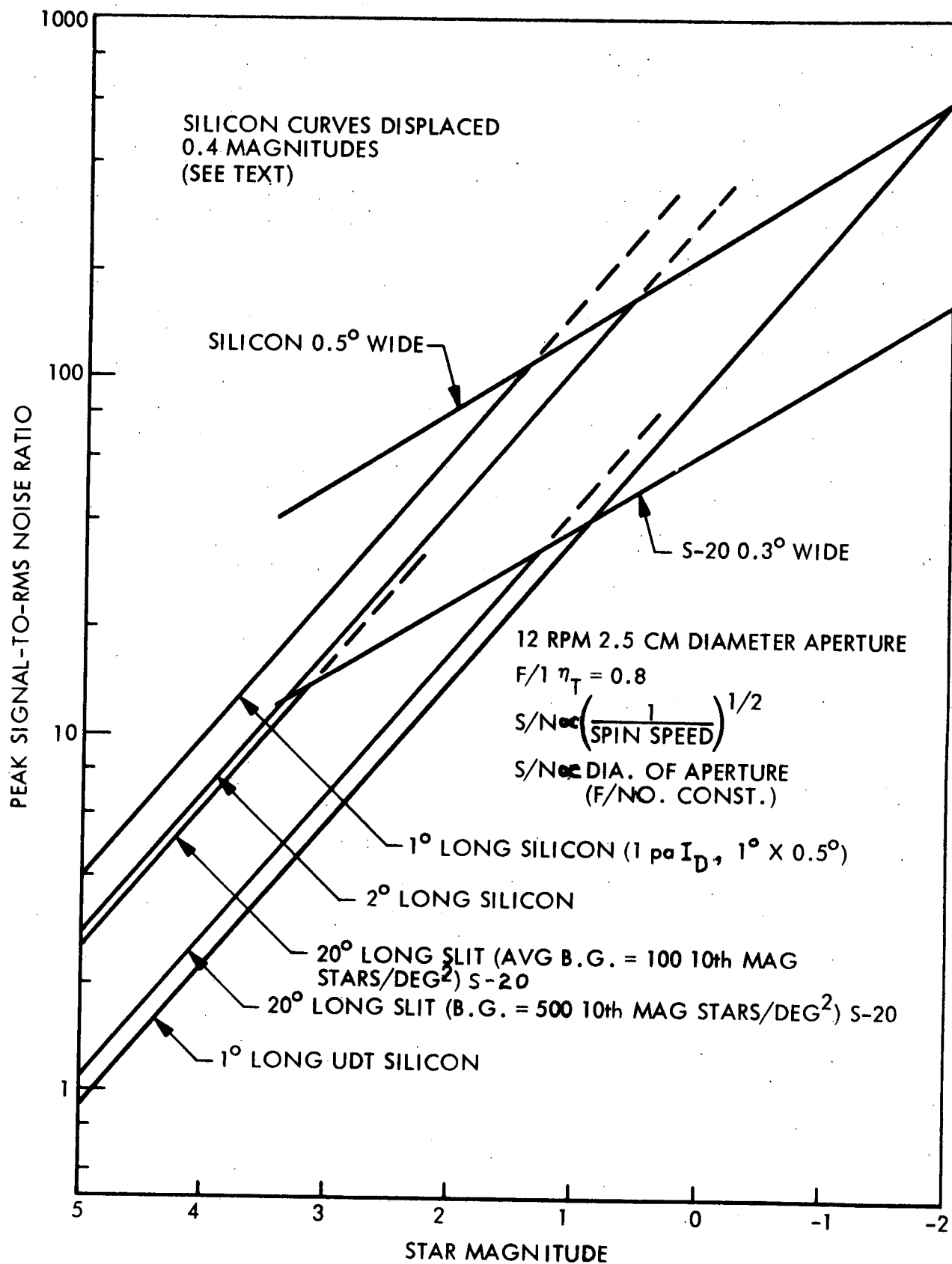


Figure 7-4 Signal-to-Noise Ratios of Silicon Detectors and Photomultiplier Tubes Used in Star Scanners

the developmental detector technology as reported by Fairchild and IMSC Microelectronics. The curve labeled UDT is the larger dark current technology commercially available from United Detector Technology, Inc. As in the photomultiplier case, the noise has the square root of area dependence so the signal to noise ratio depends on the detector length but not the width. The detector becomes signal noise limited at higher signal light intensities, just as in the photomultiplier case. Again the transition between the two regions is smoothly rounded but has been omitted from the figure.

Figure 7-4 is a similar plot of signal to noise versus light intensity showing both the silicon diode detector and the S-20 photomultiplier. The sensor parameters are the same as for the previous two sets of curves, but in order to make a more realistic comparison between the two types of detectors for this star sensor application, the silicon curves have been displaced toward lower light levels by 0.4 magnitudes. This is done because, as was shown in Section 6, the silicon detector "sees" more stars in the sky brighter than a given magnitude than an S-20 detector does. The displacement of the silicon curves allows a comparison of the two detectors on an approximately "equal number of stars" basis.

The silicon detector has a much larger signal to noise ratio than the S-20 photomultiplier tube in the large signal region where both are signal noise limited. This is due to the wider spectral bandwidth of the silicon detector, and its higher quantum efficiency. These two effects mean that many more carriers will be generated in the silicon detector for a given target star than will be released from the S-20 photocathode. For the same bandwidths (same detector widths) the signal to noise ratio will be higher in the silicon detector by the square root of the current ratio. For example, if a given star target generates 6 times more current in a silicon photodiode than it releases from an S-20 photocathode, the signal to noise ratio for the silicon diode will be $(6)^{1/2}$ larger than for the photomultiplier tube when both are signal noise limited.

SECTION 8

SIGNAL TO NOISE REQUIREMENTS

The previous section developed the relationships between signal to noise ratio and various system parameters such as optics size, f/number, detector type and field of view, spin speed, and others. This section will examine the question: What signal to noise ratio is required for proper sensor operation? To do that we must show how star positions are measured from the detector output pulses, the accuracy with which the positions can be determined as a function of signal to noise ratio, and how the average false alarm rate ($\overline{\text{FAR}}$) and the detection probability P_d also depend on signal to noise ratio and threshold level. It will be shown that the structured background, that is the background stars which are below threshold but still have a reasonable detection probability, is the source of interference which places the most severe requirement on the signal to noise ratio for this application.

MEASUREMENT OF STAR POSITION IN THE SPACECRAFT FRAME

The position of a star in the spacecraft reference frame is determined by measuring time intervals between the sun generated clock reference pulse and the detector pulses generated by star images crossing the reticle slits or detector.

An example of this is shown in Figure 8-1. The particular configuration shown is representative of a single channel V-slit sensor but the concept is similar for other multiple slit or multiple detector sensors. As the sensor rotates, it sweeps a sector that is 10° in elevation angle, in this case, at a rate determined by the spacecraft spin rate. Each rotation of the spacecraft will produce a high signal-to-noise ratio pulse accurately referenced to the sun, which serves as a clock pulse for the star scanner. The azimuth of a star in view of the star sensor will be proportional to the time interval, t_1 ;

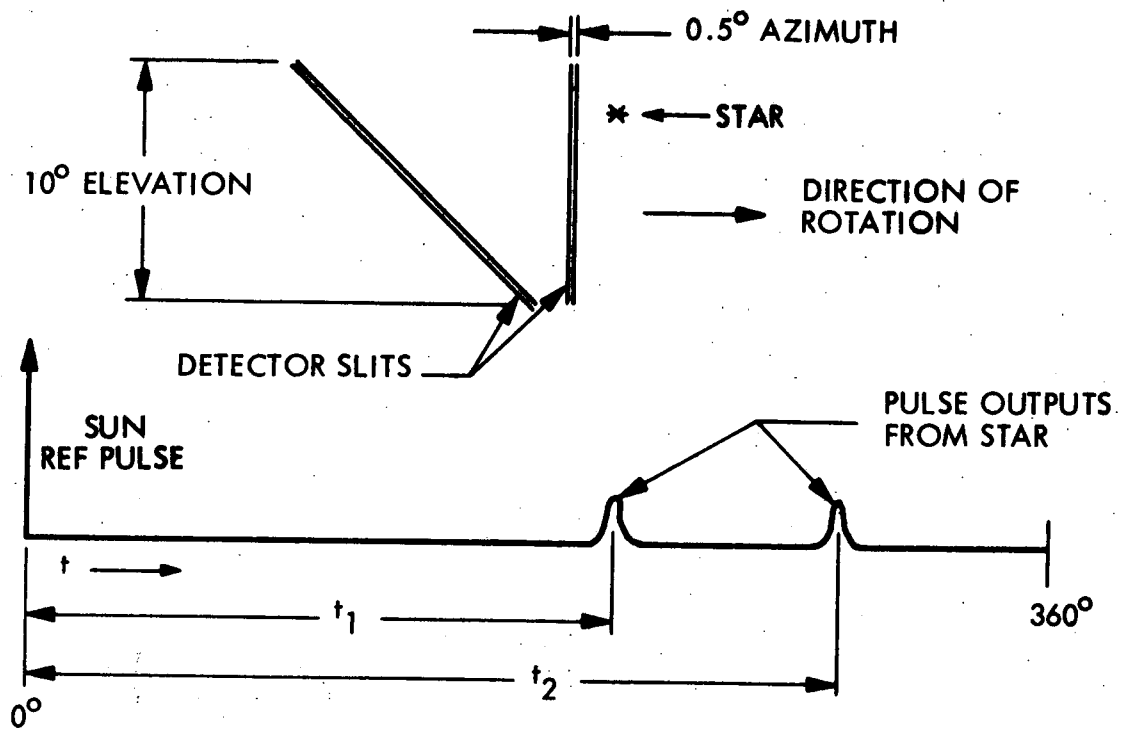


Fig. 8-1 Example of Star Position Sensing

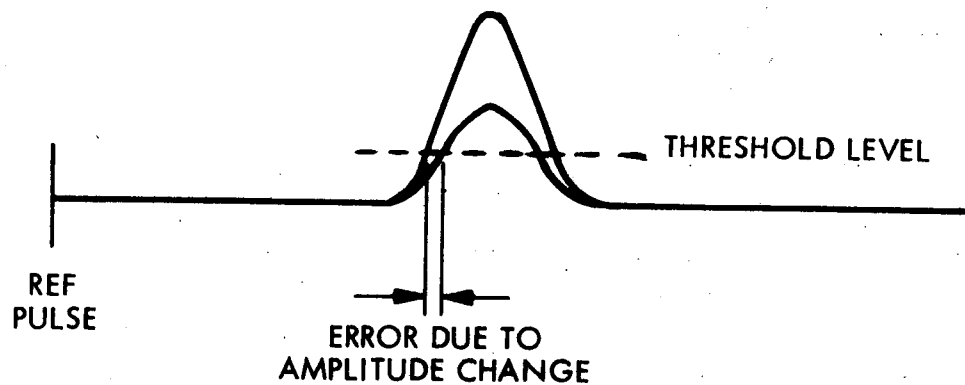


Fig. 8-2 Amplitude Error for Fixed Threshold Setting

the time between the sun reference pulse and the occurrence of the first star pulse. Time $(t_2 - t_1)$ will be a measure of the star elevation angle in the sensor field of view. Accurate position determination becomes a problem of accurate measurement of time differences.

There are several approaches to implementing time interval measurement which involve various degrees of complexity and accuracy. Perhaps the simplest is a fixed threshold crossing indication, where the interval t_1 and t_2 would be based upon the time from the reference pulse, to the time when there is a positive slope crossing of a given voltage level. This technique incurs errors in the t_1 measurement as a function of star intensity since the threshold will trigger at different times for differing input amplitudes as shown in Figure 8-2. The interval $(t_2 - t_1)$ does not have this error assuming that the same amplitude is generated at each detector or slit opening, since the threshold will trigger at the same point on each pulse resulting in a correct difference measurement. The error in the t_1 interval measurement can be overcome in at least three ways:

- (1) by making the threshold occur at a given fraction of the pulse amplitude;
- (2) by differentiating the pulse following the threshold crossing and sensing the zero crossing; or
- (3) by encoding the peak amplitude of the pulse following the threshold crossing.

A fourth, more sophisticated, technique involves performing cross-correlation following a threshold crossing and sensing the peak of the correlation, but this method is much too complicated for this application and is not considered as a serious candidate.

Encoding the peak amplitude following a threshold crossing has two distinct advantages. First, by knowing the filter response, the threshold crossing time t_1 and the peak amplitude, the time of the center of the pulse can be computed. Second, measuring the amplitude of the pulse will aid in identifying the stars, and will greatly aid in resolving ambiguities which can arise if stars are closely spaced. Because of these advantages, this technique is considered most desirable.

Errors in Time Interval Measurements

Errors from a number of sources will influence the accuracy of the interval measurement. The principal error sources are:

- (1) Input noise
- (2) Quantization (digitizing) error
- (3) Circuit drifts
- (4) Thresholding (amplitude measurement)
- (5) Baseline shift due to high pass filtering.

The quantization error can be made small enough to be insignificant and, through multiple measurements, will average the error to a negligably small value. The remaining errors except input noise will be highly dependent upon the actual design implementation. For these reasons, only the input noise error will be examined at this time.

For a measurement made on a single threshold crossing, the noise present on the leading edge is largely responsible for the error. If it is assumed that the rise time of the pulse after filtering can be approximated by

$$\tau_r = \frac{0.35}{\Delta f} \quad (\text{seconds}) \quad (8-1)$$

where τ_r = the 10-90% rise time

and Δf = 0.707 amplitude Bandwidth (Hz).

However, since

$$\Delta f = \frac{1}{2\tau_d} \quad (\text{Hz}) \quad (8-2)$$

$$\text{and } \tau_d = \frac{\alpha}{\omega}$$

where τ_d = pulse width (seconds)

α = slit or detector azimuth width (degrees)

ω = spin rate (degrees/second)

then

$$\Delta f = \frac{\omega}{2\alpha} \quad (8-3)$$

Examining Figure 8-3 it is found that the presence of noise will cause the leading edge to rise or fall relative to its mean value. By approximating the leading edge between the 10 and 90% points with a straight line, a perturbation in amplitude σ_N is seen to produce an error in time of σ_t . Since the pulse amplitude rises 80% in time τ_r ,

$$\frac{\sigma_N}{\sigma_t} = \frac{.8A}{\tau_r} \quad (8-4)$$

The value of σ_t can be related to the angular error σ_ϕ and the rotation rate by

$$\sigma_t = \frac{\sigma_\phi}{\omega} \quad (8-5)$$

Utilizing equations (8-5), (8-4), (8-3) and (8-1) it is found that

$$\sigma_\phi = .875 \frac{\sigma_N}{A} \propto \quad (8-6)$$

If σ_N is defined as the standard deviation of a gaussian noise density function, then σ_ϕ becomes the standard deviation of the angular measurement ϕ . The ratio $\frac{A}{\sigma_N}$ represents the peak signal-to-RMS noise ratio. The ex-

pression is plotted in Figure 8-4 for detector widths of 0.1° and 0.5° . This shows that for ratios of signal-to-noise 4.4 and greater, the noise components on a single measurement can be kept under 0.1° for a 0.5° slit width. If multiple measurements (i.e. data from several revolutions) of the same star can be obtained the variance (σ_N^2) can be reduced by the number of measurements, or the standard deviation will be reduced by the square root of the number of measurements.

The accuracy as plotted in Figure 8-4, is the azimuth accuracy obtainable with a single scan of a configuration such as shown in Figure 8-5 A. One slit is at right angles to the scan direction, and a second at an angle θ to the first. Because the elevation measurement is the difference ($t_2 - t_1$), the standard deviation of the difference will be $\sqrt{2}$ larger than the standard deviation of a single measurement. The error of the elevation

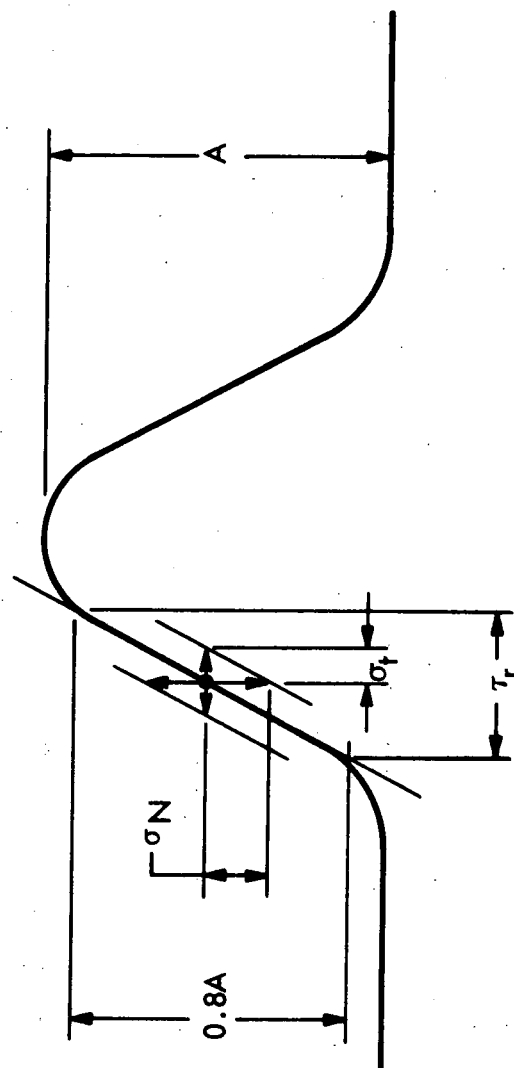


Figure 8-3 Effect of Noise on Time Interval Measurement

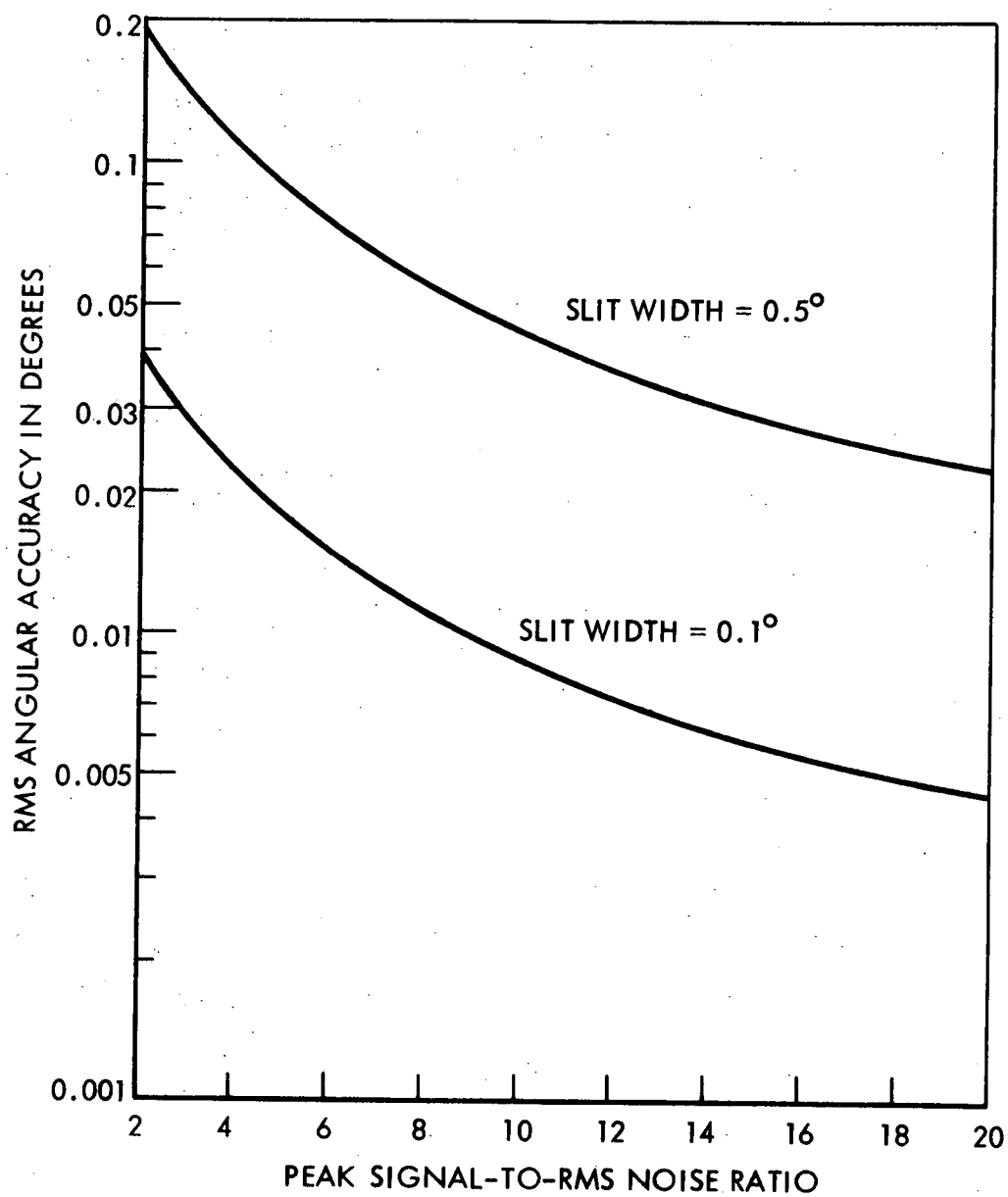


Figure 8-4 Angular Measurement Error Versus Signal-to-Noise Ratio (Single Look)

V-SILT CONFIGURATIONS

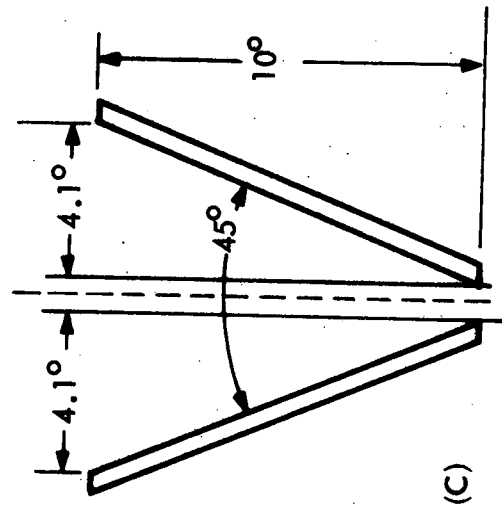
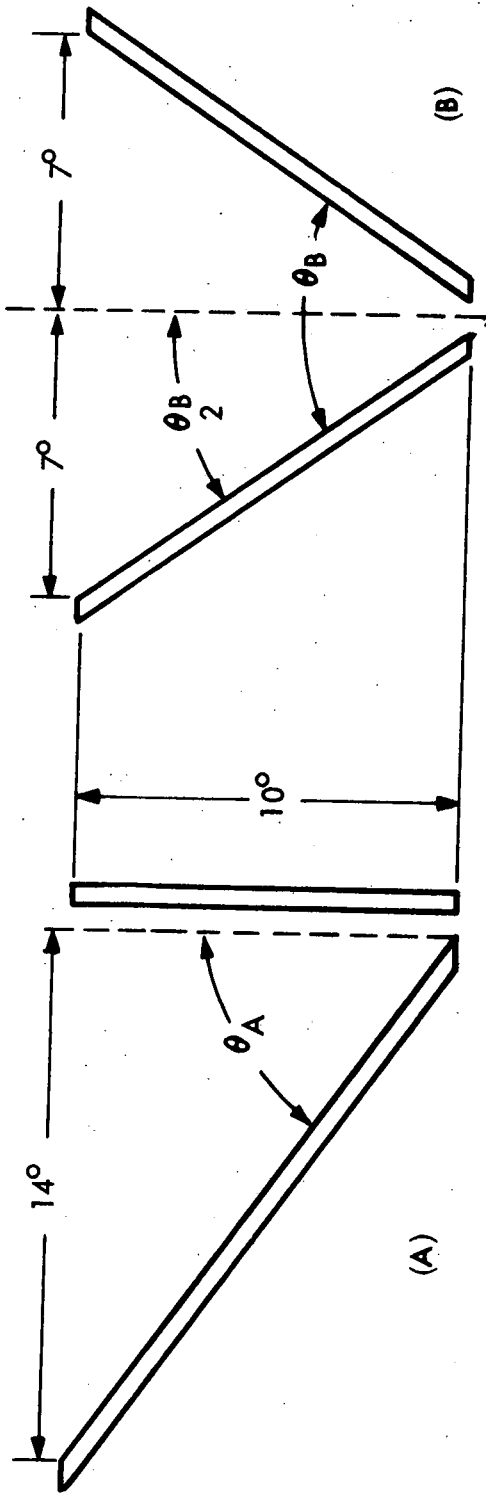


FIGURE 8-5

will then be $\sigma_a = \sqrt{2} \frac{\sigma_a}{\tan \theta}$

So for σ_a to equal σ_e , that is for the azimuth and elevation errors to be equal

$$\tan \theta = \sqrt{2} \quad \theta = 55^{\circ}44'$$

So if the elevation f.o.v. is 10° , then the angled slit must extend 14° in the azimuth direction.

The situation is somewhat different for the reticle pattern B, where now both slits are angled symmetrically about a center line. The elevation measurement is still the difference $t_2 - t_1$, and the previous considerations hold, where now

$$2 \tan \frac{\theta_B}{2} = \tan \theta_A$$

for equal elevation accuracies.

The azimuth measurement is different for pattern B, however, because it involves both slit crossings. The time that the star crosses the center line of the reticle pattern is given by

$$t_1 = \frac{t_1 + t_2}{2}$$

Just as in the difference measurement, the standard deviation of the sum is $\sqrt{2}$ larger than the standard deviation of an individual measurement. Dividing by 2, however, brings the net azimuth error for the single sweep down to $1/\sqrt{2}$ of the error present in pattern A, and the symmetrical approach is superior for this reason. We essentially gain the accuracy benefits of two separate azimuth measurements in single scan. Configuration B is better from a stray light baffling viewpoint, too, because the maximum baffle f.o.v. angle is smaller for the same azimuth dimension, i.e. one can draw a smaller circle about pattern B.

Actually, the large angles shown in both pattern A and B are larger than are desirable from a stray light viewpoint. An included angle of 45° as is shown in pattern C, where the azimuth dimension is only about 9 degrees, is much more reasonable from stray light considerations. Here we are trading off accuracy in the elevation dimension to gain a benefit in stray light rejection. This is perfectly acceptable since we have more

accuracy than required anyway. For the 45° angled slits, the elevation error is about 1.7 times the azimuth error for a single measurement, and Figure 8-4 shows us that we can obtain an elevation error of less than 0.1 degree for a signal to noise ratio of only about 8, even with the 0.5° wide slit, and the azimuth error will be smaller by the factor $1.7 \times \sqrt{2} = 2.4$.

The accuracy with which the spin axis may be determined having measured the star azimuth and elevation positions with a certain accuracy is a complicated problem which depends on the number of stars measured and their relative positions. When only one or two stars are detected, along with the sun aspect and azimuth measurements, depending on the type of sensor employed, there are cases where the accuracy is poor because the case is "near degeneracy." Such cases are very unlikely, however, and for most cases when more than the minimum number of stars are detected, the accuracy of spin axis determination is comparable to or greater than the measurement accuracy on each individual star. If the vehicle is stable (without nutation or precession), successive revolutions will allow reduction in the errors by the factor $1/\sqrt{n}$ where n is the number of revolutions.

Although the leading edge of the pulse was approximated as a straight line for the purpose of estimating the error caused by noise components, the bandpass filters that would be used in this application will not produce a straight leading edge for a rectangular pulse input. It will instead have a slope which varies with amplitude, with the maximum slope in the vicinity of one-half the peak amplitude. It is, therefore, desirable that the threshold be set near the one-half peak amplitude point. If a fixed threshold is used then it should be command adjustable so that it can be set to operate near the 50% amplitude of the bulk of the pulses. Higher amplitude pulses will cause the circuit to trigger at a lower percent of peak amplitude and a lower slope causing a greater error for the same S/N. In a given orientation if the brighter stars are seen often enough, the threshold could be commanded to a higher level which increases the accuracy. Alternately, additional complexity could be included to provide a circuit that would always make the measurement at the same percentage amplitude point or to sense the peak of the pulse.

FALSE ALARM CONSIDERATIONS

The presence of noise in a system implies that at some time a mistake may be made in assuming a signal was present when in fact it was due to a random noise fluctuation. In a device which produces an output each time the voltage rises above a given value, it is important to know approximately how often an output will be caused by noise instead of signal. This is a common problem and has been solved and documented. One convenient source can be found in the Electro-Optics Handbook published by RCA (reference B 2) since it is applied to this exact case. The assumptions for the calculations are that the noise into the detector can be classified as white gaussian noise, and that a matched filter is used for signal detection. Both of these assumptions are reasonable for this particular case, where the noise is shot noise due either to background generated current or dark current. The average false alarm rate ($\overline{\text{FAR}}$) is given by the expression:

$$\overline{\text{FAR}} = \frac{1}{2\sqrt{3} \tau_d} \exp(-I_t^2/2I_n^2) \quad (8-7)$$

where

τ_d = pulse width

I_t = threshold level

I_n = RMS value of the input noise

or

$$\frac{I_t}{I_n} = \sqrt{-2 \ln(2\sqrt{3} \tau (\overline{\text{FAR}}))} \quad (8-8)$$

Since,

$$\tau_d = \frac{\alpha}{\omega}$$

$$\overline{\text{FAR}} = \frac{x}{T_s}$$

where x = number of false alarms/spin period

T_s = spin period.

$$\tau(\overline{\text{FAR}}) = \frac{x\alpha}{360^\circ} \quad (8-9)$$

Equation (8-8) can be solved in terms of spacecraft revolutions per false alarm for a given detector or slit width. This is shown plotted in Figure 8-6 for detector widths of 0.1° and 0.5° . The figure shows that the false alarm rate drops very rapidly as the threshold level is raised. If a detector width of 0.5° is used, only 1 false alarm will occur in 10 revolutions at a threshold to noise ratio of 3.9.

If inclined detectors or reticle slits are used, an additional qualification can be placed upon the data to reduce the false data output, namely, to process only those pulses which are followed by a second pulse within the required time interval. An estimate of the probability of getting a false alarm within a given period knowing the average false alarm rate may be calculated. Using the Poisson probability density function, the probability of K false alarms in interval (b-a) is:

$$P[K / (b-a)] = \frac{e^{-\lambda(b-a)} [\lambda(b-a)]^K}{K!} \quad (8-10)$$

where λ = average number of false alarms/time interval

(b-a) = interval of time

Let $\lambda = \frac{1 \text{ false alarm}}{\text{rev.}}$

$$(b-a) = \frac{10^\circ}{360^\circ} \text{ rev.}$$

$$\lambda(b-a) = \frac{1}{36}$$

The probability of 1 false alarm in interval (b-a) will be:

$$P(1/36) = \frac{e^{-1/36} (1/36)^1}{1} = .027$$

Therefore with an average false alarm rate of 1/rev, 1000 false alarms will be the expected number of false alarms in 1000 revs and on approximately 27 occasions the false alarm will be followed by a second false alarm within the qualifying time interval. If the false alarm rate is 1/10 revs, then

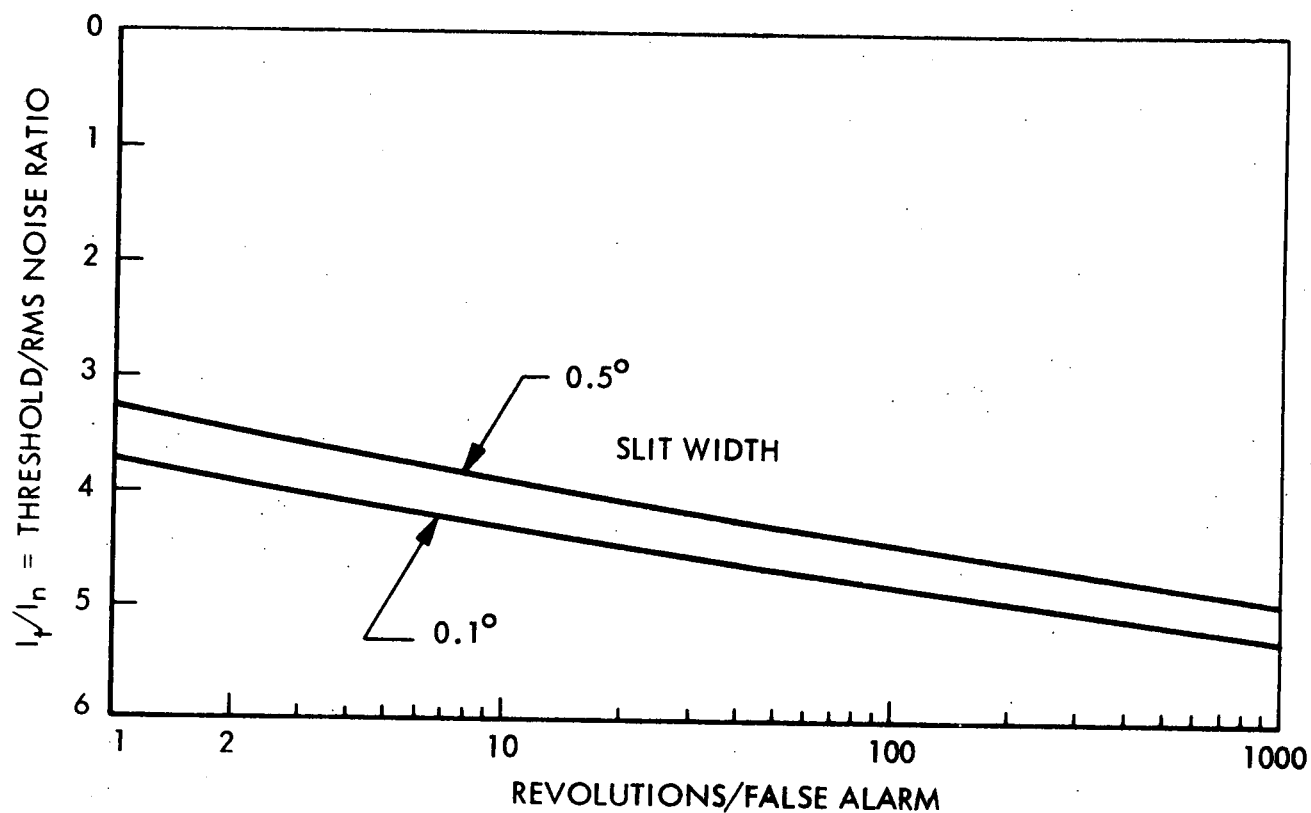


Fig. 8-6 Threshold/RMS Noise Ratio vs. False Alarm Rate

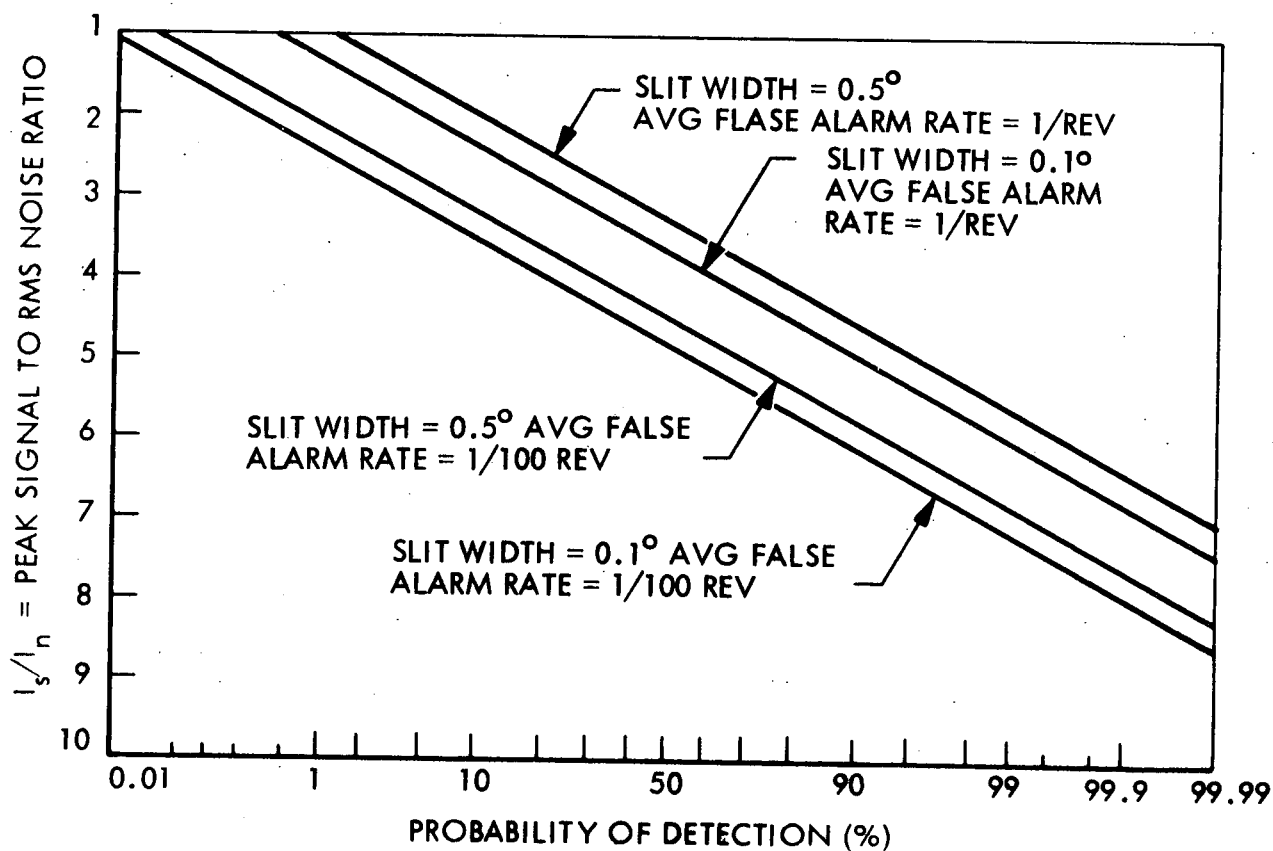


Fig. 8-7 Signal/Noise vs. Probability of Detection

the probability of a false alarm in any 10^0 interval will be reduced to 2.77×10^{-3} .

The circuitry required to do this time discrimination so as to only transmit pulses which fall in pairs within the allowed time intervals adds complexity and increases costs while it degrades reliability. A tradeoff must be made between these complexity, cost, and reliability considerations and the benefits to be gained by reducing telemetry requirements.

Probability of Detection

Although it is desirable to minimize false alarms, it is equally desirable to have a high probability of detection when a pulse does occur. The probability of detection can be expressed as

$$P_d = \frac{1}{2} \left[1 + \operatorname{erf} \left(\frac{I_s - I_t}{\sqrt{2} I_n} \right) \right] \quad (8-11)$$

where I_s = peak signal level after passing the band pass filter.

The above expression can be put in terms of average false alarms/rev. and plotted as shown in Figure 8-7. The curves show that for a slit width of 0.5° and $(\overline{\text{FAR}})$ of one per revolution, a 90% probability of detection will be obtained at a peak signal-to-RMS noise ratio of 4.6. For 1 false alarm per 100 revolutions, the signal-to-noise must be about 5.8; an increase of only 26%.

INTERFERENCE DUE TO STRUCTURED BACKGROUND

The false alarm rates we have just calculated are due to random noise fluctuations exceeding threshold, and, as we have seen, a threshold to noise ratio of about 5, and a signal to noise ratio of 6 or 7 is sufficient to provide very high probability of detection and a very low false alarm rate. These calculations have neglected interference due to structured background.

The background is not the uniform diffuse extended source we have assumed when we calculated background current and shot noise, but instead consists mostly of stars which are discrete point sources of varying intensity in a non-random distribution. As the sensor scans the sky, the light striking the detector will fluctuate as the various stars come in and out of the sensor field of view. Most troublesome from a noise standpoint, are the comparatively bright stars which are below threshold level, but because of the random noise they have a reasonable probability of detection. The probability of detection can be calculated from Equation 8-11 given earlier as

$$P_d = \frac{1}{2} \left[1 + \operatorname{erf} \left(\frac{I_s - I_t}{\sqrt{2} I_n} \right) \right] \quad (8-11)$$

For a fixed threshold and noise, the probability of detection may be calculated as a function of star intensity. If we choose a nominal detection probability we wish to use as minimum, say 0.9, then for any given signal to noise ratio for the limiting magnitude star where $P_d = 0.9$, the probability of detection for brighter or dimmer stars depends on the magnitude difference ΔM . Such a curve is shown in Figure 8-8, where the signal to noise ratio refers to a star at the limiting magnitude which has $P_d = 0.9$. For a low signal to noise ratio of 5, it can be seen from the curve that a star a full magnitude dimmer than the limiting magnitude star with $P_d = 0.9$ will still have a 4% probability of detection. The curve steepens rapidly for larger signal to noise ratios and begins to approach the ideal situation which is a perfect step function where stars brighter than a cutoff have 100% probability of detection, and stars below the cutoff never are detected.

For a typical sensor configuration, the average number of pulses from the stars below the limiting magnitude can be calculated from the curves of Figure 8-8, and the star population versus intensity relations presented in Section 6. Assuming a sensor which scans 6% of the sky per revolution (10° elevation f.o.v. centered at 45° aspect angle), the average number of pulses per revolution from stars dimmer than certain limiting magnitudes is shown in Figure 8-9. If we place the limiting magnitude at 3.0, for example,

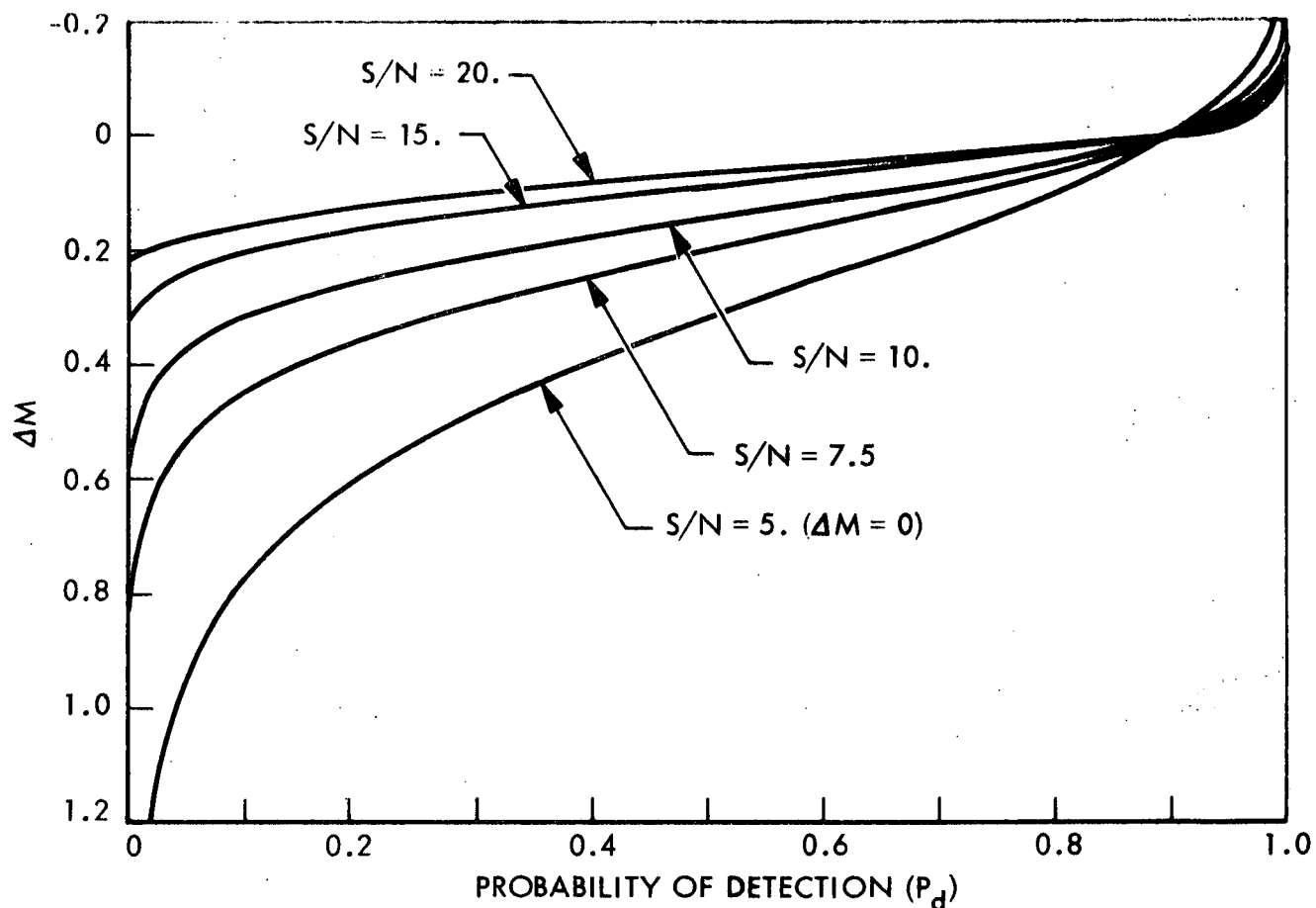


Fig. 8-8 Probability of Detecting Stars Below Limiting Magnitude

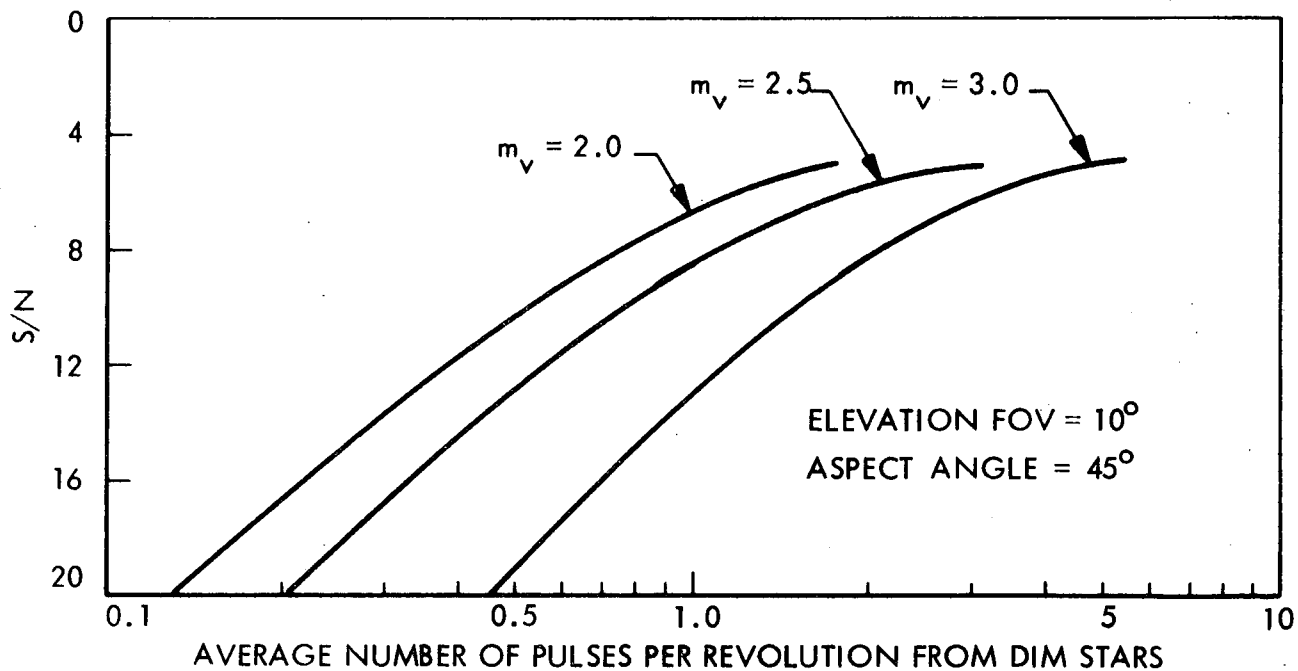


Fig. 8-9 Average Number of Pulses from Stars Dimmer than Limiting Magnitude for Typical Sensor Configuration

and we desire an average of one pulse per revolution from dimmer stars, then the signal to noise ratio must be at least 13 for the third magnitude star. The situation is much better if we can set the limiting magnitude at a brighter level, say magnitude 2.5 or 2. This is because as the limiting magnitude is reduced, the number of stars in a given interval ΔM above the limiting magnitude also decreases. It is apparent from the figure that if we require a limiting magnitude larger than two (which we do for the worst case conditions), then this structured background noise imposes a more severe requirement on the signal to noise ratio than the false alarm rate due to random noise.

PRECEDING PAGE BLANK NOT FILMED

SECTION 9

STRAY LIGHT - SOURCES, SYMPTOMS, AND CURES

Previous sections have discussed several sources of system noise which limit sensitivity and interfere with the proper operation of star scanners. Stray light is a source of interference that differs in many ways from the other noise sources, and has proven to be a problem in many star sensor systems. Rejection of stray light is a major design problem, and because of its importance, this entire section is devoted to it.

Many aspects of the stray light problem are covered in this section, beginning with the sources of stray light, the mechanisms by which it interferes with proper sensor operation, and the total stray light rejection required in the sensor. Rejection of stray light is accomplished by a combination of the baffle, the optical system, the configuration of the focal plane, and the information processing performed on the detector signals. Important parameters associated with each of these components are presented, along with the principles and criteria important for sensor design. Baffle design is a complex problem, and a number of designs have been developed or proposed by various groups in the past for similar applications. The study team reviewed a number of potential designs, have selected one as being most promising for this application, and have developed a set of parameter curves for this particular design.

The stray light rejection problem is so complex that accurate calculation for real baffles and optical systems is extremely difficult. The only way to have confidence in the overall rejection capability of the sensor system is to measure the rejection on the actual system or components of it. Unfortunately, current measurement techniques are not adequate to measure the large rejections required, and we recommend two techniques which can be developed into measurement systems with sufficient capability to measure the rejections required for this star scanner application.

SOURCES OF STRAY LIGHT

All stray light comes from the sun, either directly, or after reflection from objects such as planets, the moon, or spacecraft appendages. The sun itself is the most intense of all the stray light sources; on the stellar magnitude scale it is a source of approximately -26.8 visual magnitude, which is nearly 10^{12} brighter than a third magnitude star, about the dimmest star the sensor must detect. At Venus, the intensity of the sun is about double what it is at the earth.

Sunlight reflected from planets or spacecraft appendages can vary widely in total brightness depending on the geometrical factors involved, but will always be less intense than light from the sun directly. The sun, however, is a small area source which subtends an angle of only about 30 minutes at the earth, while a planet can subtend a very large angle, approaching a full hemisphere, when the spacecraft is close to the planet. The large subtended angle can make baffling for planetary albedo nearly as difficult as baffling for the sun, and in some cases can restrict operation over a larger total solid angle.

Reflection from spacecraft appendages is generally a lesser problem than direct sun illumination or planetary albedo, because we have control over the placement of the sensor and the appendages. The best arrangement is to position the sensor such that all structure is behind the plane which defines the baffle opening; then there is no way for light reflected from the spacecraft to enter the baffle except by diffraction at the edge. Actually, as long as all structure is placed outside the sun rejection angle of the baffle, there should be no problem. The baffle should have a sun rejection angle of 35 degrees or so, and it should not be difficult to place the sensor or the spacecraft such that this requirement is met. If possible, the surfaces which can reflect light into the baffle interior should be diffuse reflectors (to eliminate specular flashes of light) and have low reflectivity.

Another class of reflectors which must be treated differently is particles which may "float" near the spacecraft. These could be particles resulting from thruster firing, or coming from the surfaces of the spacecraft, perhaps knocked off by micrometeorite impacts, or from other sources. When these

particles are illuminated by the sun (as they will be except when they are in the shadow of the vehicle) they will appear to a sensor viewing them as a point source of light. Such particles may be distinguished from true stars by their motion when viewed on successive revolutions, by their intensity if it is significantly higher than star targets, and by their failure to fit into the pattern of the other stars viewed.

STRAY LIGHT REJECTION REQUIRED

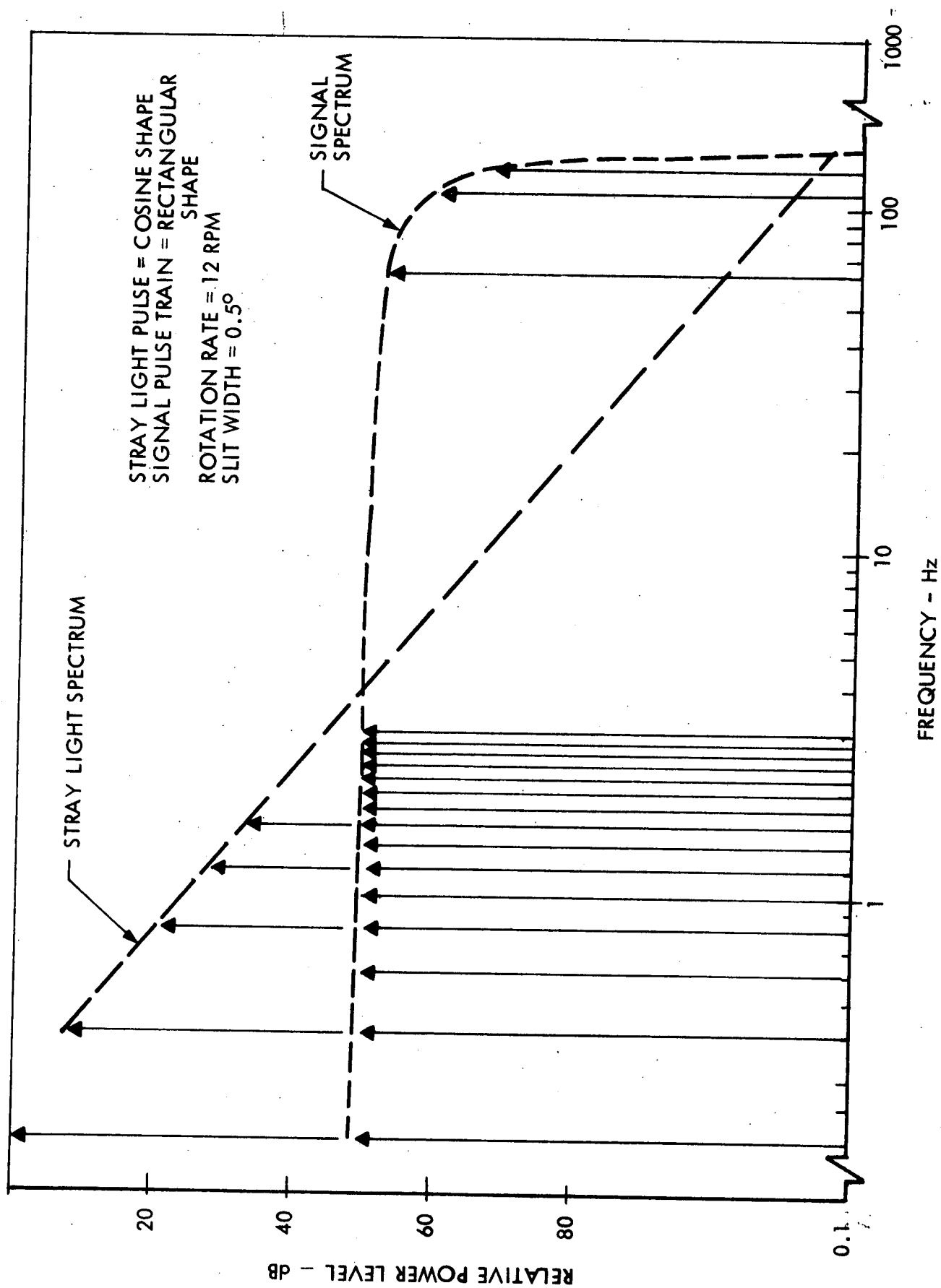
Stray light can interfere with proper operation of the star scanner in basically two ways; it can increase the random noise, and it can appear as a signal. The random noise is shot noise due to the current generated in the detector. If the total current is increased significantly above existing currents such as background generated current or dark current, the total noise increases and the sensor is degraded. Thus the baffle and optical system must keep the light intensity at the detector focal plane low enough so that the current generated by the light is less than these other currents.

The second mechanism by which stray light can interfere with sensor operation is by generating spurious signals. Since the vehicle and sensor are spinning, the angles between the stray light source and the sensor are constantly changing with time, so the light at the focal plane and thus the detector current will be modulated by this motion. The waveform of this modulation depends on the source geometry, and the detailed characteristics of the baffle and optical system, but with a small area source (such as the sun) and some simplifying assumptions about the sensor baffle characteristics, the light at the focal plane will vary approximately as a half wave rectified cosine wave. The intensity will be a maximum when the sensor is oriented closest to the sun, and will fall to zero with a rotation of 90 degrees. It will remain zero for the next half revolution, then rise to maximum during the last 90 degrees of the revolution. The assumptions for this calculation are that the baffle opening is circular, and that a constant fraction of the light striking the interior baffle surfaces reaches the focal plane. A real baffle will undoubtedly have a more complex stray light waveform, but the cosine pulse is probably a reasonable approximation.

Figure 9 - 1 shows the power spectrum of a cosine stray light pulse and for comparison a signal pulse of equal amplitude from a 0.5 degree wide detector. The spin speed is 12 RPM. Power is plotted on a relative decibel scale with zero taken as the level of the fundamental component of the stray light pulse which occurs at the spin frequency of 0.2 Hertz. For equal peak amplitudes, the stray light pulse contains more power because the duration is larger, and its frequency spectrum is larger at low frequencies. The stray light spectrum decreases at higher frequencies and falls below the power spectrum of the signal pulse at about 4 Hertz. A larger amplitude stray light pulse dominates to higher frequencies, of course. Thus, to eliminate the interfering stray light pulse, high pass filtering must be employed with the cutoff frequency dependent upon the relative amplitudes of the signal and stray light. It is desirable to utilize a filter with a cutoff rate exceeding the 40 db/decade fall-off rate of the straylight; hence at least a 3 pole design should be considered.

Because high pass filtering eliminates some signal energy as well as noise or interference energy, a method of stray light elimination other than by filtering might be considered, namely cancellation. Implementation of this requires knowledge of the amplitude, waveform, and time of occurrence of the stray light pulse and then subtracting this wave from the total signal. This is difficult to accomplish even if the stray light signal does not vary, but in this case it will surely vary with sun aspect angle, and other sources such as planetary albedo will enter, so it becomes much too complicated an approach for this application.

Stray light reaching the sensor focal plane will generally be more or less uniformly distributed over the sensitive detector area, due to the nature of the scattering and reflection mechanisms involved in the process. This means that the currents generated by the stray light will be proportional to the detector area. A solid state sensor which employs a number of detectors to make up the full field of view, enjoys a distinct advantage due to reduced detector area over a single channel sensor such as one employing a photomultiplier tube. A second advantage of the solid state array is that a stray light signal will affect all channels at once and thus



FREQUENCY SPECTRUM OF SIGNAL PULSE AND STRAY LIGHT PULSE OF EQUAL AMPLITUDE
 FIGURE 9-1

can more easily be distinguished from a true star crossing which will affect only one detector at a time.

The total stray light rejection required will thus depend on the details of sensor construction, since it depends on the existing noise sources (background or dark noise) and the sensitive areas of the detectors. Anticipating the preliminary sensor designs, we will assume, for purposes of calculating the stray light rejection required, two different sensors. One employs an S-20 photomultiplier detector and a reticle pattern consisting of two slits, each 10 degrees in elevation and 0.3 degrees wide. The optical system is $f/2$ with a five centimeter diameter aperture. The second sensor employs an array of eight silicon diode detectors, each 2.5 degrees x 0.5 degrees, with a 3.2 centimeter, $f/1$ optical system.

Rejection can be defined in a number of ways, and we have adopted two definitions useful for this application which will be referred to as definitions (A) and (B).

(A) Rejection (A) is the ratio of the light striking the detector when the stray light source is in the sensor field of view (imaged on the detector), to the light striking the detector when the stray light source is at a given angle or position outside the sensor field of view.

(B) Rejection (B) is the ratio of the light intensity from an out-of-field source which strikes the sensor and baffle, to the light intensity on the sensor focal plane.

Definition (A) is only applicable to the entire sensor, and depends in detail on the detector or reticle configuration and, because the source is imaged, depends on the geometry of the source. Definition (B) can be extended to components of the sensor, such as the baffle itself, by substituting the light intensity at the output of the component in place of the intensity at the focal plane. Under both definitions, the rejection required depends on the currents produced in the detector. Rejection must be such that currents from stray light do not exceed the total detector

current in the absence of stray light. The sun is the brightest source of stray light so we will calculate the rejection required for this source. Since we are interested mainly in currents produced in the detector it is convenient to calculate the sensor response to a known star of the same spectral class as the sun, and then make appropriate intensity conversion. The star α Centaurus is such a star, being of class G2V, just as the sun, and having a visual magnitude m_v of -0.28. The sun has a visual magnitude of -26.8, so the intensity difference is $10^{0.4(26.8 - 0.28)} = 10^{10.6} = 4 \times 10^{10}$. Reference P2 lists the response of the silicon detector and S-20 photocathodes to α Centaurus as 0.758×10^{-12} amps/cm² and 0.709×10^{-13} amps/cm² respectively. These values are for no atmospheric attenuation, 100% telescope transmission, and are per square centimeter of telescope aperture. Similar values for the sun (if the detectors were linear) would be larger by the factor 4×10^{10} . Based on these values, we can now calculate the required off axis rejection required for the sensors for both definitions (A) and (B).

STRAY LIGHT REJECTION REQUIRED FOR THE PHOTOMULTIPLIER SENSOR

The photomultiplier sensor is limited by background radiation which, on the average, is equivalent to 100 tenth magnitude stars per square degree. The area of the reticle slit is $2 \times 0.3^\circ \times 10^\circ = 6$ square degrees, so the total background on the detector is equivalent to 600 tenth magnitude stars. The response of the S-20 detector to a zero magnitude A0 star is 0.827×10^{-13} amps/cm². The background and sun radiation enter through the same optical system, so the aperture size and optical transmission do not affect the ratio.

Rejection (Definition A)

The reticle slit is narrower than the sun's image, so only about 80% of the sun's light will fall on the detector when the sun is imaged on it.

$$R_A(P.M.) = \frac{\text{current from sun}}{\text{current from 600 tenth mag stars}}$$

$$= \frac{(4 \times 10^{10})(0.709 \times 10^{-13} \text{ amps/cm}^2)(0.8)}{(600)(10^{-4})(0.827 \times 10^{-13} \text{ amps/cm}^2)}$$

$R_A(P.M.) = 4.57 \times 10^{11}$

Rejection (Definition B)

The situation is different for definition (B), since we must calculate the light per unit area, and hence current per unit area. The optical system is $f/2$. The background current per detector area can be calculated as follows:

$$\frac{I}{A_D} = \frac{(I/A_o) A_o}{A_D}$$

where $A_o = \pi/4 D_o^2$

and $A_D = (f_1)^2 \Omega$ where Ω is the solid angle detector field of view

$$= \frac{(I/A_o) \pi/4 D_o^2}{\Omega (f_1)^2} = \frac{\pi (I/A_o)}{4\Omega (f/no)^2}$$

The solid angle in this case is 6 square degrees
 $= 1.836 \times 10^{-3}$ steradian

So the rejection required (definition B) is

$$R_B(P.M.) = \frac{\text{current from sun/collector area}}{\text{background current/detector area}}$$

$$= \frac{(4 \times 10^{10}) 10.709 \times 10^{-13} \text{ amps/cm}^2}{\frac{\pi(600 \times 10^{-4})(0.827 \times 10^{-13} \text{ amps/cm}^2)}{4 (1.836 \times 10^{-3})(2)^2}}$$

$R_B(P.M.) = 5.34 \times 10^9$

Note that this definition results in a required rejection nearly two orders of magnitude smaller than that required using definition (A).

STRAY LIGHT REJECTION REQUIRED FOR THE SILICON DIODE DETECTOR SENSOR

The sensor employing silicon diode detectors is not limited by background radiation as is the photomultiplier detector, but is limited rather by the dark current of the detector. For the f/1, 3.2 cm diameter optical system, the 2.5 degree by 0.5 degree detector will have a dark current of about 4 picoamperes. This dark current is typical of the low dark current detectors as developed by Fairchild and Lockheed Microelectronics. Again we calculate the currents generated by the sun by correcting the α Centaurus values by 4×10^{10} .

Rejection (Definition A)

$$\begin{aligned} R_A(\text{Si}) &= \frac{\text{current from sun}}{\text{dark current}} \\ &= \frac{n + A_o (4 \times 10^{10}) (I/A_o) \propto \text{Cent.}}{I_D} \\ &= \frac{(0.8)(8)(4 \times 10^{10})(0.785 \times 10^{-12} \text{ amps/cm}^2)}{4 \times 10^{-12}} \end{aligned}$$

$$R_A(\text{Si}) = 4.85 \times 10^{10}$$

The rejection required by definition A, for the silicon sensor is just about a factor of 10 less than that required by the photomultiplier sensor.

Rejection (Definition B)

As in the photomultiplier sensor, we are interested in the currents per unit area. The detector area is

$$A_D = (f_1)^2 \Omega$$

where f_1 = focal length = 3.2 cm

and Ω = solid angle f.o.v of detector = 2.5×0.5 square degrees = 3.82×10^{-4} steradians

The rejection required is:

$$\begin{aligned} R_B(\text{Si}) &= \frac{\text{sun generated current/collector area}}{\text{dark current/detector area}} \\ &= \frac{(4 \times 10^{10}) (0.758 \times 10^{-12} \text{ amps/cm}^2)}{4 \times 10^{-12} \text{ amps}/(3.2 \text{ cm})^2 \times 3.83 \times 10^{-4} \text{ ster.}} \end{aligned}$$

$$R_B(\text{Si}) = 2.97 \times 10^7$$

Using definition (B), the off axis rejection required by the silicon sensor is less than that required by the photomultiplier sensor by a factor of about 180. The two systems differed by less than a factor of ten when compared using definition (A). We now must examine the question: Why is there this difference and which comparison is most valid?

The difference between the definitions are somewhat subtle and center about the way the noise sources scale with detector area and the effects of imaging of the sun under definition (A). Because we image the sun in definition (A), as long as the detector is larger than the sun image, the numerator of the ratio is constant. The denominator, for both sensor cases, increases as the detector field of view increases, so this definition leads to a smaller rejection for a larger detector. This occurs because the stray light contribution must be less than the existing noise sources, and these noise sources increase with area. This definition is somewhat unrealistic, however, since for a given sensor baffle, optical system, and sun position, the stray light will be distributed over the focal plane, so the contribution of the noise source will scale with area in the same way as the other noise sources. If the two sensors are compared on an equal field of view basis, we must correct by the ratio of the field of view = $6^\circ/1.25^\circ = 4.8$, resulting in the silicon sensor requiring less rejection by a factor of 45.

Definition (B) is more realistic in the sense that it recognizes that the stray light is diffusely distributed in the focal plane and thus the detector area does not influence the required rejection. The f/number does enter this calculation however, and if we compare the two systems on the basis of equal f/number, we again find the silicon detector sensor requires less rejection by a factor of 45. Thus we have excellent agreement between the two rejection definitions, if we are careful to make our comparison on the basis of equal sensor fields of view (definition A) or equal optical f/numbers (definition B).

We conclude that definition (B) offers the most direct comparison of the required stray light rejection, primarily because definition (A) results in the unrealistic situation that the larger the detector the less stray light rejection is required. Two points are clear in any case. First, the

silicon detector sensor is significantly superior as far as its susceptibility to stray light, and second, one must carefully state the definition of stray light rejection since the required values can vary widely depending on definition.

BAFFLE PRINCIPLES

The baffle is the first, and in some respects the most important, of the sensor components which reject off-axis radiation. In this application, the baffle will be called upon to perform the lion's share of the job. Its function can be stated simply: Keep off axis radiation from entering the sensor optical system.

The baffle relies on geometric shielding, so it is impossible to prevent light sources at very small angles from the field of view from illuminating at least part of the optical system. The optical system itself must reject such light. The function of the baffle is rather to shield the optical system from bright sources at larger angles outside the field of view. In this application, a reasonable requirement might be to reject sunlight at angles exceeding 30 or 35 degrees from the center of the field of view.

If perfectly black surface coating materials were available, baffle design would be trivial. A simple tube extending from around the entrance aperture of the optical system, coated with such a perfect absorber, would perfectly shield the optical system for sources outside the rejection angle. Reflections would be eliminated, and the only mechanism whereby light could enter is by diffraction. For real baffles coated with real materials operating with visible light, reflection easily dominates diffraction, which can then be neglected for most purposes.

Baffle design is a very complex problem involving a large number of variables, and consequently there is no one design which is universally accepted as best for most applications. There are several design principles, however, which all successful baffles observe, and these are as follows:

- (1) All baffle structure must be placed outside the sensor field of view. This means that any light reflected or diffracted from these baffle surfaces will not be imaged by the optical system directly on the detector.

(2) The surface area of the baffle which can be directly illuminated and which also views the optical entrance aperture should be minimized. This generally means that baffle rings or other structures be employed so that only the edges of such structures can be illuminated and view the lens. Such edges are usually sharpened to minimize their area. In this structure, most light rays undergo more reflections and thus greater attenuation before reaching the optical system.

(3) If the rejection required is greater than is practical with one baffle, a second baffle stage can be added which shields the first stage. In such a configuration the area illuminated which views the optical system (item 2) can be made zero.

(4) Depending on design details, the surfaces at the baffle should be either:

- (a) Black diffusely reflecting surfaces
- (b) Black specular reflecting surfaces
- (c) Highly reflecting and accurately polished (mirror) surfaces.

There are a number of "schools of thought" on baffle design and the surface coatings. The black surfaces are intended to absorb the radiation and the highly reflective surfaces are used in designs where the light is to be reflected back out the entrance. The specular designs are sensitive to small surface irregularities and deformations, particularly the highly reflective type, and are much more difficult and expensive to produce. The diffuse surfaces can be made the most absorptive (blackest), and are the easiest to manufacture. Primarily for these reasons, we favor the black diffuse surface coatings for all internal baffle surfaces, while external surfaces can be finished as required for thermal or other reasons.

BAFFLE DESIGNS REVIEWED

The study team reviewed a number of baffle designs which have been used in various applications or which have been proposed. These included the single stage cone, the two stage cone, the truncated two stage cone, and modifications of these. Also considered were the specular reflection

ellipsoid, a cavity type baffle, the CDC hybrid baffle, and a multiple knife edge baffle. These designs are described in reference R 22, and table 9-1, which compares these designs under several criteria, is taken from this source.

The criteria by which these designs are judged are these:

- (a) Ease of fabrication
- (b) Past performance or experience
- (c) Number of edges
- (d) Volume and dimensional efficiency
- (e) Sensitivity to deformation and surface defects
- (f) Sensitivity to diffraction
- (g) Is the illuminated first edge visible directly?

The simplest form of baffle is the simple cone. This configuration allows the aperture to view an illuminated surface, the illuminated portion varying with angle to the interferring source. It is easily fabricated but offers only limited rejection performance.

The two stage cone (dual baffle) provides an outer baffle to prevent illumination of viewed surfaces for sources outside a particular angle for the optical axis. It, too, is fairly easily fabricated and offers much better rejection than a single stage baffle.

The truncated two stage cone acts in a similar manner and reduces the area of illumination on the outer baffle surface but at the expense of permitting an illuminated baffle edge to be viewed. The total volume and length of the baffle are reduced by the truncation, but the fact that the first edge is now viewed by the optics negates one of the primary reasons for the second baffle stage.

The specular reflection ellipsoid baffle is designed to reflect light back out the entrance rather than absorbing it within the baffle, but it is difficult to fabricate and is very sensitive to surface defects. Here, too, the illuminated first edge views the optics.

The cavity baffle employs the principle of creating "light traps" for light rays outside of the field of view. Black specular surfaces might be employed here. The design gets very large for highly absorbtive traps.








Configuration	Ease of Fab.	Past Perf.	No. of Edges	Vol/Dim. Eff.	Sens. to Imperfection	Sens. to Diffraction	First Edge Illuminated:
 Single Stage Cone	1	--	1	Poor	Medium	Poor	Yes
 Two Stage Cone	2	Bendix	2	Good	Good	Good	No
 Truncated Two Stage Cone	4	Kollsman	2	Good	Medium	Poor	Yes
 Specular Reflection Ellipsoid	7	NASA Technical Input	2	Medium	Poor	Medium	Yes
 Cavity Baffle	3	Study	1	Poor	Medium	Poor	Yes
 CDC Hybrid	5	Computer Study	2	Medium	Good	Medium	No
 Multiple Knife Edge	6	JPL MM 69	Several	Good	Medium	Medium	Yes

TABLE 9-1 BASIC SUNSHIELD CONFIGURATION TRADEOFF CHART

The CDC Hybrid baffle employs an outer baffle similar to the outer stage of the two stage cone, and employs a cavity or "light trap" arrangement of baffle edges at the inner stage. This design can be considered a type of two stage cone baffle.

The Multiple Knife Edge baffle is a variation of the Truncated Two Stage Cone employing "light traps" in both the outer and inner baffle. The edges in such a design must be carefully ground and polished to razor sharpness.

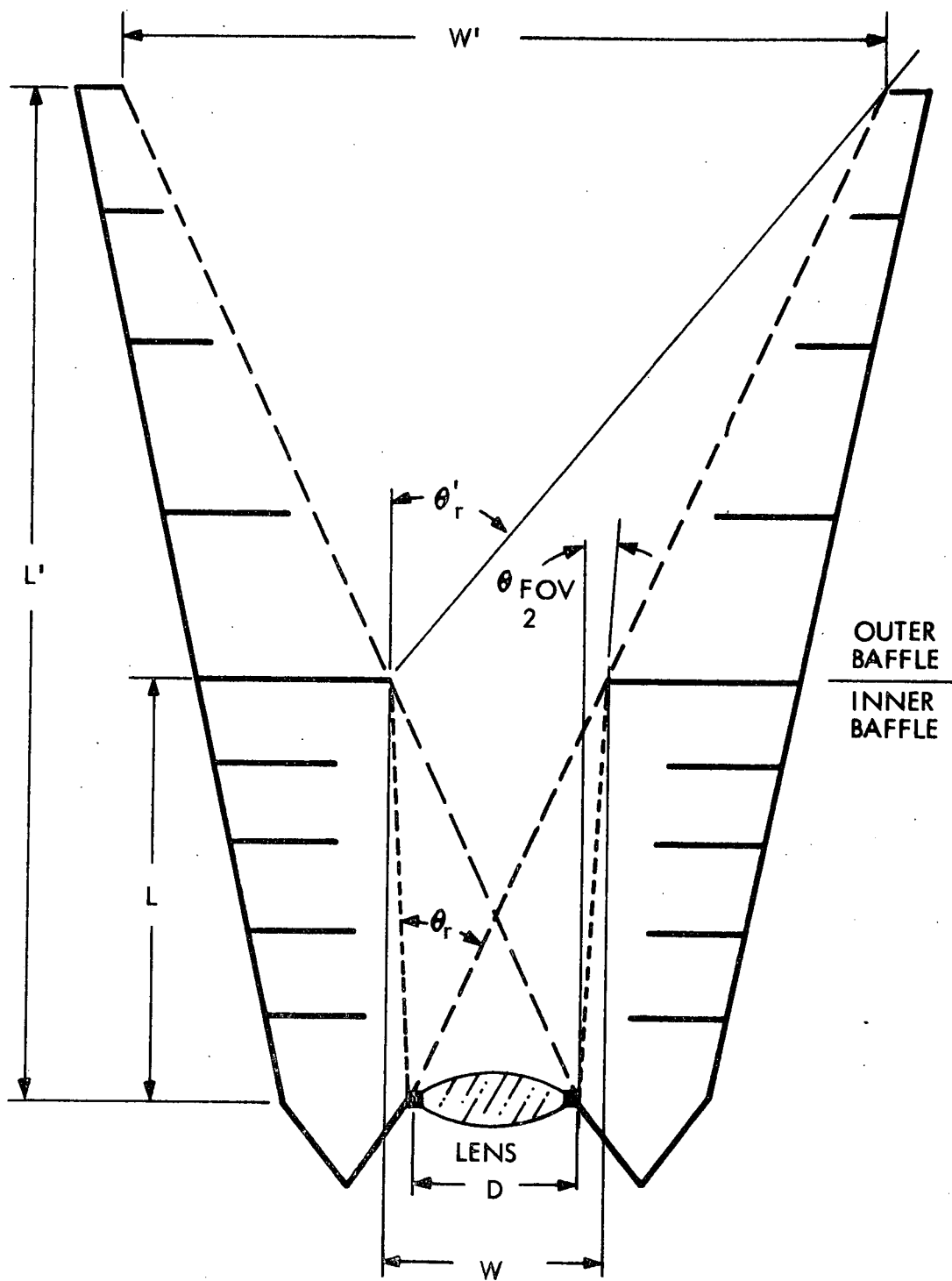
RECOMMENDED BAFFLE DESIGN

The two stage cone baffle achieves the overall highest marks in the comparison of Table 9-1. It is fairly easy to fabricate, uses a minimum number of edges, has good volume and dimensional efficiency, is quite insensitive to surface defects and is insensitive to diffraction. The illuminated first edge is not viewed by the optical system, in fact, for source angles outside the rejection angles, no illuminated surface or edge can reflect or diffract directly into the optical system. This two stage cone configuration is the basic design recommended.

Actually, the simple cone surface can be improved upon significantly at some additional complexity in fabrication, by replacing the smooth cone surface with a recessed surface and baffle rings. Such a design is shown in Figure 9-2, where the original cones are now represented by the dashed lines. These surfaces are now defined by the optical entrance aperture, and the two major baffle edges. All other edges and surfaces are recessed back from these cones, with baffle rings placed to reflect light several times before it can reach the optical aperture.

Parametric Design Curves for Two Stage Baffle

The dimensions of the cones which define the two stage baffle can be determined for any specific case in a straight forward manner. The inner baffle cone must flare out from the optical system aperture at the field of view angle so as to just stay outside the field of view. The second stage cone begins at the end of the first stage cone and flares out at a steeper angle as shown in figure 9-2. The only remaining question is



TWO STAGE BAFFLE

FIGURE 9-2

where does the first cone end and the second cone begin?

The baffle rejection angle θ_r' is the angle outside of which a source can only illuminate the outer baffle directly; the inner baffle is completely shielded geometrically. The rejection angle is a function of the field of view angle, the lens diameter, and the lengths of the inner and outer cones. We have developed a computer program which calculates the relative lengths of the inner and outer baffles such as to minimize the rejection angle, and plots a series of parametric curves.

If we normalize all dimensions to the aperture diameter (i.e., for $D = 1$) then the length L of the inner baffle which minimizes θ_r' is given by

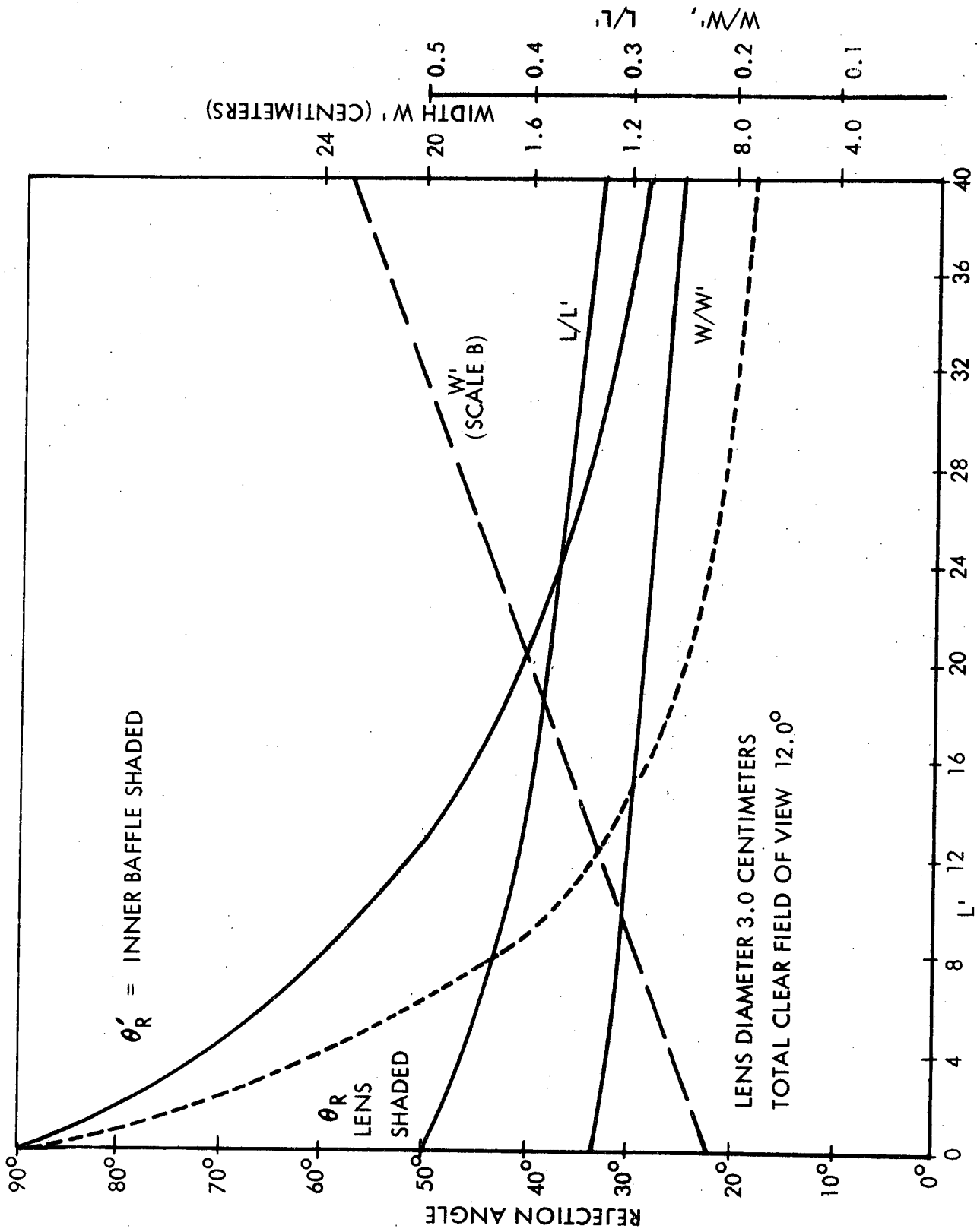
$$L = \frac{-1 + (1 + 2L' \tan(\theta_{FOV}/2))^{1/2}}{2 \tan(\theta_{FOV}/2)} \quad (9-1)$$

A typical set of parameter curves as generated by this computer program is shown in Figure 9-3. This is for a 3 centimeter diameter aperture and a total sensor field of view of 12 degrees (6 degree half angle).

For a given rejection angle, or the maximum length or width, the other baffle parameters can be determined from the curves in the figure. For example, if the required rejection angle θ_r' is 35 degrees, we find that the overall length of the baffle L' is 27.2 centimeters. The width of the outer baffle (w') is 19 centimeters for the length of 27.2 centimeters, and the inner baffle is 5.12 centimeters (w/w' times 19 centimeters). The length of the inner baffle is 10.1 centimeters (from L/L' times 27.2 centimeters), and no part of the lens will be directly illuminated for angles outside 22 degrees (from the θ_r curve).

If the baffle length could be as long as 40 centimeters, the outer baffle width (w') would be 23.2 centimeters and the rejection angle θ_r' decreases to 29 degrees.

A similar set of curves is shown in Figure 9-4, where the field of view is now 15 degrees and all dimensions have been normalized to the diameter of the optical aperture.



BAFFLE PARAMETERS AS A FUNCTION OF BAFFLE LENGTH

FIGURE 9-3

TWO STAGE BAFFLE

$\theta = 15^\circ$ FOV

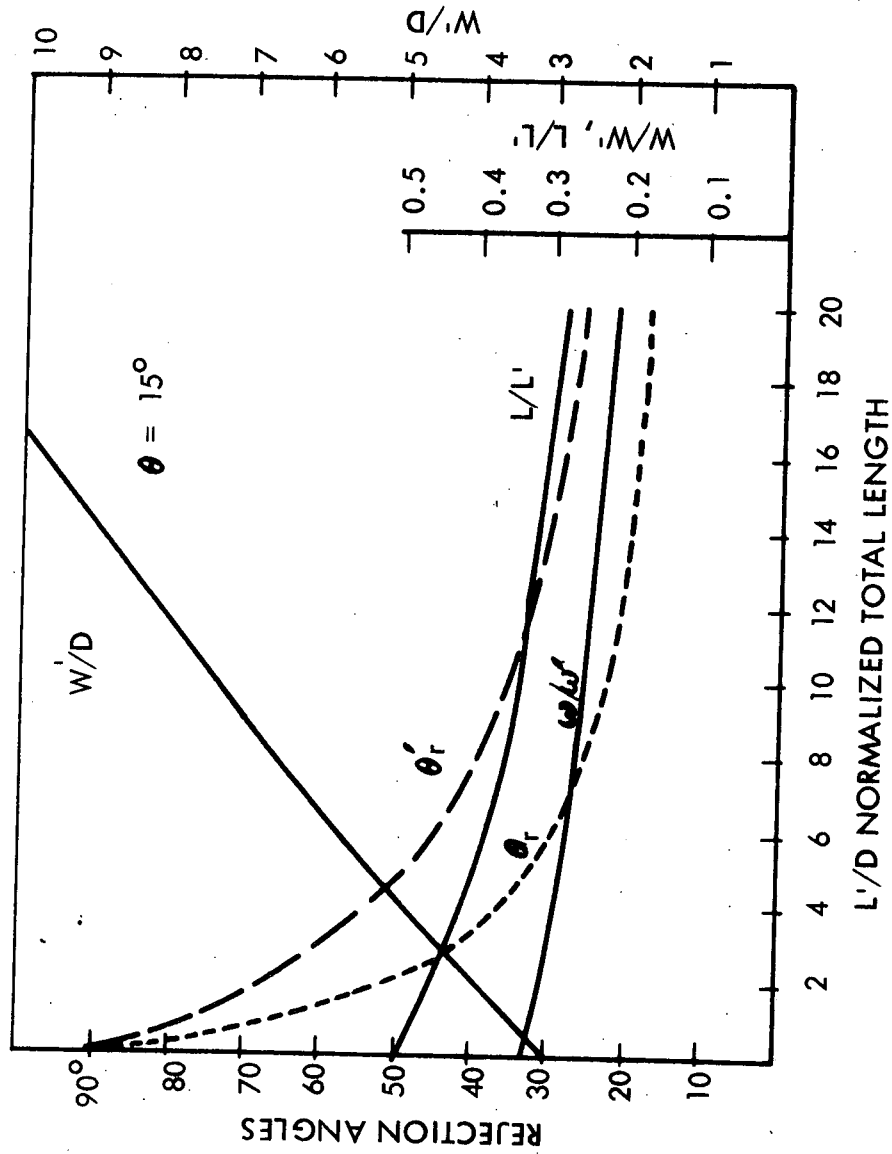
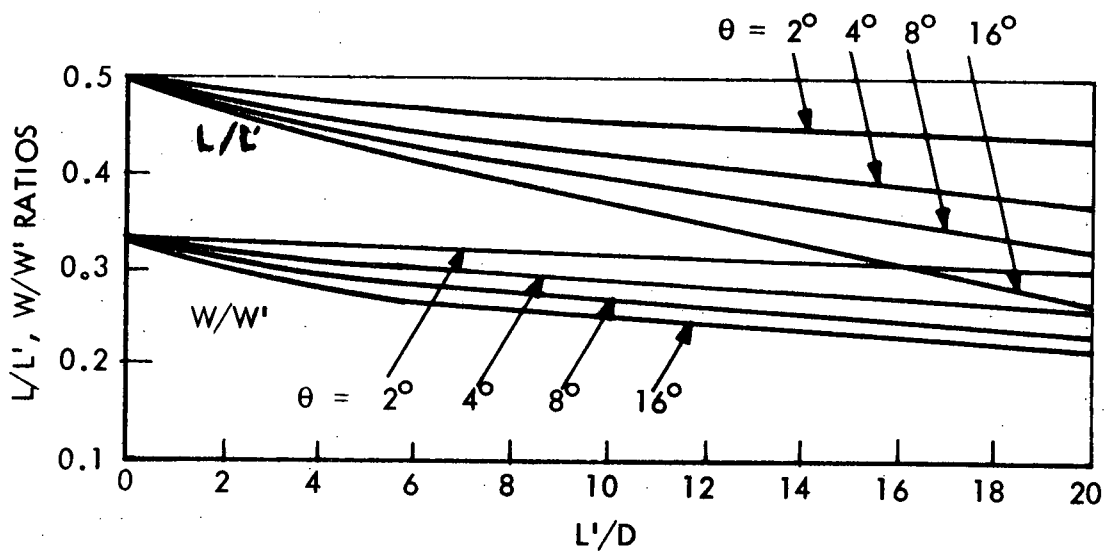
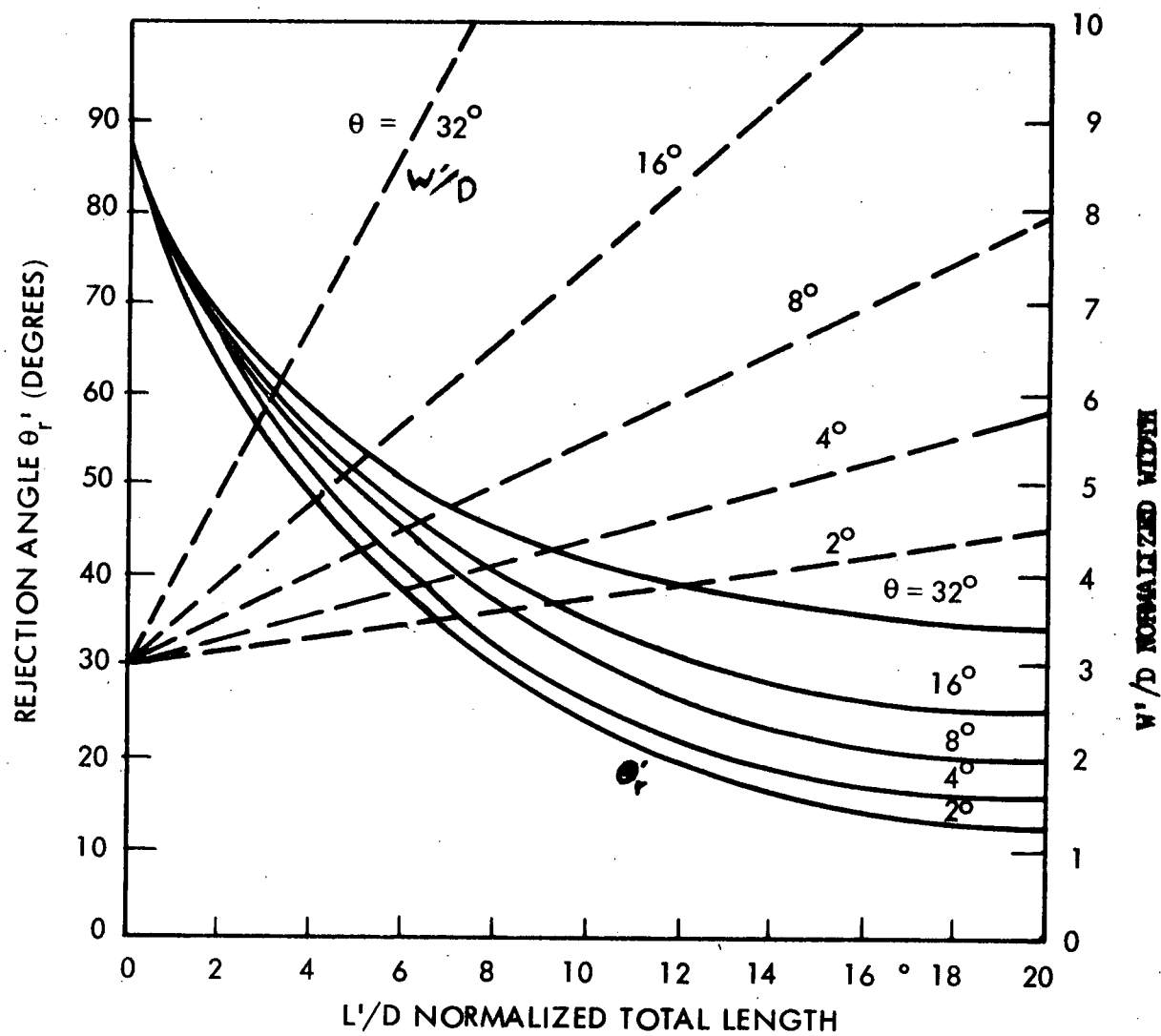


FIGURE 9-4



HAFFLE PARAMETERS FOR VARIOUS FIELDS OF VIEW

FIGURE 9-5

LENGTH AND WIDTH OF TWO STAGE BAFFLE

TOTAL FIELD ANGLE θ_{FOV}	4°	8°	16°	32°
Total Rejection Angle θ_r	L'/D	w'/D	L'/D	w'/D
20°	14.8	4.9	20.0	7.7
			--	--
30°	8.4	4.1	10.1	5.5
			15.0	9.8
				--
35°	6.8	3.9	7.8	5.0
			10.7	8.0
				23
				--
40°	5.4	3.7	6.2	4.6
			8.0	6.85
				14.9
				16.2
50°	3.7	3.5	4.0	4.0
			4.8	5.4
				7.3
				9.7

TABLE 9-2

Figure 9-5 shows another set of parameter curves for field of view angles of 2, 4, 8, 16 and 32 degrees. It can be seen that as the field of view is increased, the rejection angle increases markedly for a given total baffle length, or for a given rejection angle the length must increase. For example, for a rejection angle of 35 degrees, a normalized length of 6.1 is required if the field of view is 2 degrees, but the length must be 7.8 for an 8 degree field of view, and it must be longer than 20 for the 32 degree sensor. Even more dramatic is the width increase with field of view, which is shown in the dashed curves. The L/L' and w/w' ratios are shown at the bottom of the figure. Table 9-2 shows some of these values for various rejection angles taken from Figure 9-5.

STRAY LIGHT REJECTION OF TWO STAGE BAFFLE

How good is this two stage baffle we have described, and is it good enough to meet the required rejection criteria presented earlier? Unfortunately it is impossible to provide an exact numerical answer to the first part of the question, because the geometry we propose with the recessed walls and baffle rings makes precise calculations very difficult. We can show, however, for realistic coating materials such as 3M Black Velvet paint, and some simplifying assumptions about the geometry, that the two stage baffle when combined with the off axis rejection of the lens will meet the stated criteria.

For purposes of calculation, we assume the simplest form of two stage baffle, that is, the simple cone surfaces themselves. Since we are using black surfaces which only reflect a few percent of the light incident upon them, we only consider light which is reflected two times. Light that is reflected more often will be attenuated further and will add only a negligible amount to the total light at the focal plane.

The rejection definition we use here is definition (B) described earlier. For a given intensity incident upon the baffle from the sun, we calculate the intensity at the aperture of the optical system.

We have made this calculation for total fields of view of 4, 8, 10, and 16 degrees, all with a normalized length, L'/D , of 11. For each baffle we have calculated two cases: for light incident at the rejection angle (which is different for each baffle), and for light incident at 45 degrees from the optical axis. The rejections for these baffles are tabulated in Table 9-3, along with some of the baffle parameters. These values assume a total diffuse reflection of 5 percent for the baffle coating materials, which is typical of a good material such as 3M Black Velvet. These rejections are proportional to the square of the reflectance (since we consider only two reflections) so these rejection ratios can be corrected for other total reflectance values. For instance, if the coating material has a reflectance of 6 percent, these values would be multiplied by $(5/6)^2 = 0.695$.

SENSOR OPTICAL SYSTEM

The optical system is the second part of the sensor which rejects stray light. Since all surfaces of the baffle are outside the sensor field of view, all light reaching the lens after reflection or diffraction from the baffle is outside the field of view. A perfect optical system images all this light off the edge of the detector or reticle slit. The optical cavity must be carefully designed to prevent such light from reaching the detector after further reflection. Perfect systems do not exist, of course, and in real systems there are a number of ways in which small amounts of this out of field light will be directed toward the detector.

There are basically two types of optical systems, reflective systems which use mirrors, and refractive systems using lenses. In addition, there are combinations such as the Bowers and Schmidt systems which combine refractive and reflective elements. Reflective systems are all "folded" systems which are more difficult to baffle than in-line refractive systems,

OFF-AXIS REJECTION FOR TWO STAGE BAFFLE ($L'/D = 11$)

Total Field of View Angle θ_{FOV}	Rejection Angle θ_r	Inner Rejection Angle θ_r	w'/D	L/D	Rejection for $\rho = 0.05$ $\theta_{in} = \theta_r$	$\theta_{in} = 45^\circ$
4°	24.3°	14°	4.3	4.74	2.2×10^7	3.85×10^7
8°	25.5°	17°	5.49	4.19	8.2×10^6	1.60×10^7
10°	30°	18°	6.5	4.07	7.8×10^6	1.36×10^7
16°	37.8°	22.5°	7.7	3.42	3.55×10^6	6.25×10^6

TABLE 9 - 3

particularly when small f /numbers and wide fields of view are required. Paths can exist in folded optical systems whereby light can reach the detector by circumventing the optical elements. Reflective systems, also, often have "spiders" or other support structures in the field of view which can reflect off axis light and greatly degrade the stray light rejection of the optical system.

Refractive systems, although they have their own set of problems, do not suffer from these difficulties which are present in mirror systems, and generally promise superior performance for the f /numbers and fields of view required in this star scanner application. Most instruments covered in the technology survey use refractive optical systems, and this is the design approach recommended. The following discussion deals specifically with stray light mechanisms in refractive systems, but many of the comments can be applied to the reflective systems as well.

Stray Light Mechanisms in Optical Systems

There are a number of mechanisms within any real optical system which degrades it from the ideal system so that some out of field light reaches the detector. These mechanisms fall into two basic categories: scattering of various types, and multiple internal reflection. The star scanner must minimize these effects to maximize the rejection of stray light.

Scattering is a general term describing a number of related physical phenomena which can occur when waves (such as light waves) interact with other structures (in this case, the elements of the optical system) so that some of the energy exits at angles other than would be predicted by the reflection or refraction laws. Scattering is usually the result of non-uniformities in the materials, and can be associated with both the surfaces and bulk of the optical materials. The surface scattering is due to surface defects (e.g., scratches), imperfections in the coating materials, and contamination. The bulk scattering can be due to macroscopic defects such as bubbles, or microscopic defects such as color centers.

Scattering measurements performed on simple optical systems at Perkin-Elmer Corporation (Reference 01) have shown that careful selection of

materials, surface polishing, and cleaning can lead to a total diffuse scattering of about 10^{-4} of the incident radiation. This is probably a practical minimum scattering which one could expect to achieve in an optical system for the Pioneer Venus star scanner.

The second general mechanism contributing to the stray light, internal reflection, depends on the quality of anti-reflection coatings and the number of surfaces in the system. If we consider a series of flat plates, and assume that the reflection at each interface is small, it is easy to show that the total light which is multiply internally reflected and which leaves the stack in the same direction it enters, is given approximately by

$$I = I_0 \rho^2 (1 + 2 + \dots + N-1)$$

where I_0 is the incident intensity

ρ is the reflectivity per surface

N is the number of surfaces.

Thus the total contribution due to internal reflection increases as an arithmetic progression on the number of surfaces.

Real optical systems, of course, do not consist only of flat surfaces stacked together, so the above relation is significantly modified, because many rays are directed out the sides of the system. Curved surfaces can focus and concentrate the stray radiation also, and this is the real danger of multiple internal reflection. Any optical design must be carefully examined to determine if there are any internal reflection paths which could focus and image off axis light onto the detector. The edges of the lenses must be carefully treated also to absorb light reaching them and prevent reflection back into the lens.

Optical System Design Criteria

These scattering and reflection mechanisms which occur in optical systems lead to several criteria which can be used in designing and comparing potential optical systems. These criteria are listed below.

(1) Materials should be selected for low scattering characteristics. Glasses and other optical materials vary considerably in their content of bubbles and microscopic defects, as well as their ability to take a good polish. The best optical grade fused quartz is one of the best materials in this regard.

(2) Surfaces should be "superpolished" by any of the commercial techniques which have been developed in the last few years. Most of these methods are similar and based on the experimental work of A. F. Bennett and J. M. Bennett at the Naval Weapons Center, China Lake. (Reference P 20 presents some theoretical scattering curves for various surface finishes.) The polished surfaces should be carefully AR coated.

(3) Since scattering and internal reflection depend on the number of surfaces and total path length through the optical materials, the number of such elements should be minimized. This means that in this star scanner application where we have shown that we have more than sufficient accuracy with detectors as wide as 0.5 degrees, we should allow a sizable blue to simplify the optical system.

(4) The edges of the lenses should be coated with a material designed to absorb rather than reflect light reaching these surfaces. One such material is "Luxorb", developed by the Northrup Corporation for star sensor applications, and comes in several formulations to match the indices of refraction of various glasses.

(5) Contamination on the surface is one scattering mechanism which we can't control after the vehicle is launched. A safety factor should be included by providing the system with an "over designed" baffle to allow some contamination to settle on the lens before compromising sensor operation due to stray light. Fortunately, the two stage baffle appears to have sufficient off axis rejection for the sample cases studied to provide this safety margin.

BAFFLE MEASUREMENT TECHNIQUES

Because the off axis rejection capabilities of the baffle and optical system depend on so many parameters and involve complicated geometry, the only way to have confidence in the performance of sensor is to test it.

Unfortunately, conventional baffle measurement techniques are not sufficiently sensitive to measure the very high rejection ratios required in this application, so improvements must be made in the measurement capability.

Baffle measurements are normally performed in a room with a bright source of collimated light such as a laser or an arc lamp. A typical measurement set-up is indicated schematically in Figure 9-6. The light beam is expanded so that it uniformly illuminates the entrance aperture of the sensor baffle. The angle between the sensor and the light source is varied by either rotating the sensor or moving the light source in an arc about the sensor.

There are two mechanisms which limit the rejection ratios which can be measured by such a technique. First is scattering due to the air and dust particles in the air. This scatters light directly into the field of view of the optical system, which focuses it on the detector. Performing this measurement in a clean room can reduce the dust scattering, but, for visible light, Rayleigh scattering in the air can still be significant. Such a limitation can be removed completely, of course, by performing the measurements in a vacuum chamber.

The second limiting mechanism is backscatter from the wall or other structure which is in the sensor field of view. Some of the light reaching this surface will be reflected into the sensor field of view. Of course, this surface should be made as low reflectance as possible, such as a black honeycomb or other cavity type surface, and placed as far back as possible. If the back wall has a total reflectance of 1 per cent, and is located 5 meters from the sensor which has a 32 centimeter diameter baffle coated with a 5 percent reflectance material, then the maximum rejection that can be measured with such an arrangement is less than 10^7 (definition B). This calculation considers reflection from the baffle interior only, ignoring reflections from other walls and surfaces which will degrade the capabilities of a real measurement system below this level. Depending on the sensor type and construction details, the measurement system must be capable of measuring rejection ratios up to several orders of magnitude larger than this calculated measurement capability.

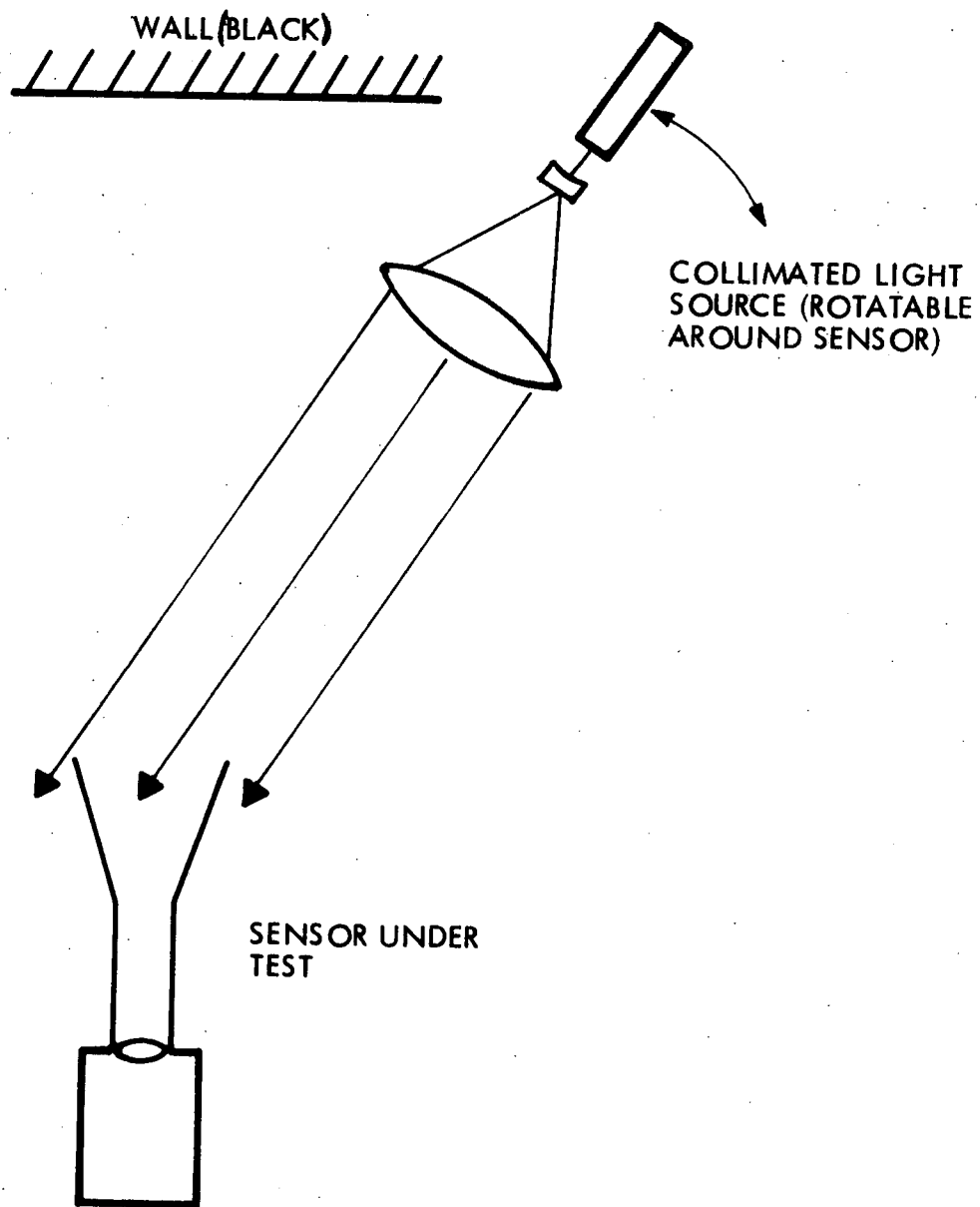


Figure 9-6 Conventional Baffle Measurement Technique

Measurements at IMSC in filtered air have shown that the limiting rejection ratio that can be measured without undue effort is about 10^7 (definition A), and it is considered unlikely that improvements could be made to this basic method that would reduce air and dust scattering and wall reflections to the levels required for this program. Other methods must be employed which do not have these limitations, and we suggest two possible techniques which could be developed to provide the required measurement capabilities.

Potential Baffle Measurement Techniques

The first technique is proprietary to the Lockheed Missiles and Space Company since it was conceived long before the initiation of this study. It involves discrimination against reflection from the back wall which the sensor views by the differences in the time required for the light to traverse the various path lengths. Light travels at a speed of about 3×10^{10} centimeters per second, or as a rule of thumb, about one foot per nanosecond. Reflection from a wall x feet away would return to the sensor $2x$ nanoseconds after the direct beam. The method requires light pulses which are shorter in duration than this delay time, such as can be produced in lasers by several techniques. A very fast detector, such as a specially designed photomultiplier, will be required in place of the regular detector used in the sensor. The entire measurement must be performed in a vacuum chamber to eliminate air and dust scattering which is not discriminated against by the technique.

The second technique involves breaking the total measurement into two measurements, one on the baffle assembly itself, and one on the optical system. The attenuations achieved with each system separately will be measurable in air without special precautions, but the measurements must include angular as well as total intensity information and the results of the two measurements then combined by numerical integration in a computer. The measurement on the baffle, for example, will involve mounting the baffle in a light tight box with an auxillary sensor which is movable behind the baffle. All light reaching the sensor must come through the baffle, so the angular intensity

distribution can be "mapped" by moving the sensor about to view the baffle exit aperture at various angles. A similar angular measurement would then be performed on the unshielded optical system to produce a "map" of its sensitivity to out of field light. The results of the two measurements would then be combined to obtain the total sensor rejection.

The first technique has the advantage of being more direct in that it measures the rejection of the complete sensor, but it requires a complex laser and electronic system and a good size vacuum chamber with mechanisms to move the source and/or sensor during the test. The second technique, although less direct, can be performed in air without such an elaborate set-up. This could also be used as a convenient tool for baffle and optical system design because it reveals more information about the detailed characteristics of each component.

SECTION 10

PRELIMINARY SENSOR AND SYSTEM DESIGN

Based on the attitude determination requirements, and the stellar, detector, baffle, and optical system characteristics, a preliminary design concept has been developed which meets the requirements. We are actually taking two approaches, since two separate types of sensor systems can perform this function. First is what we call the "traditional" design approach, which consists of a photomultiplier tube detector with a "V-slit" reticle. Such an instrument would be similar to instruments now in service, although the baffling, the optical system, and the electronics are different for this design. The second design approach uses an array of silicon detectors, and is a significant departure from the traditional sensor, but offers a number of significant advantages such as potentially smaller size, lower susceptibility to stray light interference, and greatly increased reliability.

This section describes the preliminary design requirements, the basic design parameters for the two sensor approaches, and a baseline approach to the information processing.

PRELIMINARY DESIGN REQUIREMENTS

To meet the system attitude determination requirements as stated in Section 4, a set of sensor system design requirements has been developed. The next section discusses how the mission requirements and consequently the sensor and system requirements might be relaxed to simplify the sensor or realize other advantages. The sensor and attitude determination system requirements which determine the preliminary design are these:

(1) Two sensors must be employed, and oriented on the spacecraft in such positions and angles that at least one of them will be operational for all possible attitudes of the vehicle. One should be oriented pointing up toward one spin axis, and the other pointing down toward the other end of the spin axis. Since it is not desirable to point too close to the spin axis (elevation field of view and optical resolution must increase), a good compromise position is to orient the sensors at aspect angles of 45 and 135 degrees.

104

(2) Both sensors should be operational in the normal cruise mode. This provides complete redundancy for this mode which is a reference position. If need be, due to failure of one of the sensors, other attitudes can be obtained by "open loop" control from this reference position even if the new attitude is such that the remaining sensor is not operational because of sun angle. To provide a band of reasonable width about the cruise position where both sensors are operational, the baffle rejection angle must be smaller than the angle from the sensor to the sun in this mode. A baffle rejection angle of 30 to 35 degrees will provide an operational band of ± 10 to 15 degrees when the sensors are mounted at aspect angles of 45 and 135 degrees.

(3) A sun aspect angle sensor should be included in the attitude determination system. The sun can be used as a well identified star which is located in both aspect and azimuth, reducing the requirements on the star sensor. Knowing sun position in two axes greatly simplifies star identification and the attitude may be determined by observing only one (identified) star. There is a limit to how much we can relax the star sensor requirements because we must avoid a critical failure path through the sun aspect sensor, so the star scanner must be able to determine attitude independently, without relying on sun aspect angle information, for most vehicle attitudes.

This still represents a significant reduction in star scanner performance requirements, because the system can be designed for star availability closer to average rather than the worst case star condition which is much worse than average. The sun aspect sensor also provides considerable redundancy.

The sun aspect sensor can be a small, light weight, simple instrument. For instance, a pinhole camera concept could be used because of the high light intensity available, and a position sensing silicon photodiode using the lateral photoeffect might be a convenient detector. We did not examine the sun aspect angle sensor further since it is outside the scope of the study.

(4) For all attitudes except those where the sun appears within the baffle rejection angle, and at normal cruise spin speed (assumed to be 12 RPM), each sensor must provide sufficient information so that the vehicle attitude can be determined when the sun aspect and elevation are known. If the sensor scans 6% of the sky, for example, it must be able to detect a third magnitude star (2.5 magnitude silicon) since under the worst case conditions only one third magnitude or brighter star appears in the scanned field.

(5) The same must be true at maximum spin speed (120 RPM), except we require that each sensor only provide attitude information for 75% of all attitudes not compromised by the sun. Operation at all intermediate spin speeds and as low as 5 RPM is also required, which means that the electronic bandwidth must track the spin speed over this range. Although the signal to noise ratios at 120 RPM are lower than those at 12 RPM by more than a factor of three, the worst case star distribution which dictated the design for the cruise RPM is so much worse than average, that 75% of the time at least one star brighter than second magnitude will be visible. This means that if requirement (4) above is satisfied, and the filters track the spin speed, then this requirement is automatically satisfied.

(6) An average of only one "false" pulse per revolution will be allowed at cruise RPM when the threshold is set for 90 percent probability of detection on a third magnitude star. Most of these "false" pulses are due to dimmer stars, and this criteria sets the minimum signal to noise ratio requirements.

(7) To provide a safety margin for degradation of the instrument, the design should provide at least a 50% larger signal to noise ratio than required. One might reason that the photomultiplier tube should have a larger safety margin because of its known degradation mechanisms and the fact that it is a single channel and thus more vulnerable to failure. On the other hand, the very low leakage silicon detector technology is developmental, so perhaps its safety margin should be larger. For simplicity, and to facilitate direct comparison, we have assumed the 50% margin for

both sensors. These nominal designs can easily be adjusted for other values if desired.

PRELIMINARY SENSOR DESIGNS

Based on the design requirements, a set of design specifications have been developed for the two basic concepts. Both sensors measure star position in both elevation and azimuth, and have an elevation field of view of 10 degrees and are designed to be mounted on the spacecraft at aspect angles of 45 and 135 degrees. The baffle rejection angle for each is 35 degrees to allow a ± 10 degree band around cruise orientation where both sensors are operational. In spite of detector differences, the electronic signal processing is similar for the two approaches, and both employ band pass filters which track the spin speed.

Photomultiplier Tube Sensor

The photomultiplier tube sensor design is basically similar to existing designs with a few specific differences. The phototube is the EMR type 541 E which is the glass-kovar ruggedized tube with an S-20 cathode. The 541 N is the same tube with a bi-alkali cathode material. Tubes of this type have been flown in star scanners and other space instruments. If the Kovar in the tube is a problem, the ceramic tube, types 510 E or 510 N could be substituted.

This design uses a "V-slit" reticle, each slit 0.3 degrees wide by 10 degrees elevation in a 45 degree "V" configuration. This "V" angle is chosen as a tradeoff between accuracy of measuring the elevation angle, and the stray light requirement of minimizing the field of view.

The signal to noise requirements and the 50 per cent safety factor indicate that we should design for a signal to noise ratio of 20 for a third magnitude star at 12 RPM spin speed. The signal to noise curves for the photomultiplier sensor indicate that a 5 centimeter diameter aperture is required to achieve this signal to noise ratio. This assumes a background about midway between the 100 tenth magnitude stars per square degree average

background and the 500 tenth magnitude stars per square degree typical of bright areas.

The f/number does not directly affect the photomultiplier sensor sensitivity, but the focal length must be short enough to keep the image size smaller than the cathode sensitive area, and should also be kept short to minimize the sensor length and volume. We have chosen an f/2 optical system which can give sufficient resolution (less than 0.3 degrees blur) with only two elements. The number of elements is minimized for to maximize stray light rejection.

The baffle must have a 12 degree circular field of view to contain the reticle pattern. With the aperture of 5 centimeters, the baffle must be 45 centimeters long and 32 centimeters in diameter to reject sunlight outside 35 degrees.

Because the photomultiplier tube is susceptible to damage from high light levels, two protection mechanisms are provided to prevent this problem. A circuit is incorporated which monitors the anode current and reduces the power supply voltage when it gets above a threshold level. A second mechanism which is activated by a small solid state sensor mounted at the edge of the baffle will close a shutter if the sun threatens to get too close to the field of view so that it might damage the cathode surface.

The electronic signal processing techniques employed in this sensor are discussed later in this section.

Silicon Diode Sensor

The silicon detector sensor is a significant departure from the photomultiplier tube design, and offers several advantages such as smaller size, lower susceptibility to stray light, lack of damage mechanisms, and much better reliability.

The detector focal plane consists of an array of silicon diode detectors. The number chosen depends on several involved tradeoffs centering around the complexity of the electronic processing, which goes up as the number of detectors, and the sensitivity of the instrument, which also goes up as the

number of detectors goes up. Sensitivity as a function of number of detectors can be determined from the curves of Section 7 where detector length is the variable parameter. The complexity as a function of number of detectors depends on the information processing techniques employed and their hardware implementation. For example, if very little processing is done such as only simple filtering, thresholding, and amplitude measurement without any correlation with other channels, and if integrated circuits are designed and built for this application, then adding additional channels adds very little to the cost, size, or weight. In such a case, a larger number of detectors which increases sensitivity and which would allow a smaller aperture and baffle might be an effective tradeoff.

We have chosen an array of eight silicon detectors arranged in four pairs of 45 degree "V's". Each pair is only about 2.5 degrees in elevation, and each detector is 0.5 degrees wide. The "V" arrangement is retained to provide adequate elevation axis information, but if more detectors were employed, or if one was willing to sacrifice elevation accuracy, a staggered linear array with some overlap of elements could be employed instead, with an increase of sensitivity due to a decrease in detector area.

A signal to noise ratio of 20 for the minimum star is required at 12 RPM spin speed, just as in the photomultiplier sensor, but because there are more red stars in the sky, this minimum star is 2.5 magnitude (silicon) rather than the third magnitude (visual) star required by the photomultiplier tube sensor. This requires an aperture diameter of 3.2 centimeters.

The f/number must be kept as small as possible for the silicon detector so we have chosen an f/1 system of three elements, which will provide an acceptable blur size throughout the ± 5 degree field of view.

Since the detector array is 10 degrees long but only a couple degrees wide, the baffle field of view need not be circular, but rather can be oval. A baffle 11 degrees by 4 degrees will be sufficient, and must be 28 centimeters long and have a maximum opening of 19 centimeters to reject sunlight 35 degrees or more from the optical axis.

Since the silicon detector array is not susceptible to damage by high light levels as is the photomultiplier sensor, protection mechanisms to shut off the power or to activate a shutter are not required.

Table 10-1 summarizes the basic design features of the two sensor approaches. One major difference between the two sensor approaches is the size of the stray light baffle required. Figure 10-1 shows the rejection angle and normalized width versus normalized length for the two field of view angles involved. The differences here are small, but when combined with the actual aperture diameters, the differences become more apparent, as shown in Figure 10-2. The baffles required for the two systems for rejection angles of 30 and 35 degrees are shown to scale in Figure 10-3. It is readily apparent from the picture why it is important to minimize the required aperture diameter and thereby minimize the baffle size.

ELECTRONIC DATA HANDLING DESIGN

The purpose of the electronic data handling system is to accept the broadband signals coming from the photomultiplier or silicon detectors, filter these signals to maximize the signal to noise ratios, detect star crossings, encode the star crossing information, and present the encoded information to the telemetry system for transmission. This can be done in a wide variety of ways, and many additional functions can be added which can reduce the total telemetry requirements by performing correlation or other analysis on the data to discard false alarms, validate good data, and compress its format. In order to make a judgment about many of the more complex schemes, the study team has examined some of these possibilities. Our general conclusion, however, is that the benefits to be gained by reducing the telemetry requirements by these complex data analysis schemes are not sufficient to justify their inclusion. This is because they involve significantly increased design and manufacturing costs and some additional weight and power, they invariably do not preserve all the information which could be of benefit if sent to the ground for processing,

SENSOR DESIGN SPECIFICATIONS

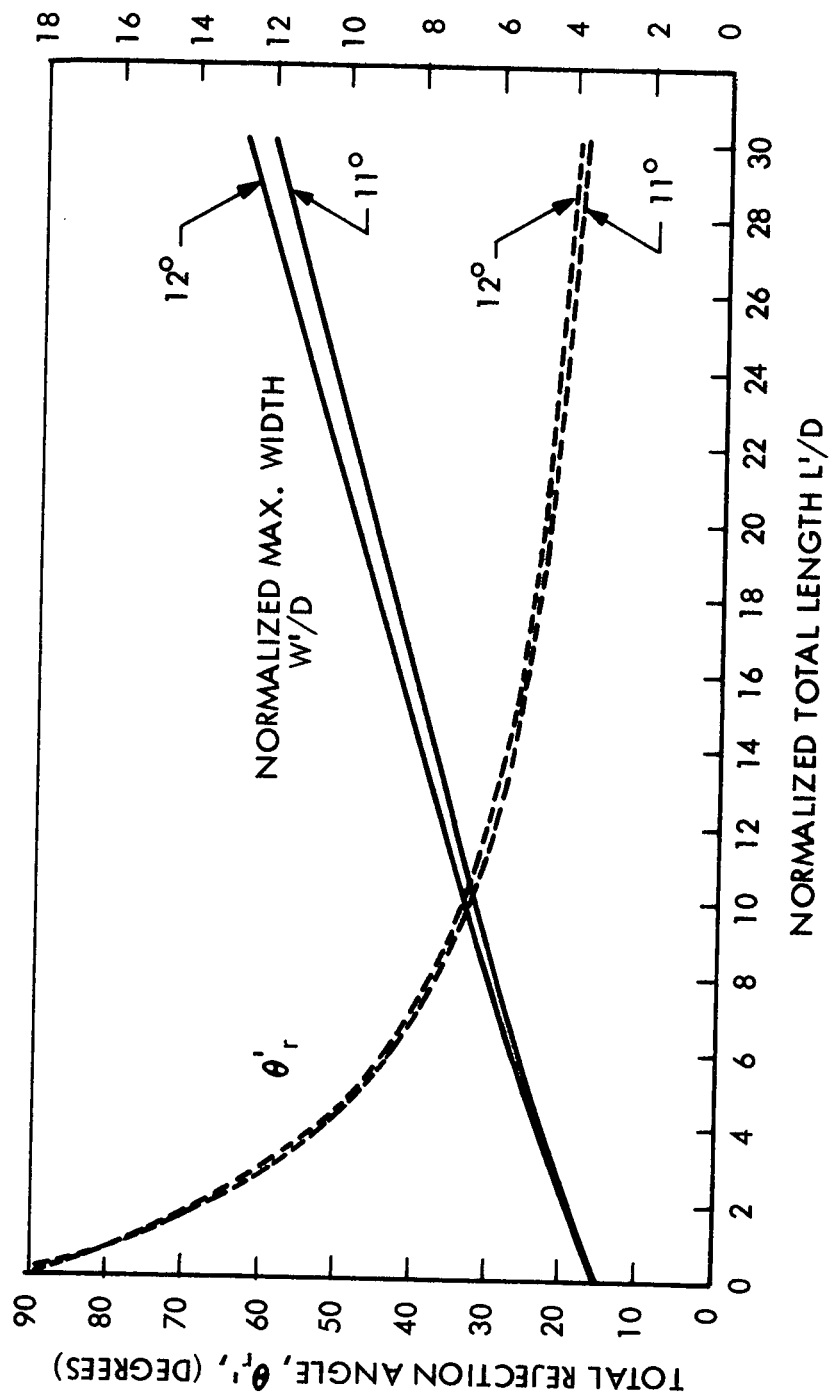
PHOTOMULTIPLIER TUBE SENSOR

- RMR 541 E tube
- Two slits in 45 degree "V" 0.3 wide
10 degree elevation
- S/N of 20 for 3rd magnitude star at 12 RPM
- Aperture diameter = 5 cm
- Two element f/2 optics
- 120 circular FOV baffle 45 cm long,
32 cm diameter rejects outside 35 degrees
- Two level high light level alarms to turn off
P M tube power and activate shutter
- Power: 1 watt
- Weight: 1.8 KG (excluding baffle)

SILICON DETECTOR SENSOR

- Eight silicon detectors
- Each detector 0.5 degrees x 2.5 degrees
10 degree elevation FOV
- S/N of 20 for 2.5 magnitude (sl) star
at 12 RPM
- Aperture diameter = 3.2 cm
- Three element f/1 optics
- 110 x 40 baffle 28 cm long, 19 cm maximum
opening rejects outside 35 degrees
- No protection mechanisms required
- Power: 1/2 watt
- Weight: 1 KG (excluding baffle)

TABLE 10-1



BAFFLE PARAMETERS VS LENGTH

FIGURE 10-1

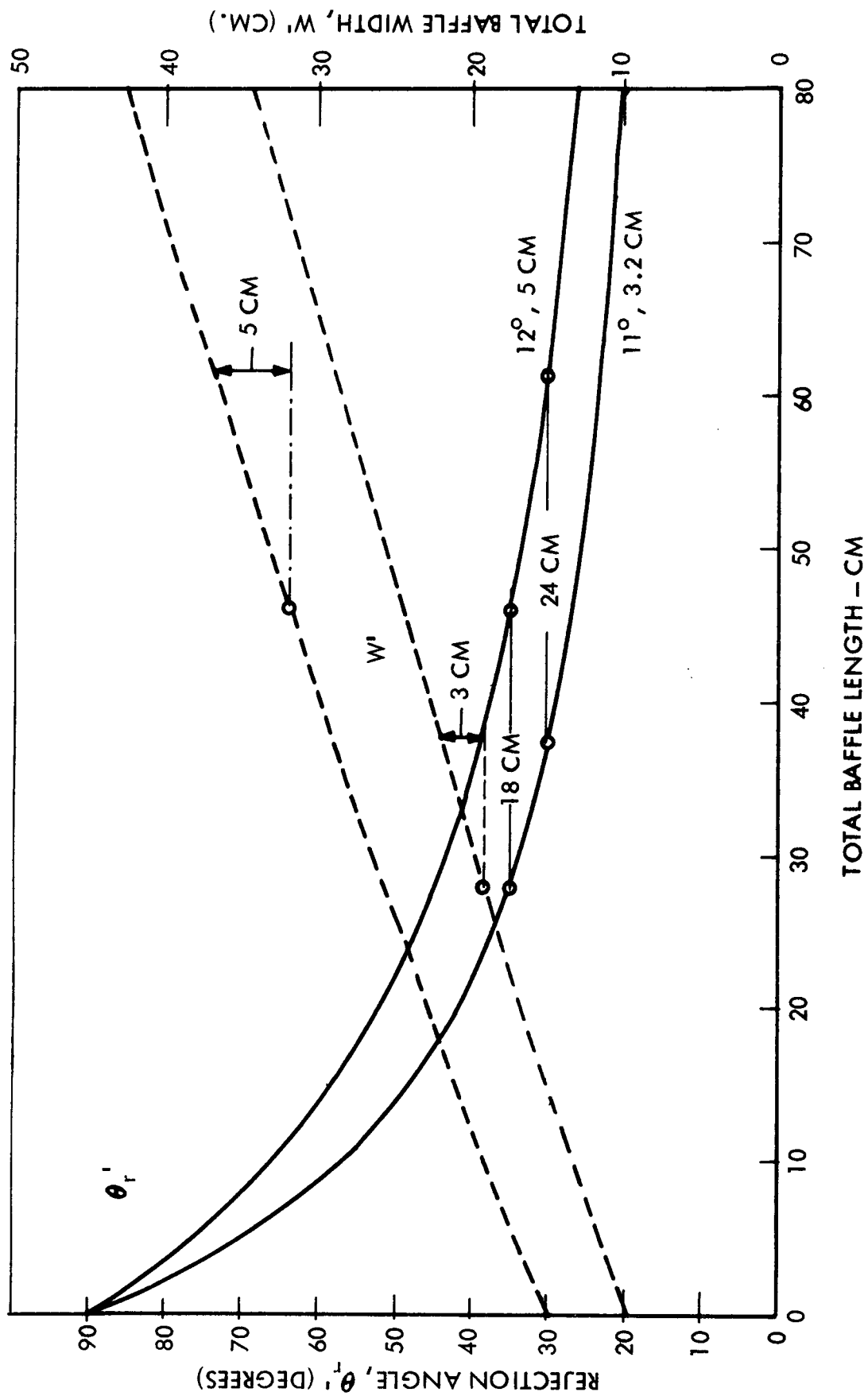
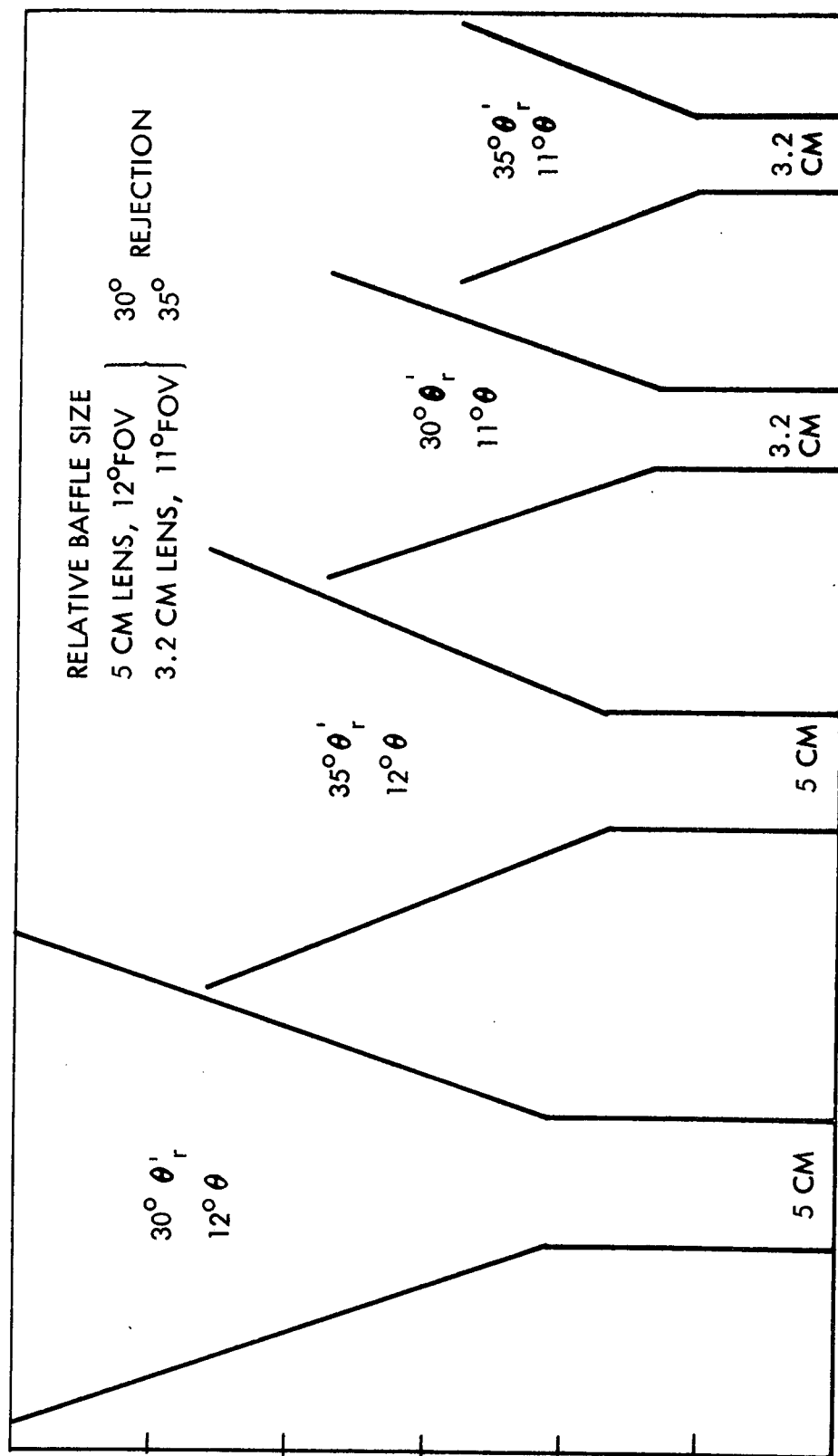


FIGURE 10-2



COMPARISON OF BAFFLE SIZE

FIGURE 10-3

they compromise the total system reliability, and they "mask" sensor internal operation so that a malfunction can not be diagnosed as easily. Instead, data rate can be controlled by a commandable threshold (desirable for other reasons, too) which could be raised to a level such that only the brightest objects in the sensor scan would be detected.

The baseline electronic design for both sensors, then, is fairly simple. It is assumed that a pulse will be available from the sun which will serve as a time reference for measuring all star crossings. The output of the detector is amplified and passed through the bandpass filter. This filter is an approximation to the optimum filter determined by the details of the signal and noise frequency spectra, and consists basically of a high pass and a low pass filter in cascade. The bandwidth and center frequency of the filter must be adjusted as the spin speed is varied. This filter can be implemented by various techniques including:

- (a) Active filtering using off-the-shelf integrated circuit modules.
- (b) Charge transfer or "bucket brigade" devices in a custom integrated circuit design.
- (c) Digital filtering using custom integrated circuit designs.

All of these methods can utilize the sun reference pulse repetition rate as the input for bandwidth control.

The filtering section is followed by a command adjustable threshold sensor which determines when a preset voltage level has been exceeded. The signal produced by this threshold crossing initiates the following:

- (1) Readout of the time counter (started by the sun reference pulse).
- (2) Enable the peak measuring circuit and the associated analog to digital converter which measures the amplitude of the pulse and digitizes the information.

The digital output of the time counter and the peak measuring circuit are placed in a storage register which is sampled by the telemetry. An intermediate buffer may be required depending on telemetry requirements.

(3) When the signal falls below threshold again, a reset signal is generated which returns all components to their original state, ready for the next pulse to be received.

The measurement of the peak pulse amplitude is only one of several ways in which the star crossing time can be accurately determined, but as mentioned in Section 8, it is recommended over other possible methods because it most easily resolves possible ambiguities which can arise when stars are closely spaced, it facilitates star identification, and it is easy to implement in hardware.

Amplitude Measurement

The method of encoding amplitude suggested is one providing constant percentage error regardless of input amplitude. This is possible by utilizing a fixed increment digital encoder preceded by a log amplifier. Since a log amplifier has an output amplitude that is related by a constant factor to the logarithm of the input amplitude, the encoding resolution will represent the same percentage error of the input amplitude over the total encoding range. For example, if the peak input signal is expected to have a dynamic range of 100/1 and the digital encoder is capable of encoding the log amplifier output into 128 increments, then the percentage error represented by one encoding increment is approximately 3.7 percent for any input amplitude within the dynamic range. If, instead, a linear amplifier output were encoded for the above example, the encoding accuracy for a maximum signal level input would be 0.78 percent for a one resolution cell error, however, for a signal level a factor of 10 lower, the error would be 7.8 percent. Thus the percentage error increases with decreasing amplitude which is undesirable. The number of levels chosen for encoding will be a function of the input signal to noise ratio and the accuracy requirements for the sensor.

The photomultiplier sensor with its single information channel will require only a single set of electronics which perform the above functions. Unless weight, space, and power are at an extreme premium, this circuitry would most likely be made up of discrete components and/or commercially available integrated circuits. The expense of designing, building, and qualification testing custom integrated circuits which would perform the

required operation on a couple of chips or so is probably not justified, although this approach would likely increase the reliability of the circuitry.

The second sensor design involves several detectors (nominally eight) and requires a separate set of electronics for each. In this situation it is much more important to minimize the size, weight, and power requirements of each channel, and thus the design and construction of custom integrated circuits to perform such functions becomes more attractive. Once we have constructed the integrated circuits, additional channels can be included in the design for very little extra cost. A detailed analysis based upon firmer design parameters may well show that there are two distinct categories of multiple detector sensors. One using discrete components would be limited to a relative few channels, while the other using integrated circuits would not be so limited by the electronics and would use many more detectors to increase sensitivity so that the optics and baffle sizes could be reduced. The question of whether or not to employ custom integrated circuits also depends heavily on the number of sensors to be built.

Data Transmission Requirements

The data transmission requirements for the star scanner will be influenced by the accuracy required in encoding amplitude of the pulse, and the threshold crossing time. Each star viewed will cross each slit of the V-slit sensor or two detectors in the multiple detector sensor. In the simple logic scheme used as the baseline design, each crossing will involve a crossing time measurement and an amplitude measurement. More complex schemes where the two crossings are recognized as being due to one star can reduce the data requirements by requiring only one amplitude measurement (or perhaps an average of the two), and a fewer number of bits on the time measurement of the second pulse. Some information is lost in this process, however.

The data word for encoding the crossing time will be required to encode a 360 degree sector to approximately 0.1 degree accuracy. To estimate the number of bits required it was assumed that the RMS accuracy required would be 0.1 degree and that a uniform probability density function would describe the random variable. With these assumptions

$$\sigma = \frac{a}{2\sqrt{3}}$$

where σ = standard deviation

a = resolution element size

If $\sigma = 0.1^\circ$, $a = 0.3464^\circ$ requiring 1039 resolution elements. Since 1024 elements will be produced by 10 bit accuracy, no more than 11 bits should be required.

Assuming the use of log encoding for the amplitude information it is anticipated that no more than 7 bits will be required. This is based on a dynamic range of 100 and a maximum encoding error of 2 percent. The data collected per star crossing is thus 11 bits plus 7 bits or 18 bits total per crossing.

The data rate transmitted to the ground will depend on the number of stars crossing threshold per scan revolution and the spin speed. Each star crossing generates 18 bits of data or 36 bits per star per revolution. The maximum spin speed of 120 rpm or 2 revolutions per second would then produce 72 bits per second per star. For attitudes when the high gain antenna cannot be used, the data capacity of the telemetry could easily be exceeded. This could be handled, however, since each scan will produce the same data (ideally at least) and the storage registers can be sampled at a much slower rate if required. The amount of data taken per revolution can also be limited, of course, by raising the threshold to reduce the number of stars detected.

The above values are correct for the photomultiplier sensor, which has only one information channel. The silicon detector sensor with its multiple detectors requires additional bits to identify the particular detector which received the light signal. Three bits per star crossing will identify each detector out of the eight in the array. This information adds considerable redundancy and allows powerful discrimination against false alarms and stray light interference.

Sensor Comparisons

The major physical features of the two sensor designs was summarized earlier in Table 10-1. The photomultiplier sensor somewhat surprisingly turns out to require a significantly larger aperture than the silicon diode array sensor. This is because although the photomultiplier has inherently greater sensitivity than the silicon detector, its larger area receives much more background radiation, it has much lower quantum efficiency and a narrower spectral bandpass, and because of the spectral region of operation, must sense higher magnitude (dimmer) stars.

Table 10-2 compares the two sensors in terms of complexity, reliability, and costs. The single channel of the photomultiplier sensor requires much less electronics than the several channels of the silicon diode sensor. On the other hand, all the detector channels of the silicon detector sensor are identical, and this unit does not require the high voltage power supply and the two protection mechanisms that the photomultiplier sensor requires. The overall complexity of the two approaches is about the same, particularly if custom integrated circuits are employed in the information processing channels which reduces the part count per channel tremendously.

The reliability of the two sensor systems is radically different. On one hand, the photomultiplier sensor employs a single detector which can be degraded or permanently damaged by high light levels, and which requires protection mechanisms, one of which is a mechanical device. A high voltage power supply is required which is generally considered to have much lower reliability than the low voltage supplies required in the silicon detector sensor. The silicon sensor features a number of parallel channels, and can operate acceptably even with several of them not functioning. The silicon detectors are inherently more rugged than the photomultiplier tube and do not require the protection mechanisms, particularly the mechanical shutter, which can be prone to failure. The silicon detector sensor is clearly superior as far as reliability is concerned.

SENSOR COMPARISON

	<u>PHOTOMULTIPLIER TUBE SENSOR</u>	<u>SILICON ARRAY SENSOR</u>
Complexity	Single channel H.V. power supply Protection mechanisms	Several identical channels
Reliability	Single channel "Fragile Tube" High voltage	Multiple parallel channels Rugged components Low voltages
Costs		
Development	---	30-50 P.C. more
Test equipment	Same	Same
Sensor (w/o electronics)	Same	Same
Electronics	---	Same - 20 P.C. more

TABLE 10-2

What are the costs of the two sensor systems? We have divided the costs into four categories: development costs, test equipment costs, sensor fabrication and assembly excluding the electronics, and the electronics costs.

The development costs for the photomultiplier sensor will be significantly less than for the silicon diode sensor. The photomultiplier sensor is a "traditional design" and can use some existing components such as power supplies and protection circuitry currently used on other sensors. The optical system and baffle must be developed for this purpose for both sensor systems. The silicon detector technology is still developmental and will entail more costs on this account. Over all, we estimate that a silicon diode sensor will cost about 30 to 50% more to develop for this Pioneer Venus application than a photomultiplier detector sensor of a more traditional design.

The test equipment costs will be about the same for the two systems, since they have the same operating requirements. The photomultiplier system will require testing of the protection mechanisms which are not required of the silicon diode sensor, but this is probably not a significant fraction of the whole.

The costs of the sensors without the electronics is about the same for the two approaches, since the basic hardware consisting of the physical housings, the optics, and the baffle are similar in the two cases. This cost is certain to be small compared to the electronics in any case.

The relative electronic costs include a number of variables which are difficult to assess. The costs of the silicon detectors themselves are more or less unknown, and the costs of producing the integrated circuits for this application will vary considerably depending on the number of units produced, since the initial costs of the circuit artwork is high compared to the costs of producing the circuits once the artwork and masks are made. For example, a set of masks to produce the custom circuits required for a sensor may cost about \$50,000, but the individual circuits may be produced for \$100 or so after this is completed. We estimate that

the electronics cost to produce six sensors (enough for two flights plus spares for a third), will range from about the same for the two approaches up to about 20% more for the silicon diode array sensor.

One cost item which has not been included and which can vary considerably, is the costs of qualification testing of components and assemblies. Since a wide variety of requirements can be imposed, we have omitted this item from the cost comparisons. Such costs should be included, of course, in making the final tradeoff comparisons between the two systems.

Both the photomultiplier tube sensor and a sensor using silicon diode detectors can meet all the requirements of the Pioneer Venus mission. The photomultiplier system is a more traditional design but is larger, heavier, and less reliable than the silicon diode sensor which is more developmental and will cost somewhat more to develop and to build. The silicon diode sensor is significantly less susceptible to interference due to stray light.

SECTION 11

OPTIONS TO SIMPLIFY ATTITUDE DETERMINATION SYSTEM

The system we have described so far will meet all the attitude determination requirements as listed in Section 4. It will provide attitude information at all spin speeds and orientations. Its multiple sensors and the inclusion of the sun aspect sensor provide considerable redundancy so that one sensor can fail completely and the system will still provide adequate attitude information for most orientations. Because of this complete capability, the system as described provides complete flexibility to modify the mission profile essentially at will at a later date, unconstrained by any limitations of the attitude determination system.

This section examines ways in which these attitude determination requirements might be relaxed to simplify the attitude determination system or to reduce costs, size, weight, power, or exact other benefits. The sensor system requirements can be reduced in essentially four ways. They are:

- (1) Relax the redundancy requirement and give up the ability to operate in all possible orientations.
- (2) Reduce the maximum spin speed requirement and/or the requirement to operate over a wide range of spin speeds.
- (3) Reduce the sensitivity requirements by relaxing the requirement to operate at the worst case orientation.
- (4) Reduce accuracy requirements.

Reduce Redundancy Requirements

The complexity, weight, and power requirements of the attitude determination system are cut nearly in half if only one sensor is employed rather than two. The ability to measure attitude in the cruise (reference) position is retained, but the redundancy is lost. This option is particularly unattractive for the photomultiplier sensor which has a critical failure path through its single detector channel. The silicon detector sensor with its

much higher reliability is more of a candidate here. Complete attitude determination ability is retained over more than a complete hemisphere, and if the silicon sensor is designed so it will recover sufficiently fast, a reduced capability over the other hemisphere will be available except when the sun actually comes within the field of view of the silicon detector and heats it. This sort of operation with the photomultiplier sensor would require the shutter to cycle off and on once per revolution which seems very risky, since the shutter needs to "hang-up" only once momentarily to destroy the detector. A safer approach would be to chase the shutter and "open loop" control from the reference cruise orientation.

Reduce Spin Speed Requirements

The sensor system can be simplified if the requirement to operate at all spin speeds is relaxed. If a fixed cruise spin speed is chosen, and the sensor is only required to operate at this speed, a fixed filter rather than a variable filter could be employed, with a significant reduction in the complexity of electronic circuitry, and a subsequent increase in reliability. If operation at a higher speed is required, the orientation could be determined at the cruise speed, and then the vehicle could be "spun-up" with little chance that the attitude would be changed by the operation. The speed would then be reduced and the attitude remeasured to add confidence to procedure. This relaxation in the spin speed requirement, however, does not serve to reduce the sensitivity requirement, since that is determined by the ability to operate with the worst case star distribution at cruise RPM. The sensitivity can be reduced, however, by reducing spin speed at cruise, since the signal to noise ratio will vary inversely as the square root of the spin speed. Another way is the next item, reducing the requirement to operate in all possible orientations.

Relax the Requirement of Operating in All Orientations.

As shown in Section 6, the stars are not arranged in the sky in a regular fashion, and thus there exist worst case distributions and worst case orientations for the spacecraft spin axis. These worst cases are very rare, but are

Preceding page blank

sufficiently worse than average, so the requirement to work in all possible orientations is fairly severe. If this requirement were relaxed somewhat, say to 80 percent of all orientations, a considerable reduction in the required sensitivity would result, and the sensor could be made significantly smaller.

Reduce Accuracy Requirement

At first thought, reducing the accuracy requirement of the sensor and attitude determination system is an obvious way to simplify the system and reduce the required sensitivity. Such is not the case. As shown in Section 8, high accuracy measurements can be made at fairly low signal to noise ratios, and the real requirement on the signal to noise ratios comes from the necessity of limiting false pulses due to the dimmer stars. About the only benefit to be directly attributable to reducing the accuracy requirement is a reduction in the telemetry data bandwidth by reducing the number of bits of quantization. This procedure makes star identification increasingly difficult, however, since identification is primarily based on accurate measurement of angular separation between stars. Reducing the elevation angle accuracy of individual star positions might be desirable, since it would allow a staggered linear silicon detector array of smaller area rather than the pairs of "V-slits" detectors. The only significant impact this would have on the spin axis accuracy would occur when only a single star was observed per scan. Again star identification becomes more difficult. In general, very little is gained by relaxing the attitude determination requirements beyond the 0.1 degree to 1.0 degree range.

Combinations

The four methods of relaxing the system requirements as discussed above can be combined in a number of ways to produce various configurations. For instance, only one sensor could be used, which reduces redundancy, but it could be a silicon detector sensor with a fixed filter operating only at one speed which is a highly reliable configuration, thus tending to offset the lack of redundancy. In addition, a single sensor might be designed

with a slightly larger aperture to provide a larger safety factor in the signal to noise ratios. Such combinations are numerous and fairly obvious and will not be further detailed.

SECTION 12

SURVEY OF APPLICABLE STAR SCANNER TECHNOLOGY

A survey of current star scanner technology has been conducted to determine if there are any existing sensors or components which could be used, perhaps with modification, on the Pioneer Venus program. Since much of the desired information is not available in report form, we made direct inquiry, initially by telephone, with a number of industrial, academic, or governmental groups which have been involved in star sensor design, development, manufacture, or operation. In all, fifteen separate organizations were contacted. These groups, along with their addresses, telephone numbers, and the names of the person contacted are listed below.

1. Goddard Space Flight Center
Greenbelt, Maryland
(301) 474-9000 (Bill Hibbard)
2. Avco Corporation, Systems Division
201 Lowell Street
Wilmington, Massachusetts 01887
(617) 657-5111 (Albert Merlisni)
3. TRW Systems Group
One Space Park
Redondo Beach, CA.
(213) 535-2036 (Pat Hutching)
4. International Telephone and Telegraph Corp.
Electro-Optical Laboratory
15151 Bledsoe Street
San Fernando, CA. 91342
(213) 362-1511 (Leo Cardone)
5. American Science and Engineering, Inc.
11 Carleton Street
Cambridge, Mass. 02142
(617) 862-6222 (Bruce Stanton)
7. Adcole Corp.
330 Bear Hill Rd.
Waltham, Mass. 02154
(617) 890-3400 (Ralph Abbott)

8. Singer-General Precision, Inc.
Kearfott Division
1150 McBride Avenue
Little Falls, New Jersey 07424
(201) 256-4000 (Sol Shapiro)
9. Control Data Corporation
Minneapolis, Minnesota
(612) 853-3218 (Joe Carroll)
10. Ball Brothers Research Corp.
Boulder Industrial Park
P. O. Box 1062
Boulder, Colorado 80332
(303) 441-4000 (John Sand)
11. Quantic Industries, Inc.
999 Commercial Street
San Carlos, CA. 94070
(415) 591-9411 (Dick Ronald)
12. Kollsman Instrument Corp.
575 Underhill Blvd.
Syosset, N. Y. 11791
(516) 921-4300 (Jim Connors)
13. Perkin-Elmer Corp.
Boller & Chivens Division
South Pasadena, CA. 91030
(213) 682-3391
14. Astro Mechanics, Inc.
8500 Research Blvd.
Austin, Texas
(512) 452-8815
15. Applied Physics Lab
John Hopkins University
Scaggsville, Maryland
(301) 953-7100 (Fred Schenkle)

Information received through contact with these organizations is listed below. There are a number of sensor systems covered in the survey which have some applicability to the Pioneer Venus mission. The parameters of these sensors are summarized in Table 12-1, and the modifications to these sensors which would be needed to enable them to meet the Pioneer Venus requirements are discussed in the text.

Program	S ³	OSO-7	ATS-3
Manufacturer	Goddard Space Flight Center	Ball Brothers	Control Data Corporation
Sensor Type	Photomultiplier-Reticle-Single Slit	Photomultiplier-Reticle	Photomultiplier V Slit
Size (inches)	8 x 1 1/2 dia.	13 x 4 Dia.	6 x 12 x 18 incl ball release mech.
Weight (lbs)	3	10	25
Power (watt)	1	1.25	.75
Spin Rate RPM	4 to 7	30	100
Magnitude	+3.5	+4.5	2.5
Sun Angle (deg)	90	Night Orbit	28
Accuracy	.1°(3σ)	.03	1.5 min.
Detector	Photomultiplier	Photomultiplier	Photomultiplier EMR 541-E-01-14
Field of View (deg)	25 x .3 Single slit	10 elevation V slits	12
Optics & Aperture	Refractive 1.25	Refractive	3.5 Refractive
Reliability	NA	NA	NA
Status	Operational	Operational	Operational for 6 months
Comments	Slow Spin Rate EMI Susceptible	Night Orbit only	Experiment ended after 6 months

1. 4

Program	SAS-A,B	SAS-B	SCANNER
Manufacturer	American Science and Engineering	Johns Hopkins Applied Physics Laboratory	Honeywell Radiation Center
Sensor Type	Photomultiplier N Reticle	Photomultiplier N Reticle	Photomultiplier Reticle
Size (inches)	10 x 5 Dia. (SAS-A)	130 in ³	21.5 x 8.0 x 16.0
Weight (lbs)	10	4.75	42.19
Power (watt)	.65	.4	1
Spin Rate RPM	.1 to 1	.1 to 3	60 to 120
Magnitude	+5	+5	+3
Sun Angle (deg)	40	60	45
Accuracy	1.0 Min.	1 min.	20 sec.
Detector	Photomultiplier	Photomultiplier EMR 541	Photomultiplier EMR 541A
Field of View (deg.)	10 x 5	10 elevation 5 between parallel slits	6 x 6
Optics & Aperture	Refractive	2 Refractive	Refractive 2.75
Reliability		NA	.664 (1000 hrs.)
Status	SAS-A Operational	To be flown Fall 1972	Operational
Comments			Destroyed after one flight

TABLE 12-1, SECTION 2

Program	SPARS	Pioneer Jupiter	Pioneer Venus	Pioneer Venus
Manufacturer	Control Data Corp.	TRW Systems Group	Control Data Corporation	Kollsman
Sensor Type	Solid State	Solid State	Solid State	Solid State
Size (inches)	N/A	6 1/4 x 4 1/2 x 6	5.5 Dia. 3.3 long	7.6 x 4.5 Dia.
Weight (lbs)	N/A	2.5	1.6	5.4
Power (watt)	N/A	.5	.8	1.0
Spin Rate RPM	N/A	2 to 5.8	75	75
Magnitude	N/A	Canopus	0 mag silicon	0.0 Silicon
Sun Angle (deg)	N/A	50 (with sun shade)	N/A	30
Accuracy	N/A	0.5° (3σ)	3 min	.3 (1σ)
Detector	Cadmium Sulfide Selenide	Silicon	Silicon PIN Photodiode	Silicon
Field of View (deg.)	4 elevation	.5 x 40 Single slit	45	45 elevation
Optics & Aperture	Concentric 2025	Cassegrain Bowers	2.1 effective aperture Cassegrain	Refractive
Reliability		0.98 (3 yrs.)	NA	0.91 (2 yrs.)
Status	Prototype	Operational	Proposed	Proposed
Comments	High Accuracy Very Slow Rates	Usable on bright stars only		

TABLE 12-1, Section 3

Goddard Space Flight Center. Goddard Space Flight Center (GSFC) designed and built the Scanning Celestial Attitude Determination System (SCADS) for use on the Small Scientific Satellite (S^3) program. The SCADS is an operational system which is being successfully flown. The system is a photomultiplier-reticle type, 8 inches long by 1.5 inches in diameter, weighing about 3 pounds. Its field-of-view, defined by a single reticle slit, is 25 degrees by 0.3 degrees. It can detect stars to +3.5 magnitude to a 3σ spin orientation accuracy of 0.1 degrees. It consumes 1 watt of power and was designed to operate at a spin rate of 4 revolutions per minute.

Problems with satellite wobble caused the initial information from the star scanner to be severely degraded. However, when the satellite spin rate was increased to 7 revolutions-per-minute, the wobble was eliminated and the SCADS sensor operated as designed. The S^3 experimenters also noticed a noisy sensor output at the lower satellite altitudes. This noise disappeared at the higher altitudes and was attributed to strong ionizing radiation at the lower altitudes which caused scintillation in the photomultiplier tube. The SCADS sensor seems to be very susceptible to EMI when in orbit, so the experimenters feel it would be advisable to incorporate noise rejection circuitry and additional shielding and filtering in future sensors.

The SCADS Sensor would require extensive modification to meet the Pioneer Venus requirements. These modifications would include:

(1) The 3.2 centimeter diameter aperture would have to be increased to about 5 centimeters to provide sufficient sensitivity for the spin speeds to be covered. At the same time, the optical system could be simplified to reduce the large number of elements of the present design. A larger photomultiplier tube may be required because of this change.

(2) An effective baffle must be added, since the SCADS is designed to only work when oriented more than 90 degrees from the sun. The large (25 degree) field of view makes this difficult.

(3) SCADS uses a single slit reticle which we feel is not as desirable for the Pioneer Venus star scanner as the V-slit reticle, although it is acceptable. Changing to a V-slit would allow a reduction in the elevation field of view and simplify the baffle design.

(4) The electronic circuitry must be modified to accommodate the wide range of spin speeds to be encountered. Other changes may be necessary to make the sensor output compatible with the telemetry interface and available information bandwidth. Because of current EMI experience, filtering and noise rejection circuitry should be included.

These modifications constitute a complete redesign of the sensor although some components, such as photomultiplier tube power supply, may be directly used.

System Division of AVCO Corporation. AVCO was to build the Magnetic Storm Satellite (MSS) for NASA. This was to be a fairly conventional photomultiplier-reticle system. All of the star scanner parts had been ordered and breadboard tests had just begun when the MSS program was cancelled. Work on the instrument ceased immediately and it was never completed.

TRW Systems Group. TRW has built a solid state single axis Canopus star sensor which is presently operational on the Pioneer Jupiter spacecraft. This device utilizes a solid state silicon detector having a .5 degree by 40 degree field-of-view. It weighs 2.5 pounds, is 6.25 x 4.5 x 5.9 inches in size (without sun shade) and consumes under 1/2 watt of power. It is designed to operate with a spin rate of 2 to 5.8 revolutions-per-minute, and has a reliability of 0.98 for 3 years.

The star sensor requirements for this Jupiter mission are very much different than the Pioneer Venus requirements. This instrument is only a "pipper" which provides a roll reference by detecting one star, Canopus.

It could not readily be converted into a device to satisfy the Pioneer Venus requirements. It does not have the sensitivity to track the dimmer stars which is required of the Pioneer Venus Star scanner. To increase its sensitivity would be major undertaking. The aperture would have to be increased or a more sensitive detector utilized. Its spin rates are not compatible and its single axis configuration should be converted to a dual axis mode. All this requires modification of the device to such an extent as to constitute a completely new sensor design.

ITT Electro-Optical Laboratories. ITT has specialized in the image dissector type of star sensor, and all of their sensors are built using this device which they manufacture. In the image dissector system, scanning is done electronically in the dissector tube and thus the need for a mechanical scanner, necessary if the space vehicle is stabilized, is eliminated. Electronic scanning in this way greatly increases the star sensor's electronic complexity, and, as a result of this, ITT image dissector sensors have complex electronics. For spinning vehicle applications such as the Pioneer Venus, it is simpler and much more efficient to use the vehicle motion to provide the scanning for the sensor. The image dissector is applicable to a star tracker on a 3-axis stabilized vehicle, but is of no interest for this Pioneer Venus application.

American Science and Engineering. American Science and Engineering (AS&E) has built the star scanner presently operating on the Small Astronomical Satellite A (SAS-A). The company is also building a similar star scanner to be flown on the SAS-B. These are photomultiplier "W slit" reticle systems. Although the physical configurations of the two units are slightly different, both have similar parameters. They are designed for spin rates of .1 to 1 revolution-per-minute. They can detect stars to fifth magnitude to an accuracy of 1 arc minute. They have refractive optical systems and fields-of-view defined by the reticle of 10 degrees by 5 degrees. They both consume under 1 watt of power. The SAS-A is approximately 10 inches long by 5 inches in diameter without the sunshield. The SAS-B is odd shaped and approximately the same volume as the SAS-A. Both weigh about 10 pounds.

The SAS Sensors would require considerable modification to meet the Pioneer Venus mission requirements, because they are designed for much higher accuracy and much slower spin speeds. They use a Super-Farron lens system, for example, which is a very fast, high resolution system, while the Pioneer Venus program requires a much simpler system to reduce weight and enhance stray light rejection.

Honeywell Radiation Center. Honeywell built a star scanning system in the early sixties which was flown on an Aerobee Sounding Rocket. This was a conventional photomultiplier-reticle system designed to operate at a spin rate of 60 to 120 revolutions-per-minute. The system weight was 42 lbs and its dimensions were 21 x 8 x 16 inches, including the sun shade. It had a 20 arc second accuracy on third magnitude stars. It had refractive optics and a multiple V slit reticle giving a 6 degree x 6 degree total field-of-view. It was designed to operate 45 degrees from the sun line with a .664 reliability for 1000 hours. The device consumed under 1 watt of power. The scanner operated successfully but was destroyed after the first flight when the rocket went off course and landed in the ocean.

Honeywell is presently building a star scanner for the Air Force Space Precision Altitude Reference System (SPARS) Program. This sensor is a fairly large device designed for very high accuracy and very slow spin rates. It uses solid state detectors in a multiple slit configuration, and is not applicable to the Pioneer Venus mission because of the radically different design parameters.

Adcole Corporation. Adcole has built one star scanner for NASA Goddard but it is no longer interested in star scanners, and we were unable to obtain details of their earlier work.

Singer General Precision Incorporated, Kearfott Division. Kearfott is doing some classified star sensing work for the Air Force, but it is not directly applicable to our requirements. Kearfott had specialized in systems using vidicon tubes as detectors, which like the ITT image dissector sensors discussed above, are useful in star tracking systems from 3-axis stabilized vehicles, but have little applicability to star scanning systems on spinning vehicles. These systems generally have high performance, especially when tracking in bright backgrounds, but they are quite complex. The vidicon must be scanned with precisely generated electronic waveforms and thus complex electronic scan generation circuitry is required. Since the vidicon is a hot filament tube reliability can also be a problem. High power

consumption is also characteristic of these systems. It is recommended that complex television type systems, such as vidicon star sensors, not be used on the Pioneer Venus mission.

Control Data Corporation. Control Data Corporation (CDC) has built several starmapping systems including the Advanced Technology Satellite-3 (ATS-3) and the initial SPARS cadmium sulfide-selenide detector star scanner. The ATS-3 was a photomultiplier-reticle system operating at a 100 revolution-per-minute spin rate, measuring 6 x 12 x 18 inches and weighing about 25 pounds. It could detect stars down to 2.5 magnitude with an accuracy of 1.5 arc minutes. It had a 3.5 inch objective aperture and was operational for 6 months after which time problems with the satellite resulted in the star scanner experiment being terminated. It utilized a double "V" slit reticle with an overall field-of-view of 12 degrees. With a sun shade it could operate to within 28 degrees of the sun line. The star scanner also included a mechanism to release a reflecting ball for a separate experiment to be done with the ATS-3 vehicle.

CDC recently completed the preliminary development of the SPARS solid state star scanner. The company designed, built, and successfully tested this device which used cadmium sulfide-selenide as the detection material. The CDC SPARS star scanner was a fairly large device designed for very high accuracy and slow spin rates (1 revolution per 90 minutes). It used a concentric optical system having a 2.25 inch effective aperture. Its field-of-view was 4 degrees in the elevation direction. This device is not suitable for the Pioneer Venus mission because the very slow spin rates it was designed to operate at are not compatible with the higher rates of Pioneer Venus. The very high accuracy provided by this sensor is also not required by the Pioneer Venus units. CDC is no longer working on this starmapper since Honeywell, the prime SPARS contractor, decided to build the SPARS star scanner itself.

CDC has proposed a small solid state star scanner using a silicon detector to one of the Pioneer Venus system study contractors. The proposed

device is 5.5 inches in diameter and 3.3 inches long. Its weight is 1.6 pounds and it consumes 0.8 watts of power. It has a 3 arc minute accuracy on zero magnitude silicon stars at a 75 revolution-per-minute spin rate. The instrument has a 2.1 inch effective aperture Cassegrain optical system, a field-of-view of 45 degrees in the elevation direction, and uses a silicon P/N photodiode detector. This star scanner meets the Pioneer Venus mission requirements established by the system study contractor several months ago, but these requirements are significantly different from the requirements developed in this study. We believe that the 45 degree field of view requirement is particularly unwise for stray light rejection reasons.

Ball Brothers Research Corporation. Ball Brothers Research Corporation (BBRC) has built the Orbiting Solar Observatory-7 (OSO-7) star scanner under contract to NASA Goddard Space Flight Center. The OSO-7 star scanner is a photomultiplier-reticle device, presently in operation at a 30 revolution per minute spin rate. This scanner is 13 inches long and 4 inches in diameter. It weighs 10 pounds and consumes 1.25 watts. Its accuracy on a 4.5 magnitude star is 1.8 arc minutes. Its "V-slit" reticle has a field-of-view in elevation of 10 degrees. The sensor will operate in night orbit only.

This OSO-7 sensor could be modified to meet the Pioneer Venus requirements. It is somewhat heavier than desirable, but if a simpler optical system is employed the weight could be reduced. Of course, a sunshield baffle must be added, integrated with the optical system, to provide stray light rejection. A shutter should be added to the electrical protection circuits already employed.

The electronics must be modified to include the ability to operate over the expected range of spin speeds, and may well require additional modification to meet telemetry interface and bandwidth requirements. Modification of the physical packaging of the sensor will probably be required to interface with the Pioneer Venus vehicle, since it presently is packaged in several pieces, some rectangular, a triangular section, and the cylindrical section with the optics and photomultiplier tube.

Thus it is likely that very little of the present OSO-7 sensor design could be used without modification of some sort. Rather than try to preserve the design with so many modifications, it seems better to us to start afresh using some of the applicable design principles and concepts proven in this and/or other sensors.

BBRC has been doing developmental work on a silicon solid state star scanner. This solid state sensor is a derivative of a breadboard system which BBRC built and delivered to Comsat. The Comsat system was a startracker designed for a stabilized vehicle and thus not compatible with Pioneer Venus Probe requirements. It did, however, use a silicon slit detector which could be utilized in a spinning star scanner system.

Quantic Industries. Quantic Industries is building a star tracker for the Air Force using a silicon solid state detector. They have not built any star scanning systems and this star tracker system is sufficiently dissimilar to the Pioneer Venus requirements that its concept, design, and component hardware are not of interest in this study.

Kollsman Instrument Corporation. Kollsman Instrument Corporation has had extensive experience in the star sensing field, although most of their work has been in the gimballed star tracker area. They have proposed a star scanner for the Pioneer Venus mission to one of the systems study contractors, as did CDC. Their proposed system is 7.6 inches by 4.5 inches diameter in size and has a weight of 5.4 pounds. It consumes 1 watt of power and provides a 0.3 degree lg accuracy on a zero magnitude silicon star at a 75 revolution-per-minute spin rate. It uses refractive optics and has a elevation field-of-view of 45 degrees. Its reliability is 0.91 for 2 years. With a sun shield, Kollsman claims the star scanner can operate 30 degrees from the sun line. This current study shows that this proposed system as well as the CDC proposed system with 45 degree fields-of-view make baffling to reject stray light extremely difficult. A field-of-view of 15 degrees or less is much more reasonable from a stray light rejection viewpoint.

Perkin-Elmer Corporation. Perkin-Elmer builds large astronomical telescope systems and a variety of other optical instrumentation but does not make any suitable star scanner hardware.

Astro Mechanics, Inc. Astro Mechanics Inc. specializes in large astronomical telescope systems and does not build any suitable star scanner systems.

Applied Physics Laboratory of John Hopkins University. The Applied Physics Laboratory (APL) is building a star sensor for use on the SAS-B. This is a photomultiplier-reticle system which is similar to the American Science and Engineering SAS star sensors. The star scanner weighs 4.75 lbs. and occupies a volume of 130 cubic inches. Its power consumption is 0.4 watts. It uses a 2 inch refractive optical system and an N slit reticle with a field-of-view in elevation of 10 degrees. The scanner operates at a spin rate from 0.1 to 3 revolutions-per-minute to within 60 degrees from the sun line. The system provides a 1.0 arc minute accuracy when detecting fifth magnitude stars. Plans are to fly this system in the fall of 1972. Because it is designed for high resolution and slow spin speeds, the optics and electronics require extensive redesign, and a much improved sunshield must be added to reduce the stray light rejection angle from 60 degrees to 35 degrees or so. APL does not normally build devices for sale to outside contractors.

SUMMARY OF TECHNOLOGY SURVEY

This survey has shown that several organizations have built instruments similar in some ways to that required on the Pioneer Venus mission. They are:

- Goddard Space Flight Center
- American Science and Engineering
- Honeywell Radiation Center
- Control Data Corporation
- Ball Brothers Research Corp.
- Applied Physics Lab of John Hopkins University

Table 12-1 summarizes the major parameters of the systems built by these organizations, the two Pioneer Venus star scanner proposals, and Pioneer Jupiter Star "pipper". It can be seen from the table that most of the operational starmapping systems built to date have been of the reticle-photomultiplier type. Also, most of the systems built to date have operated at slower spin rates than desired for the Pioneer Venus mission. Several of the systems described could be modified to perform the Pioneer Venus mission satisfactorily, but in all cases considerable modification is required and/or will involve additional constraints on the vehicle and mission. Based on our analysis of the survey data, we feel that a completely new design, based on the proven design principles demonstrated in these sensors, rather than modification of one of them, is the cost effective approach which will allow the most freedom to optimize the instrument for this specific application.

SECTION 13

CONCLUSIONS

From the information developed in the study, several conclusions may be drawn concerning the application of star scanner systems to the Pioneer Venus mission.

(1) A star scanner system can meet all attitude determination requirements. This will require two sensors mounted on the spacecraft at aspect angles of 45 degrees and 135 degrees. A baffle must be included to reject off axis light (from the sun or planetary albedo) outside 35 degrees. A sun aspect angle sensor should be included in the attitude determination system.

(2) The star sensor design can be either a "traditional" type using a photomultiplier and a V-slit reticle, or it can employ an array of silicon diode detectors. The silicon diode sensor offers many advantages including smaller size, less power, much greater reliability, and a significantly lower susceptibility to interference from stray light, but is more developmental and thus will cost more for development.

(3) The information processing in the spacecraft should be kept simple to increase reliability and minimize complexity and cost. A number of fairly elaborate schemes could be employed to validate and condense the data, but all such methods eliminate some information which can be of use. It is desirable to minimize the data rate, which can be accomplished with a simple command adjustable threshold to limit the number of stars detected.

(4) Stray light is a major problem in star scanner systems. A two stage cone type baffle is recommended for this application, and the optical system should be designed for low scatter characteristics. The silicon detector sensor has advantages in this regard.

(5) The stray light rejection capability required of the sensor is very high (up to 10^{12} , depending on sensor details and rejection definition). The problem is sufficiently complex that the only way to assure that the sensor will meet the requirements is to directly measure the rejection.

Unfortunately, conventional measurement techniques are not adequate and improved methods must be developed. Two methods are suggested which potentially could be developed into measurement facilities capable of measuring the high rejection ratios required.

(6) None of the sensors covered in the technology survey will meet the requirements of the Pioneer Venus mission without extensive modification. Several sensors, such as SCADS, QSO-7, and the SAS sensors, employ some of the design concepts applicable to a Pioneer Venus sensor, but all would require a completely new baffle and a redesigned optical system compatible with the baffle. To meet the spin speed requirements the electronics must be modified and repackaging would likely be required to interface with the Pioneer Venus spacecraft. In some cases the size of the optical system must be increased to provide the required sensitivity. All these sensors are the photomultiplier-reticle type, and some components from these sensors which have been proven in flight hardware such as the photomultiplier power supply, protection mechanisms, and reticle designs, could be used directly in this application. To provide a sensor capable of meeting all the Pioneer Venus requirements, it is felt that rather than modification of any existing design, the most cost effective approach is development of a new design based on these proven concepts where applicable.

(7) There are several ways in which the requirements can be relaxed to simplify the sensor system, or reduce size, weight, power, or cost. These include reducing redundancy, reducing the ability to operate at all attitudes, and reducing the spin speed and speed ranges. Reducing accuracy does not significantly simplify the system. If the requirements are reduced, some of the sensors covered in the survey may be applicable with fewer modifications. Unless the cruise mode and all other orientations are restricted so that the sensor always points away from the sun, all sensors would require a completely new baffle and optical system at a minimum.

SECTION 14

REFERENCES

BOOKS

- (B1) Quasius, Glen and McCanless, Floyd, Star Trackers and System Design, Spartan Books, 1966.
- (B2) RCA Corporation, Electro-Optics Handbook, RCA, 1968, Technical Series EOH-10.
- (B3) RCA Corporation, Photomultiplier Manual, RCA, 1970, Technical Series PT-61.

REPORTS

- (R1) McCanless, F., Quasius, G., and Unruh, W., Star Tracker Aerospace Reference Study - STARS, ASD-TDR-62-1056, 1963.
- (R2) Walsh, T.M. and Kenimer, Robert, Analysis of a Star-Field Mapping Technique for Use in Determining the Attitude of a Spin-Stabilized Spacecraft, NASA TN D-4637, 1968.
- (R3) Aldridge, Melvin P., and Credeur, Leonard, Investigation of an Optimum Detection Scheme for a Star-Field Mapping System, NASA TN D-5972, 1970.
- (R4) Gebel, Redames, K.H., An Analysis of Fundamental Factors Governing the Limitations in Detection of Images, ARL 68-0102, 1968.
- (R5) Andren, C. F., and Schenkel, F. W., A Star Tracker Design for Synchronous-Altitude Satellites, JHU ARLTG-869, 1966.
- (R6) Space Science Board, Venus Strategy for Exploration, Space Science Board, 1970.
- (R7) Marcotte, Paul C., Planetary Explorer Phase A Report and Universal Bus Description, GSFC, May 1971.
- (R8) Spacecraft Star Trackers, NASA SP-8026, 1970.
- (R9) Patterson, C. L., Star Trackers for Orbit and Interplanetary Space Applications, 1968, U.C.L.A.
- (R10) Carpenter, R.O.B. and Chapman, R. M., Effect of Night Sky Backgrounds on Optical Measurements, GCA 4559 FR, AD412678, 1959.
- (R11) Honeywell, Inc., Canopus Star Sensor for Lunar Orbiter Spacecraft, 4-03-10 Proposal to Boeing.
- (R12) Kleiman, Louis A. and Arehart, Raymond A., An Analytical Approach to the Determination of Stellar Fields of View, NASA TR-R-257, June 1967.

- (R13) Walsh, T. M., Keating, Jean C., and Hinton, Dwayne E., Attitude Determination of the Spin-Stabilized Project Scanners Spacecraft, NASA TN-D-4740, 1968.
- (R14) Study of a Scanning Celestial Attitude Determination System (SCADS) for a Synchronous Satellite, NASA-CR-100149, 1968.
- (R15) Nickel, D. F., Feasibility Study of Scanning Celestial Attitude Determination System SCADS for Small Scientific Spacecraft S³: Final Report, Contract Data Corp., NASA-CR-95807 (N68-29763 Microfiche) Sept. 1, 1967.
- (R16) Feasibility Study of Scanning Celestial Attitude System (SCADS) for Earth Resources Technology Satellite (ERTS) Final Report, NASA-CR-122361 (N72-18657 Microfiche) Control Data Corp., August 1971.
- (R17) Walsh, T. M., et al (NASA), A Celestial Attitude Measurement Instrument for Project Scanner, NASA-TN-D-4742 (N68-31938 Microfiche), 1968.
- (R18) Aldridge, M.D. (NASA), Investigation of the Optimum Detector Scheme for a Star Field Mapping System, NASA-TM-X-56818, August 1965.
- (R19) Weaver, J. J., Problems in the Design of a Star Mapper System, ESRO TM(P)-68 (ESTEC), (N69-15828 Microfiche) June 1966.
- (R20) Hatcher, N. M. (NASA), A Survey of Attitude Sensors for Spacecraft, NASA-SP-145, (N67-31296 Microfiche) 1967.
- (R21) Grosch, C. B., Feasibility Study for a Scanning Celestial Attitude Determination System (SCADS) For Three Axis Attitude Determination at a Command and Data Acquisition (CDA) Station, Final Report, NASA-CR-33523, (N67-23052 Microfiche) September 22, 1965.
- (R22) Jackson, D. B., SPARS Phase 1B Sunshield Development Final Report, TM-21290-52, 1970.

PAPERS

- (P1) Abate, John E., "Star Tracking and Scanning Systems, Their Performance and Parametric Design," IEEE Trans. Vol. ANE-10, No. 3, Sept. 1963.
- (P2) Forbes, F. F., and Mitchell, R. I., "Stellar Photometric Data for Six Different Photocathode Materials and the Silicon Detector", Communications of the Lunar and Planetary Laboratory, No. 141, 1968, p. 99.
- (P3) Grosch, Charles B., LaBonte, Anton E., and Vannelli, Bruce P., "The SCNS Attitude Determination Experiment on ATS-III", Spacecraft Attitude Determination Symp., 1969.
- (P4) Laverty, Norman P., "The Comparative Performance of Electron Tube Photo-Detectors in Terrestrial and Space Navigation Systems", IEEE, Vol. ANE-10, No. 3, Sept. 1963.

- (P5) Barnes, John W. and Walker, Burt, "Some Recent Advances in the Development of Solid State Celestial Trackers", Navigation, Vol. 13, No. 4, Winter 1966, p. 367.
- (P6) Schleuter, P., "Photomultiplier Tubes for Satellite Instrumentation", Applied Optics, Vol. 6, No. 2, Feb. 1967, p. 239.
- (P7) Thomas, Ronald D. and Schroyer, Gerald J., "Automatic Star Trackers for Aircraft Navigation", Navigation, Vol. 13, No. 3, Autumn 1966, p. 189.
- (P8) Forney, R. G., Szirmay, S. Z., and Bouvier, H. K., "Mariner 4 Maneuver and Attitude Control", Astronautics & Aeronautics, October 1965, p. 36.
- (P9) Favale, A. J., Kuehne F. J. and D'Agosteno, N. D., "Electron Induced Noise in Star Tracker Photomultiplier Tubes", IEEE Transactions on Nuclear Science, Vol. NS-14, No. 6, Dec. 1967, p. 190.
- (P10) Rome, Martin, Fleck, H. G., and Hines, D. C., "The Quadrant Multiplier Phototube, a New Star-Tracker Sensor", Applied Optics, Vol. 3, No. 6, June 1964, p. 691.
- (P11) Spicer, W. E., and Wooten F., "Photomission and Photomultipliers", Proc. IEEE, Aug. 1963, p. 1119.
- (P12) Engstrom, R. W., Stroudenheimer, R. G., Palmer, H. L. and Bly, D. A., "Work on Photoemission and Dark Emission Problems", IRE Trans. on Nuclear Science, Dec. 1958, p. 120.
- (P13) Chapman, D. S. J., "Signal-to-Noise Power Ratio Available from Photomultipliers Used as Star Detectors in Star Tracking Systems, A Method of Assessment", Journal Brit. IRE, March 1962, p. 209.
- (P14) Gorstein, M., Hallock, J. N., and Valge, Jr., "Two Approaches to the Star Mapping Problem for Space Vehicle Attitude Determination", Applied Optics, Feb. 1970, p. 351.
- (P15) Grusas, Pranas A., "Sattelite Attitude Determination from Celestial Sightings", J. Spacecraft and Rockets, Vol. 6, No. 9, Sept. 1969, p. 1007.
- (P16) Farrell, E. J., and Lillestrand, R. L., "Celestial Successor to Inertial Guidance", Electronics, March 21, 1966, p. 115.
- (P17) Mackison, D. L., Gotshall, R. L., Volpe, F., "Star Scanner Attitude Determination for the OSO-7 Spacecraft", AIAA Paper 72-922, Astrodynamics Conference, Palo Alto, Sept. 11, 1972.
- (P18) Grosch, Charles B., "Orientation of a Rigid Torque-Free Body by Use of Star Transits", J. Spacecraft, Vol. 4, No. 4, May 1967, p. 562.

- (P19) Hamstra, R. H., Jr., Wendland, P., "Noise and Frequency Response of Silicon Photodiode Operational Amplifier Combination", Applied Optics, Vol. 11, No. 7, July 1972, p. 1539.
- (P20) Bennett, H. E., Stanford, J. L., Bennett, J. M., "Scattering from Mirror Surfaces Used in Space Applications", paper presented at the 9th Congress of the ICO, Santa Monica, October 9-13, 1972.

OTHER REFERENCES

- (01) Robert Grosso, Perkin-Elmer Corporation, private communication.
- (02) Rudolph Dyke, Fairchild Camera and Instrument Co., private communication.